



**University of Algarve**  
**Faculty of Science and Technology**

**Water circulation pattern in the main channels of  
Ria Formosa based on tidal analysis**

DELLA PERMATA

Master Thesis of  
Erasmus Mundus Master of Science in Eco-Hydrology

**Thesis supervised by**

Professor Doutor Duarte Nuno Ramos Duarte

And

co-supervised by

Professor Dano Roelvink

2013



## **Declaração de autoria do trabalho**

Eu Della Permata declaro por minha honra ser a autora deste trabalho, que é original e inédito. Os autores e trabalhos consultados estão devidamente citados no texto e constam da listagem de referências bibliográficas incluída.

Copyright Della Permata. A Universidade do Algarve tem o direito, perpétuo e sem limites geográficos, de arquivar e publicitar este trabalho através de exemplares impressos reproduzidos em papel ou de forma digital, ou por qualquer outro meio conhecido ou que venha a ser inventado, de o divulgar através de repositórios científicos e de admitir a sua cópia e distribuição com objetivos educacionais ou de investigação, não comerciais, desde que seja dado crédito ao autor e editor.

## Acknowledgments

First of all, I would like to say grateful to God for giving me such blessed life and health during my study period in Erasmus Mundus of Ecohydrology. Without Him, I am sure I can not finish my study here. Then I would like to say my gratitude to my parents and my brother who always pray and support me whenever I need them and whenever I am down.

Many thanks to Prof. Duarte who have carefully guided me to finish my thesis. Many thanks also to Prof. Dano Roelvink who have been my nice co-supervisor, and Thanks to Prof. Luis Chicharo who accepted me in this Erasmus Mundus Master program. It was really nice experience that I have in my life. Thanks to Prof. Michael McClain who had been my program coordinator during my study period in Delft. Thank you for giving me such a chance to study in Unesco - IHE. My big grateful also want to address to Prof. Flavio Martin who had been my jury during my defense and gave me a lot of suggestions for my thesis. Then many thanks also to Prof. Erik de Ruyter for giving me a lot of encouragement and suggestion during my first two weeks in Delft. And lastly, thanks to all the professors that I can not mention one by one (Prof. Maciej Zalewsky, Prof. Alexandra Chicharo, Prof. Susana Netto, Prof. Alexandra Cravo, Prof. Leo Holthuijsen, and many) for teaching and sharing all the knowledge that you have to all of us. Thanks also to Joanna whom I had been bothering for the administration things in Faro.

Thanks also for all of my ecohydrology friends (Suha, Subham, Kyle, Enrique, Stevo, Teja, Silvia, Raquel, Li, Steffani, Mequan, emeka, Maysa, Thian, and Ashkar). I feel like I have my family here. Thanks for taking care of me, being friend with me, and encouraging me every time I feel down. I will never ever forget the moment that I spend with all of you. Tears and happiness are all together. I will miss you all.

Lastly, I would like to say thanks also to my Indonesian friends, who have been very nice to me (hani; pak eko, mas boy, pak habib, mbak ikha, pak septi, dan semua teman2 PPI portugal; kak upi, kak ira, kak ningsih, kak intan, mbak fatma, kak hesti, tia, renny, gisha, mas nawis, huda, mbak dyah, andri, pak hendiek, dan semua teman2 PPI IHE Delft; dian, melin, sita, bi chan, didi, mbak vivi dan semua anak2 JP4; anak2 kosan KP5A (stella, teteh, etc) thanks a lot...:D)

## Abstract

Ria Formosa lagoon, Southern coast of Portugal is considered as a very dynamic system. Current and water level data measurements of tidal dynamic in the main channels of Ria Formosa lagoon had been carried to figure out the hydrodynamic water circulation patterns. The aims of this study in general is to generate a recent hydrodynamic water circulation patterns based on tidal analysis, with the output of tidal dynamic characteristic (tidal propagation, tidal asymmetry and tidal distortion, energy flux and dissipation, water level and velocity longitudinal gradients, phase lag, tidal prisms, water discharge, etc) and residence time, which are used to identify the most suitable areas for seashell to grow.

Several time series of water level and longitudinal component of velocity variations data during completed tidal cycles in the 12 station points of the main channel in Ria Formosa were analyzed using harmonic analysis methods and obtained the average errors of 7.5 % velocity root mean square and 6.75% elevation root mean square, respectively. The tidal analysis results when projected in GIS platform enabled to highlight water circulation patterns in the main channel of Ria Formosa and showed the significance role of Faro-Olhão inlet and Armona inlet in term of energy, volume, and discharge, and less significance role of Sao Luis inlet. The spatial variability of residence time in each stations was obtained and showed that in the west and middle regions of Ria Formosa, a good water exchange were indicated, while in east region, a high residence time magnitude was discovered especially in the inner part of east region with 6.7 days of residence time. This finding result was combined with the average current velocity and maximum flood current and found that Nave Pegos, Culatra, Cações, and Bela Romão stations and adjacent areas are the most suitable area for seashell to grow.

The comparison study between inlet tidal cycle volume and geometric volume calculation was carried out and showed that volume difference represent in average a -38 cm of water level height difference estimation for all lagoon.

The future development of this work will allow introducing a quality level of understanding of the system in Ria Formosa and can give contribution for the fisherman as a preliminary step to find the suitable place for doing seashell aquaculture/ harvesting. Hence, from the Eco-hydrological perspective, the result of this study could be used for the decision maker as a management tool that related to anthropogenic activities such as dredging activity, inlet opening, and other activities that can give impact to the biota life in Ria Formosa.

**Keywords** : Ria Formosa, Circulation patterns, Tidal analysis, Ecohydrology, hydrodynamics.

## Resumo

O sistema lagunar da Ria Formosa localiza-se na zona costeira Sul de Portugal. Este trabalho teve por principal objectivo estudar os principais padrões de circulação da água nos canais principais, tendo por base leituras de velocidade da corrente e da variação da superfície livre, medidos em vários locais na Ria Formosa. Pretendeu igualmente estudar a propagação e a dissipação de energia da maré, os gradientes longitudinais referentes à variação da superfície livre e à velocidade da corrente, os atrasos da maré em diferentes locais, os prismas de maré, os volumes de água em circulação nos canais principais, os tempos de residência e as potenciais áreas para um melhor crescimento de bivalves tendo por base vários parâmetros hidrodinâmicos. Para o efeito foram medidas série de dados referentes à variação da superfície livre e variação da velocidade na coluna de água, ao longo de ciclos de maré, em 12 estações distribuídas na Ria Formosa, que foram submetidas a uma análise harmónica. Para a componente vertical da maré foram obtidos erros RMS médios de 6.75% e para a componente horizontal de 6.75%. Os resultados obtidos desta análise, quando projectados num sistema SIG permitiram realçar a importância das barras de Faro-Olhão e da Armona na circulação hidrodinâmica deste sistema lagunar em termos energéticos, volume e caudais, bem como uma menor importância relativa por parte da barra de S. Luís. Quando analisados os tempos de residência nas várias estações em estudo, verificou-se que as regiões Central e Oeste da ria foram caracterizadas por uma boa troca de água, enquanto nos sectores mais interiores da região Este por tempos de residência elevados de aproximadamente 6.7 dias. Estes resultados quando conciliados com as respectivas velocidades médias e velocidades máximas de enchente, permitiram definir as estações de Nave Pegos, Culatra, Cações e Bela Romão (e zonas adjacentes) com as mais indicadas para o crescimento de bivalves.

Quando comparados os volumes referentes aos prismas de maré obtidos através das séries de dados maregráficos medidos nas barras em análise, com os prismas de maré geométricos obtidos pela plataforma GIS, constatou-se haver uma diferença entre eles que se materializou numa diferença média da altura da água na laguna da ordem dos -38cm.

Este trabalho para além de contribuir para melhor conhecimento do funcionamento hidrodinâmico da Ria Formosa, e dar um contributo para as associações de mariscadores locais com estes resultados preliminares sobre as melhores localizações para os viveiros de marisco neste sistema lagunar, poderá permitir introduzir em trabalhos futuros outros parâmetros que ajudarão a definir as melhores áreas para a implementação deste viveiros.

Os resultados obtidos neste trabalho no âmbito da Eco-hidrologia, poderão ser usados não só como uma ferramenta de decisão para as entidades locais, mas também dar informações primordiais para a gestão deste sistema costeiro no que diz respeito a actividades antropogénicas, tais como a gestão de trabalhos de dragagem, a abertura de novas barras, e outras actividades que possam ter impactes no Biota da Ria Formosa.

**Palavras chave:** Ria Formosa, Padrões de circulação, Análise da mare, Eco-hidrologia, hidrodinamica.

## General Index

Declaração de autoria do trabalho.....	1
Acknowledgments.....	2
Abstract.....	3
Resumo.....	5
General Index.....	7
Table Index.....	9
Figure Index.....	10
Acronims and Abbreviations.....	11
1. Introduction.....	12
1.1. Importance of The Subject / Interest of The Subject.....	12
1.2. Thesis Framework / Theoretical Background of The Subject.....	12
1.3. Main objectives and sub-objectives.....	14
1.4. Thesis Structures Descriptions.....	14
2. State of The Art.....	16
2.1. Water level and water flow hydrodynamic.....	16
2.2. Nutrient dynamic.....	17
2.3. Dredging work and open/close inlet.....	18
2.4. Residence time.....	19
3. Study Area.....	21
3.1. Location and Characteristics.....	21
3.2. Climate.....	22
3.3. Hydrodynamics.....	23
3.4. Ecological Functions.....	24
3.5. Social and Economy Importance.....	24
3.6. Water Quality.....	25
4. Methods.....	26
4.1. Field Data.....	26
4.2. Data Treatment.....	28
4.2.1. Raw Time Series.....	28
4.2.2. Harmonic Analysis.....	28
4.2.2.1. Tidal distortion / Tidal asymmetry.....	29
4.2.2.2. Energy Flux and Dissipation.....	29
4.2.2.3. Error Calculation.....	30
4.2.3. Hysteresis Diagram Analysis.....	30
4.2.4. GIS Application.....	31
4.2.4.1. Hydraulic Geometrical Parameters Calculation.....	31
4.2.4.2. Spatial Distribution Performance.....	31
4.2.4.2.1. The mean velocity ( $\bar{u}_n,t$ ) in the water column.....	31
4.2.4.2.2. The mean velocity in the channel cross section ( $\langle \bar{u}_n,t \rangle$ ).....	32
4.2.4.2.3. The mean velocity in the channel cross section during flood and ebb ( $\langle \bar{u}_n \rangle_{\text{flood}}$ and $\langle \bar{u}_n \rangle_{\text{ebb}}$ ).....	32
4.2.4.2.4. Net Velocity.....	33
4.2.4.2.5. Water Discharge ( $Q_n$ ) and water volume ( $V_n$ ).....	33
4.2.4.2.6. Residence Time (RT) calculation.....	33
4.2.4.2.7. GIS performance.....	34
4.2.4.3. Comparison study of tidal inlet volume and annual critical geometry volume of the lagoon.....	36

5. Result and Discussions .....	37
5.1. Harmonic Analysis Fit and Proper test of the data .....	37
5.2. Longitudinal and Temporal gradients of water level and velocity in the main channel .....	44
5.2.1. Longitudinal gradients of water level and velocity in the main channel .....	44
5.2.2. Temporal gradients of water level and velocity in the main channel .....	54
5.2.2.1. For all stations .....	54
5.2.2.2. For inlets .....	58
5.2.2.3. For West Region of Ria Formosa .....	61
5.2.2.4. For middle region of Ria Formosa .....	64
5.2.2.5. For East region of Ria Formosa .....	66
5.3. Volume and Discharge of flood and ebb phase .....	70
5.4. Spatial variability of residence time .....	71
5.5. Preliminary study in determining the suitable area for seashell ponds using Arc GIS .....	73
5.6. Comparison study between inlet tidal cycles volume and geometric volume .....	75
6. Conclusions .....	79
7. References .....	81

## Table Index

Table 4.1. Coordinate location of the stations.....	27
Table 4.2. The tidal height (H) and tidal period (T) of the tide in each stations (TP measurement).....	28
Table 5.1. The tidal velocity amplitude and phase of tidal harmonic constituents M2 and M4 for each stations .....	38
Table 5.2. The tidal height / elevation / water level amplitude and phase of tidal harmonic constituents M2 and M4 for each stations .....	38
Table 5.3. The tidal height / water level amplitude and phase of tidal harmonic constituents M2 and M4 (Baptista, 1987).....	39
Table 5.4. Root Mean Square calculation.....	39
Table 5.5. Tidal Distortion and Tidal Asymmetry Analysis (amplitude ratio and flood/ebb strength comparison).....	40
Table 5.6. Flood / Ebb Dominance based on Tidal Phase Period.....	42
Table 5.7. Tidal energy flux and dissipation for each stations due to M2 and M4 tidal constituent.....	42
Table 5.8. Tidal energy dissipation along the channel stations and the reference distance among the adjacent station in Ria Formosa .....	43
Table 5.9. Water level gradient among adjacent stations at 0 hour, 3 hours, 6 hours, 9 hours and 12 hours.....	45
Table 5.10. Velocity gradient among adjacent stations at 0 hour, 3 hours, 6 hours, 9 hours, and 12 hours.....	45
Table 5.11. tidal amplitude of harmonic analysis and raw data in all stations .....	57
Table 5.12. Phase Lag.....	58
Table 5.13. Phase lag among the inlets in Ria Formosa .....	61
Table 5.14. The slack water for all stations .....	70
Table 5.15. Volume and Discharge of flood and ebb during tidal cycle .....	71
Table 5.16. Inlet tidal prisms during spring and neap tide (Pacheco et al., 2010).....	70
Table 5.17. Spatial variability of residence time in all stations .....	72
Table 5.18. Residence Time, Average current velocity, and Maximum Flood Current for each stations in Ria Formosa lagoon.....	74
Table 5.19 . Inlet tidal cycle volume.....	76
Table 5.20. The difference estimation between inlet tidal cycle volume and geometrical volume.....	78

## Figure Index

Fig 3.1 Location map of the Ria Formosa System (offshore bathymetry in meters) with location of inlet sections (1–Ancao / Sao Luis Inlet; 2– Faro–Olhao Inlet; 3–Armona Inlet; 4– Fuzeta Inlet; 5–Tavira Inlet; and 6 – Cacela Inlet). (Dias and Sousa, 2009a). .....	22
Fig 4.1. Tides parameter locations which are currently being measured by MareFORMOSA project, in Ria Formosa (red pins) .....	26
Fig 5.1. Region division in Ria Formosa (West region : Sao Luis inlet, Centro Nautica, Bar de Gina ; Middle region : Faro Olhao inlet, Quatro Aguas, Nave Pegos, Canal Cacoas, Culatra, Boia V3; East region : Armona inlet, Bela Romao, Marim, Boia V3, Culatra). .....	44
Fig 5.2. Water circulation patterns inside the main channel of Ria Formosa based on water level gradient at 0 hour (at high water in Faro Olhao inlet).....	46
Fig 5.3. The tidal current circulation patterns inside the main channel of Ria Formosa at 0 hour (at high water in Faro Olhao inlet).....	47
Fig 5.4. Water circulation pattern inside the main channel of Ria Formosa based on water level gradient at 3 hours (at ebbing period in Faro Olhao inlet).....	48
Fig 5.5. The tidal current circulation pattern inside the main channel of Ria Formosa at 3 hours (at ebbing period in Faro Olhao inlet).....	49
Fig 5.6. Water circulation pattern inside the main channel of Ria Formosa based on water level gradient at 6 hours (at low water in Faro Olhao inlet).....	50
Fig 5.7. The tidal current circulation pattern inside the main channel of Ria Formosa at 6 hours (at low water in Faro Olhao inlet).....	50
Fig 5.8. Water circulation pattern inside the main channel of Ria Formosa based on water level gradient at 9 hours (at flooding period in Faro Olhao inlet).....	51
Fig 5.9. The tidal current circulation pattern inside the main channel of Ria Formosa at 9 hours (at flooding period in Faro Olhao inlet).....	52
Fig 5.10. Water circulation pattern inside the main channel of Ria Formosa based on water level gradient at 12 hours (at high water).....	53
Fig 5.11. The tidal current circulation pattern inside the main channel of Ria Formosa based on velocity/tidal current gradient at 12 hours (at high water).....	53
Fig 5.12. Water level variation for all stations.....	55
Fig 5.13. Velocity variation for all stations.....	55
Fig 5.14. Hysteresis Diagram for all stations.....	56
Fig 5.15. Water level variation for inlets.....	59
Fig 5.16. Velocity variation for inlets.....	59
Fig 5.17. Hysteresis Diagram Analysis for inlets.....	60
Fig 5.18. Water level variation for west region of Ria Formosa.....	62
Fig 5.19. Velocity variation for west region of Ria Formosa.....	63
Fig 5.20. Hysteresis Diagram Analysis for west region of Ria Formosa.....	64
Fig 5.21. Water level variation for middle region of Ria Formosa.....	65
Fig 5.22. Velocity variation for middle region of Ria Formosa.....	65
Fig 5.23. Hysteresis Diagram Analysis for middle region of Ria Formosa.....	66
Fig 5.24. Water level variation for east region of Ria Formosa.....	67
Fig 5.25. Velocity variation for east region of Ria Formosa.....	68
Fig 5.26. Hysteresis Diagram Analysis for east region of Ria Formosa.....	69
Fig 5.27. Spatial variability of Residence time .....	73
Fig 5.28 Spatial variability of Maximum Flood Current (m/s) in Ria Formosa lagoon.....	75
Fig 5.29 Spatial variability of Average Current Velocity (m/s) in Ria Formosa lagoon.....	75
Fig 5.30 Ria formosa condition during high water level.....	76
Fig 5.31. Ria formosa condition during low water level.....	77

## **Acronims and Abbreviations**

ADP - Acoustic Doppler Current Profiler

ADCIRC - Advance 3-Dimensional Circulation Model

GIS - Geographical Information System

IPS - Instituto Portuario do Sul

MOHID - Modelo Hidrodinâmico which is hydrodynamic model in Portuguese

RMS - Root Mean Square

SWAT - Soil and Water Assessment Tool

TP - Pressure Transducer

m - meter

m<sup>2</sup> - meter quadrat

m<sup>3</sup> - meter cubic

s - second

h - hour

W - watt

## **1. Introduction**

### **1.1. Importance of The Subject / Interest of The Subject**

This study will carry out the hydrodynamic part of the Ria Formosa lagoon. Since the previous researches in hydrodynamic tend to use established model to describe the Ria Formosa hydrodynamic, this study will treat the data using local approach. It will focus on the recent hydrodynamic water circulation pattern in the main channel based on real data on tidal dynamic analysis and tidal regime within Ria Formosa. Considering that Ria Formosa is a very dynamic system, so using more recent data will be considered convenient (Dias et al, 2009b). The output of this study will be the phase lag of horizontal and vertical component of the tide, tidal dynamic characteristic (tidal asymmetry and tidal distortion, energy flux and dissipation, water level and velocity gradient, tidal prisms, discharge, etc), and residence time, which will be used to identify the most suitable area for seashell ponds. Therefore, this thesis can give contribution for the fisherman to find the suitable place for doing clam aquaculture and clam harvesting. From the Eco-hydrological perspective, the result of this study could give benefit for decision maker as a management tool related to anthropogenic activities such as dredging activity, inlet opening, etc that can give impact to the biota life in Ria Formosa. Besides that, it could help the continuity of the research in order to figure out the next step for researching.

### **1.2. Thesis Framework / Theoretical Background of The Subject**

The purpose of this sub chapter is to provide the reader with the broad theoretical framework used for interpreting the research presented in this thesis on hydrodynamic water circulation pattern in Ria Formosa coastal lagoon in term of barotropic pressure gradient, tidal characteristic (tidal asymmetry and tidal distortion, energy flux and dissipation, water level and velocity gradient, tidal prisms, discharge, etc) and residence time.

Coastal lagoons are shallow water bodies which usually connected to the open sea by one or several tidal inlets between barrier islands (Newton and Mudge, 2003; Dias et al, 2009b) and are classified as inland bodies of water (Schwartz, 2005; Bjorn, 1994). The number and size of the inlets, precipitation, evaporation, and inflow of fresh water affect the condition of the lagoon. Lagoons with little or no interchange with the open ocean, little or no inflow of fresh water, and high evaporation rates may become highly saline (Kusky, 2005). These systems usually run parallel to the coastline, in contrast to estuaries that are normally perpendicular to the coast (Newton and Mudge, 2003; Dias et al, 2009b).

The mean circulation patterns of estuaries and shallow seas originate as the remainder of chaotic first-order flow episodes caused by tides, winds, and river inflow (Csanady, 1976; Reed et al., 2004). Tides are often responsible for the bulk of the kinetic energy present in estuaries. They play a critical role in determining the strength of vertical mixing, can produce significant residual (mean) circulation, and drive lateral circulations within the estuary (Seim et al., 2006). Besides tides, winds, and river inflow, the water circulation is also controlled by rainfall, evaporation, upwelling, eddies, and storms. Water circulation patterns are influenced by vertical mixing and stratification. Vertical mixing determines how much the salinity and temperature will change from the top to the bottom. Vertical mixing occurs at three levels: from the surface downward by wind forces, the bottom upward by boundary generated turbulence (estuarine and oceanic boundary mixing), and internally by turbulent mixing caused by the water currents which are driven by the tides, wind, and river inflow (Wolanski, 2007).

Water circulation patterns can affect residence time and exposure time. The residence time of water is a key variable determining the health of an estuary, particularly from human-induced stresses. Rapid flushing ensures that there is insufficient time for sediment accumulation or dissolved oxygen depletion in the estuary; thus a well flushed estuary is intrinsically more robust than a poorly flushed estuary (Wolanski, 2007). The water residence time can be determined using tidal prism. Tidal prism is the volume of water in an estuary or inlet between mean high tide and mean low tide (Luketina, 1998) or the volume of water leaving an estuary at ebb tide (Davis and Fitzgerald, 2004). If it is known how much water is exported compared to how much of the estuarine water remains, it can be determined how long water reside in that estuary. Tidal prism magnitude can be calculated by multiplying the area of the estuary by the tidal range of that estuary (Davis and Fitzgerald, 2004). During spring or neap tides, when sea level is relatively high and floods back barrier areas that are normally above tidal inundation, the cross sectional area at the entrance of the estuary increases as tidal prism increases (O'Brien, 1931).

If tidal currents at the mouth of an estuary are strong enough to create turbulent mixing, vertically homogenous conditions often develop (Kennish, 1986). In these kind of estuaries, tidal flow is greater relative to river discharge, resulting in a well mixed water column and the disappearance of the vertical salinity gradient. the freshwater - seawater boundary is eliminated due to the intense turbulent mixing and eddy effects. The width to depth ratio of vertically homogenous estuary is large, with the limited depth creating enough

vertical shearing on the seafloor to mix the water column completely. Tidal dissipation has higher values in areas where the tidal currents are stronger, as well as in the areas of transition from the sea to the lagoon (Dias and Sousa, 2009a).

### **1.3. Main objectives and sub-objectives**

The main objective of this study is to present the recent hydrodynamic water circulation pattern inside the main channel based on real data on tidal dynamic analysis and tidal regime within Ria Formosa, with the sub-objectives consist of :

- a. Determine the tidal asymmetry and tidal distortion using harmonic analysis fit and proper test.
- b. Calculate the energy flux and the energy dissipation of the tide.
- c. Establish the spatial and temporal gradients of water level ( $\eta$ ) and longitudinal component of velocity ( $v$ ) in the main channels.
- d. Calculate the phase lags of water level ( $\eta$ ) and velocity ( $v$ ) in different stations.
- e. Calculate the flood/ebb volume and discharge in each stations.
- f. Calculate the spatial variability of the residence time in each stations.
- g. Determine the suitable area for seashell ponds using Arc GIS considering the average tidal current, maximum flood current, and residence time.
- h. Calculate the geometrical water volumes for the lagoon, considering the high water and low water variation/deformation in each stations and conduct comparison study between inlet tidal cycles volumes and the geometrical volumes.

### **1.4. Thesis Structures Descriptions**

#### **Chapter 1 : Introduction**

Consist of the explanation of the importance of the subject, thesis framework/ Theoretical background of the subject and also the main objectives and sub objective of the study.

#### **Chapter 2 : State of the art**

Consist of specific knowledge related to the subject of the study in Ria Formosa and previous researches related to the subject of the study in Ria Formosa lagoon.

#### **Chapter 3 : Study Area**

Consist of the detail explanation about the study area such as the location and characteristic, climate, hydrodynamic of the study area, ecological function, social and economy importance, and water quality.

**Chapter 4 : Methodology**

Consist of the explanation about the methods that are used, the data collection, data treatment, and data analysis method.

**Chapter 5 : Result and Discussion**

The presentation and explanation about the result of the data treatment and detail analysis discussion.

**Chapter 6 : Conclusions**

Conclusions that can be withdrawn from the study.

## 2. State of The Art

### 2.1. Water level and water flow hydrodynamic

In vertically homogenous estuary, to predict the water circulation pattern, barotropic pressure gradient measurement could be applied. Barotropic pressure gradient is associated with the horizontal change surface elevation according to the hydrodynamic process described by tidal propagation, fresh water of the river inflow, coriolis acceleration, and wind motion, with the influence of the bathymetry (Pacanowski, R. C. And S. M. Griffies, 2000). Barotropic gradient is generated by a sloping sea surface and the pressure gradient is *depth independent*. For a fluid that is homogenous (i.e. the fluid's density is constant everywhere) pressure gradient will only be barotropic. Pressure gradients can also be purely barotropic if the lines of constant pressure (isobars) are parallel to lines of constant density. subsequently a barotropic pressure gradient will not generate vertical shear in the flow, but rather a depth average flow (Ghil et al, 2002).

The tides propagate into the lagoon and altered by its geometry and bathymetry (Dias and Sousa, 2009a). Tidal wave propagates into shallow region, shallow water tides usually increase, include tidal asymmetry (Dias and Sousa, 2009a). Tidal asymmetry of the vertical tide usually refers to the distortion of the (predominant) semi-diurnal tide due to the (quarter-diurnal, sixth diurnal, etc) overtides. The strength of the asymmetry depends on the ratio between the amplitude of the overtide and that of the semidiurnal tide, and the nature of the asymmetry (ebb or flood dominance) is determined by the phase difference between the overtide and the semi-diurnal tide (Wang et al., 1999).

Tidal hydrodynamic related to water level and water flow in Ria Formosa had been simulated using finite element two dimensional model (ADCIRC) (Mendonca, 2001) and using finite difference two dimensional depth-integrated mathematical model (ELCIRC) (Dias and Sousa, 2009a). Both of them used the model to produce the water flow in various inlet and produce water level variations of several station in Ria Formosa which are processed by harmonic analysis to determine the spatial distribution of amplitude and phases of the main harmonic constituents. The harmonic constituents that includes in these two studies are Z0, Msf, O1, K1, N2, M2, S2, MN4, M4, MS4, M6, and 2MS6, which more detail explanation focus on M2, S2, and M4 constituent. The result of these two studies showed the correct representation of tide level, amplitude, and phase of the diurnal and semidiurnal constituent with small error. The semidiurnal constituent have highest amplitude, followed by diurnal (Dias and Sousa, 2009a). In most places, the semidiurnal components are dominant (Van rijn, 1990). The result for M2 can be considered representative of the tide in Ria

Formosa lagoon, since it has most of tidal energy (Dias and Sousa, 2009a). The constituent non linear (M4) has been carried out and showed that the greater velocity gradient at the site, the more significant amplitude in relation to depth (Mendonca, 2001).

Besides that, the result also showed the location of flood dominance areas in Ria Formosa which are in Ancao, Armona, Fuzeta, and Cacela inlet, while ebb dominance areas occur at other inlets (Dias and Sousa, 2009a). This finding is different with the finding of Salles et al (2005) for the Ancao and Armona inlets. This is due to the fact that the duration of flood and ebb is not a determinant factor for flow dominance. Longer duration of the flood (ebb) may be associated with flood (ebb) dominance, due to the existence of strong residual circulation between inlets. In fact, the larger flood (ebb) discharge in a shorter period does not lead to stronger flood (ebb) currents (Dias and Sousa, 2009a). So it means that the discharge and the period of the ebb or flood need to be taken into consideration for determining the flow dominance.

Other similar work has been conducted by Martins et al (2003) using a model which is developed by Portuguese researchers, MOHID, to characterize the system and to understand the processes in Ria Formosa. The hydrodynamic model was forced by the tide at the open boundary and average climatological winds without considering the freshwater flow due to the low and intermittent run off to the system (Gamito, 1997; Coelho et al., 2002; Martin et al, 2003; Serpa et al., 2007). This model was calibrated and validated using local measurement and the result showed a good agreement between the model and the measured data, with small error.

## **2.2. Nutrient dynamic**

Hydrodynamic model is the first step in future studies on water quality, sediment transport, and other studies in the system (Mendonca, 2001). The study of nutrient dynamic inside Ria Formosa correspond to land drainage, waste water treatment plant, and water exchanges across the lagoon inlet had been conducted using SWAT model with Eco-Dynamo model to provide physical-biogeochemical model (Duarte et al., 2008). Ria Formosa is a shallow coastal lagoon with high productivity (Falcao and Vale, 2003). One of the sources that contribute largely for the lagoon water nutrient enrichment (ammonium and phosphate) is the bottom sediment (Serpa et al., 2007).

### **2.3. Dredging work and open/close inlet**

The acquisition of a series of topo-bathymetric surveys and oblique aerial photos (Sedimentary dynamics) had been carried out at Ancao Inlet since its artificial opening in June 1997 until for two years ahead (Vila-Concejo et al., 2003). Six years after this study, the numerical modeling of the impact of the Ancao inlet relocation has also been conducted in Ria Formosa, Portugal (Dias et al, 2009b). This research discussed on the effect of Ancao inlet relocation to the hydrodynamic pattern such as water circulation and the potential pathways of tracers in the western part of Ria Formosa in two distinct configurations: before and after the Ancao Inlet relocation by using numerical modeling method which are hydrodynamic ELCIRC and VELA/VELApart. The hydrodynamic simulation of Ria Formosa was performed using the two dimensional depth-integrated model ELCIRC which uses finite volume / finite difference Eulerian-Lagrangian algorithm and the simulation of the tracers transport was performed with the models VELA and VELApart, with the objective of studying the dispersion of tracers (VELA) and to evaluate the residence times (VELApart). The hydrodynamic model was successfully calibrated and validated against elevation, velocity, and inlet discharge data with result the relocation of Ancao inlet increases the stability of the Ria formosa lagoon: the magnitude of tidal currents, residual velocities, and tidal prism across the bar. The tracers transport simulations showed enhanced water exchanges through the Ancao Inlet and smaller residence times in the western part of Ria Formosa with the present configuration. Overall, it is concluded that the Ancao Inlet relocation had a positive contribution towards increasing the water renewal of the western part of the lagoon, thus decreasing its vulnerability to pollution (Dias et al, 2009b). This study shows that the inlet enlargement and deepening was a successful strategy, and therefore may be implemented to improve the water quality and circulation in other lagoons or estuaries, after the numerical modeling study of possible impacts (Dias et al, 2009b).

The study of inlet dredging in Faro channel also had been carried out by Pacheco et al. (2006). This study aims to study the volumetric evolution of a navigable channel, defining both erosion and accretion sectors and to compare the natural and anthropogenic processes by comparing the three bathymetric maps from the Faro channel (1985, 1994, and 2001) provided the definition of erosive and accumulative sectors and allowed the calculation of the total variation (m<sup>3</sup>) for each sector. The comparison with the values from the dredging activities in the study area given by IPS (2001) was undertaken to define the concept natural changes and anthropogenic dredging. The result of this study showed the erosion found during the period 1984-1994 is mainly related with dredging activities, while during the

period 1994-2001, both natural and anthropogenic occurred strongly.

#### **2.4. Residence time**

Residence time in Ria Formosa had been an object of researches since a long time ago. Duarte et al. (2005 and 2008) did a research on hydrodynamic modeling of Ria Formosa with Eco-dynamo using two dimensional vertically integrated hydrodynamic model based on finite difference method and a semi implicit resolution scheme. Water residence times were estimated by “filling” the lagoon with a conservative tracer and running the model until its “washout” to the sea. The result showed water residence considering a 90% washout range from less than one day near the inlet to more than two weeks at the inner area, with an average values of 11 days. Besides that, the result also showed that Faro - Olhao and Armona inlets give dominant contribution for the lagoon-sea water exchanges and the variability in water residence time at different areas of the lagoon (Duarte et al., 2005 and 2008). These result is relevant with the research done by Ana Mendonca (2001) which also indicates the good water exchange in Ria Formosa by showing the result of ebb velocity is much greater than flood velocity. Since higher ebb velocity than flood velocity means much water transfers outside the lagoon than goes inside the lagoon, so there is more new water transfer inside Ria Formosa lagoon. Finite Element Methods was used to simulate the hydrodynamic pattern of Ria Formosa and tidal current velocities as well as the relationship between semidiurnal harmonic constituent M2 and non linear harmonic constituent M4 were used to predict the ebb/flood dominance (Mendonca, 2001). In contrast to the result of these two researches, Mudge et al. (2008) found that the residence time in the inner regions of Ria Formosa is quite long, so the management models should take into account additional complexities that might arise from the much longer exchange rates of the inner lagoon (Mudge et al., 2008). Mudge et al. (2008) estimates the residence time in Ria Formosa using salinity tracers by comparing the salinity measured during tidal cycle outside and inside the lagoon, and near the outlet of the lagoon. Calculation of the residence time was based on box model worked by Hearn and Robson (2002). This change became zero in lagoons, such as the Ria Formosa in summer, where there was no freshwater inflow. Therefore, increases in salinity above that of the inflowing sea-water were due to evaporation of surface water and the length of time the water was in the system (Mudge et al., 2008).

Besides that, Mudge et al. (2007) also did a research in the relationship between water residence time and oxygen saturation in a mesotidal lagoon, Southern Portugal during summer months where there is no significant freshwater input and has high evaporation rate.

The result showed a significant linear decrease in the oxygen saturation with the increasing residence time in response to discharges of high organic carbon content wastes and potentially eutrophic phytoplankton blooms.

### 3. Study Area

#### 3.1. Location and Characteristics

Ria Formosa is a shallow coastal mesotidal barrier lagoon, which located in the southern coast of Portugal (36°58' N, 8°02' E to 37°03' N, 7°32' W) (Gamito, 1997; Coelho et al., 2002; Newton and Mudge, 2003; Duarte et al., 2008; Dias et al., 2009b; Brito et al., 2011; Guimaraes et al., 2012). It has large intertidal areas and has mean depth of approximately 3.5 m (Falcao and Vale, 2003; Nobre et al., 2005; Duarte et al., 2008; Brito et al., 2011). Based on the general explanation above, Ria Formosa can be classified as vertically homogenous estuary because of its shallowness (Gamito, 1997; Coelho et al., 2002; Newton and Mudge, 2003; Duarte et al., 2008; Mudge et al., 2008; Dias et al., 2009b; Brito et al., 2011; Guimaraes et al., 2012).

The Ria Formosa basin has an area of 864 km<sup>2</sup>, it includes 145.22 km<sup>2</sup> of wetland as well as 40 km<sup>2</sup> of salt extraction ponds, marine culture ponds, salt marsh, exposed sands, navigable channel and mud banks. The salt marshes are composed of silt and fine sand and are intersected by a high density of shallow meandering tidal creeks. The navigable channels were extensively dredged during the year 2000. The average depth of the navigable channels is 6 m although most areas are less than 2 m deep (Salles et al., 2005; Dias et al., 2009b). There are a further 25 km<sup>2</sup> of sand dunes, farmland, forest and urban land also in Ria Formosa.

Seaward, it is limited by a non continuous belt of sandy dunes formed by two peninsulas and five barrier islands that separate the lagoon from the Atlantic ocean (Coelho et al., 2002; Dias et al., 2009b; Guimaraes et al., 2012). Ria Formosa has six inlets, which are from west to east: Ancao/Sao Luis Inlet, Faro-Olhao inlet, Armona Inlet, Fuzeta Inlet, Tavira Inlet and Cacela Inlet (**Fig. 3.1**) (Coelho et al., 2002; Dias et al., 2009b; Guimaraes et al., 2012), where the water exchange between the lagoon and the sea takes place (Dias et al., 2009b; Brito et al., 2011). Among these inlets, Faro-Olhao inlet has been artificially consolidated by two breakwaters. In 1997, the Ancao Inlet, located on the western part of the lagoon, was relocated 3,500 m westward of its previous position (Vila-Concejo et al., 2003; Dias et al., 2009b), with the goal of improving the exchange of water between the western end of the lagoon and the ocean (Newton and Mudge, 2003; Dias et al., 2009b). Besides changing the inlet location, the works increased the inlet width from 600 m to about 1,000 m, as well as the inlet depth from 2.5 m to about 6 m (Dias et al., 2009b).

The existence and persistence of tidal inlets in coastal systems is fundamental for water quality, navigability, and beach/barrier stability (Dias et al., 2009b). Five small rivers

and 14 streams flow into the Ria Formosa but most of these are ephemeral and dry out completely in summer, causing freshwater discharges to be negligible relative to tidal prisms (Nobre et al., 2005; Mudge et al., 2008; Dias et al., 2009b; Brito et al., 2011). Salinities range between 35.5 to 36.9 psu all year round, due to no significant freshwater input into the lagoon (Gamito, 1997; Coelho et al., 2002; Serpa et al., 2007). There is only one major river, the Gilao near Tavira, flowing into the Formosa. The origin of the rivers is mostly from the Caldeirao mountain range (Dias et al., 2009b).

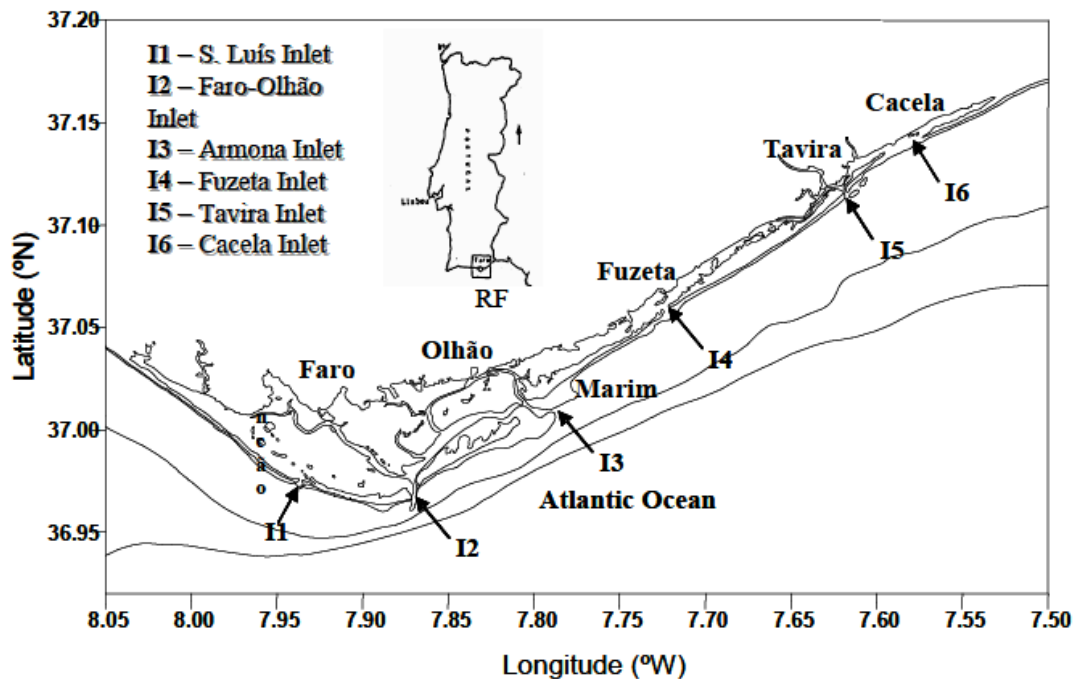


**Fig 3.1.** Location map of the Ria Formosa System (offshore bathymetry in meters) with location of inlet sections (1–Ancao / Sao Luis Inlet; 2– Faro–Olhao Inlet; 3–Armona Inlet; 4– Fuzeta Inlet; 5–Tavira Inlet; and 6 – Cacela Inlet). (Dias and Sousa, 2009a)

### 3.2. Climate

The climate of the Ria Formosa is Mediterranean (Bebianno, 1995). Rainfall is occasional, but torrential in winter (Bebianno, 1995). Based on annually and monthly data, there seems to be an increase in irregularity of annual precipitation in the basin, being the average annual precipitation value between 600 and 800 mm. The wettest month is December with about 17% of total annual precipitation, followed by November and January (about 15%). The driest months are July and August with less than 1% of annual precipitation. The maximum daily annual precipitation, for a return period of 2 years, is approximately 55 mm, whereas for a 100 years return period, it is 132 mm (Duarte et al., 2008).

### 3.3. Hydrodynamics

Only a small fraction (14%) of the Ria Formosa lagoon is permanently immersed and approximately 80% of the total area is exposed during low tides. The tides are semidiurnal, with amplitudes that range from about 0.7 m (neaps) to about 3.5 m (springs) (Gamito, 1997; Duarte et al., 2008; Dias et al., 2009b). Daily, 50-70% of the water is exchanged between the lagoon and the ocean mainly through the Faro-Olhao inlet (Gamito, 1997; Salles et al., 2005; Serpa et al., 2007; Dias et al., 2009b; Guimaraes et al., 2012). The good water exchange can be proved by the higher ebb velocity than flood velocity in Ria Formosa lagoon system (Mendonca, 2001). Tide-induced currents can be strong at the inlets and maximum values are usually found at the Faro- Olhao Inlet where they can reach 2.2 m/s and 1.6 m/s during ebb and flood respectively (Salles, 2001; Dias et al., 2009b). Tidal dissipation has higher values in areas where the tidal currents are stronger, as well as in the areas of transition from the sea to the lagoon. (Dias and Sousa, 2009a). Tidal dissipation for neap tides is considerable lower than for spring tides (Dias and Sousa, 2009a).

The tides propagate into the lagoon and are altered by its geometry and bathymetry (Dias and Sousa, 2009a). Tidal waves propagate into shallow regions, shallow water tides usually increase, include tidal asymmetry (Dias and Sousa, 2009a). In shallow areas, there is strong attenuation of M2 tidal constituent and the opposite occurs for the M4 which undergoes strong amplification, thus inducing tidal asymmetry in these areas (Dias and Sousa, 2009a). The amplitude ratio increases inside the lagoon (shallow regions) reveal tidal asymmetry is maximum at these areas (Dias and Sousa, 2009a). A significant phase delay as the tide propagates also occurs in these shallow areas (Dias and Sousa, 2009a). Tidal amplitude decreases with the distance from the lagoon inlets, while the phase lags increase, revealing a strong deformation of the tidal wave inland (Dias and Sousa, 2009a).

Neves (1988) has modeled the submergence and emergence period for the western part of the lagoon as a function of tides. The result showed that large areas of mudflats are exposed at low water but submerged at high water. The estimation for the submerged area of the Ria Formosa are 53 km<sup>2</sup> at high water and 14–22 km<sup>2</sup> at low water (Neves, 1988 in Dias et al., 2009b).

The wave climate is characterized by fair to moderate sea states (wave heights and periods in the range 1–4 m and 6–13 s respectively), predominantly approaching from west to southwest. This wave climate results in a net long shore sediment transport directed to the east, which was estimated from 100,000 to 200,000 m<sup>3</sup>/yr around Faro-Olhao Inlet (Dias et al., 2009b).

### 3.4. Ecological Functions

Ria Formosa lagoon is of high ecological importance and is recognized within Portuguese legislation as a natural park since 1987 (Bebianno, 1995; Duarte et al., 2008), also internationally as a Ramsar wetland, a protected area under the Birds Directive (79/409/EEC) and a member of the Natura 2000 Network (Dias et al., 2009b; Brito et al., 2011). The Ria provides habitat for many species of birds migrating from North of Europe (Bebianno, 1995; Coelho et al., 2002). The Ria also plays an important ecological role as breeding and nursery ground for many species, owing to its sheltered conditions (Bebianno, 1995). Its high nutrient concentration and productivity give rise to an important diversity and abundance of flora and fauna. Moreover, the combination of hydrographic factors and the nature of the substrate (predominantly sand and silt) constitute ideal conditions for the development of benthic communities (Coelho et al., 2002).

### 3.5. Social and Economy Importance

The Ria Formosa lagoon is a valuable socio-economic resource for the region mainly due to tourism, fisheries, aquaculture (especially shellfish) and salt extraction (Coelho et al., 2002; Dias et al., 2009b; Brito et al., 2011). The lagoon is very productive because of high nutrient concentrations (Bebianno, 1995; Falcao and Vale, 2003) and isolation, as well as generally good tidal water exchange (Bebianno, 1995). This productivity has given rise to the economically important fishing and mariculture industries. One of the sources that contribute largely for the lagoon water nutrient enrichment (ammonium and phosphate) is bottom sediment (Serpa et al., 2007), which coming from the open sea rather than from urban discharge (Martin et al, 2003).

The Ria Formosa is a most significant area from the point of view of fisheries, particularly with respect to the culture of molluscan shellfish. This lagoon has a long tradition of bivalve harvesting, especially of *Ruditapes decussatus*. The annual harvest of this bivalve approached 8,000 tons in 1993. Eighty percent of the bivalves (e.g. cross carpet shell, *Ruditapes decussatus*) harvested in Portugal come from this area. Approximately 100 km<sup>2</sup> are used for extensive clam culture (e.g. cross carpet shell *Ruditapes decussatus*, banded carpet shell *Venerupis romboides*, the thick through shell *Spisola solida*, the common cockle *Cerastodema edule*, the oyster *Crassostrea angulata*, the mussel *Mytilus galloprovincialis*, and *Ostrea edulis*) (Bebianno, 1995). Around 20% of the total area of Ria Formosa is occupied by on-growing banks of *Ruditapes decussatus* that are cultured throughout the entire lagoon and are the most important commercial species in the area. By

1996, a total of 1,587 clam's plots were identified in Ria Formosa (Coelho et al., 2002).

However, in recent years there has been a decrease in production, to about 3,000 tons per year. The anthropogenic pollutant releases with the ineffective clam harvest practice in Ria Formosa resulted in a massive clam mortality, that has multiple effect to the decrease of economy sector in the region (Bebianno, 1995). The mean bivalve production is currently estimated at 0.5 kg/m<sup>2</sup> (Coelho et al., 2002).

### **3.6. Water Quality**

Water quality in the lagoon has deteriorated during the last few years, due mainly to uncontrolled economic development. Untreated domestic sewage (from a population of ~150,000 people), industrial discharges, agriculture drainage, and aquaculture effluents are the major direct pollution inputs into the lagoon (Coelho et al., 2002). The high number of boats present also has an important contribution to the poor water quality of Ria Formosa. Boat traffic is largely dominated by small leisure and fishing boats. However, large commercial and fishing vessels also called into the main harbours (Olhao and Faro) (Coelho et al., 2002). The measurement of organotin concentration in water, sediment, and clams in Ria Formosa lagoon showed the acute effect occurs in the most important fishing harbour in Olhao (Coelho et al., 2002), which can cause health problem effect for the people who consume it, and cause indirect impact for Ria Formosa lagoon.

## 4. Methods

### 4.1. Field Data

In this study, the data used are the data that was collected by MaréFormosa project in which consists of time series data of water level and velocity (longitudinal component) variations, in several locations in Ria Formosa, covering complete tidal cycle. These data were taken from 12 stations in the main channel of Ria Formosa (**Fig 4.1**) and were measured in normal meteorological condition which means it is not affected by the wind, storm, and rain. The identified stations were limited in the west and central part of Ria Formosa lagoon. Those are Cais centro nautico, Bar da gina, Poita Nave Pegos, Quatro Aguas, Sao luis inlet, Faro-Olhao inlet, Canal Cacoos, Culatra, Boia V3, Armona inlet, Marim, and Bela Romao. The Bela Romao station was considered as a reference control of Fuzeta inlet in the eastern part of Ria Formosa, due to its significant role in Ria Formosa lagoon. The coordinate location of each stations can be seen from **Table 4.1**.



**Fig 4.1.** Tides parameter locations which are currently being measured by MareFORMOSA project, in Ria Formosa (red pins).

The current and water column pressure/depth were taken by using ADP (Aquadopp Current Profiler) of NORTEK. The pressure range of ADP piezoresistive (pressure sensor) is about 0-100 m with the accuracy of 0.25%, while the velocity range is about 10 m/s horizontal and 5 m/s along beam with 1% accuracy of measured value  $\pm 0.5$  cm/s. ADP measures current at 0.5 m interval starting from 0.4 m above the head of ADP equipment. The height of the installed equipment is 0.8 m from bottom.

**Table 4.1.** Coordinate location of the stations

stations	x (UTM)	y (UTM)
Barra Faro-Olhão	23380.87	-299044
Armona inlet	29290.71	-295059
Barra S Luís	15564.26	-297957
Cais Centro Náutico	13102.33	-295835
Bar da Gina	12309.32	-295100
Esteiro Cações	22787.09	-296264
Boia V3	24307.06	-295167
Culatra	25659.83	-296369
Marim	28678.3	-293269
Bela Romão	31924.71	-292305
Quatro Águas	17077.1	-295254
Estaleiro Nave Pegos 46ENP	16709.33	-294315

Beside ADP, the pressure transducer level TROLL 300 and TROLL 700 were also used to measure the water level variation. The pressure transducer level TROLL 300 has the accuracy value of  $\pm 0.01\%$  FS with non vented range 30-300 psia, while pressure transducer level TROLL 700 has the accuracy value of  $\pm 0.005\%$  FS with non vented range of 30-500 psia and vented range of 5-500 psig.

Due to the limitation of ADP equipment, the measurements using ADP in each stations were conducted in different time. The ADP measurements were measured during short period of time. By using Pressure transducer equipment which installed in Faro Olhao inlet as a reference control point of the water level measurement in Ria Formosa lagoon, the long time series of water level variation for 2 years were measured.

The short period of time measurement using ADP in each stations were adjusted with the pressure transducer long time series of water level measurement in Faro Olhao inlet. Then from this time adjustment, the similar tidal height and tidal period measurement which measured in Faro Olhao inlet in those each short time series were chosen and the date occurrence of them were recorded (**Table 4.2**). Based on the recorded date, the ADP velocity and water level measurements for each stations were filtered. Hence, each stations has adjusted time series data of water level and longitudinal component of velocity variations. The tidal height and tidal period measurement for each stations can be seen in **Table 4.2**.

All data which are taken should be calibrated with the local atmospheric variation and hydrographic zero (Portuguese datum), which is negative for the value below the hydrographic zero and positive for the value above the hydrographic zero.

**Table 4.2.** The tidal height (H) and tidal period (T) of the tide in each stations (TP measurement)

No	code	station	Tidal Height (m)		Phase Period (hour)		Tidal Period (T) (hour)	Occurrence
			Flood	Ebb	Flood	Ebb		
1	1	Faro-Olhao inlet	-2.32	2.24	6.5	5.42	11.92	3/6/2011 4:15
2	5	Armona inlet	-2.34	2.32	6.42	5.83	12.25	11/9/2011 2:45
3	6	Culatra	-2.34	2.31	6.42	6.08	12.5	15/10/2011 4:45
4	7	Boia V3	-2.34	2.29	6.67	5.5	12.17	24/10/2011 1:10
5	8	Marim	-2.29	2.32	6.42	5.75	12.17	10/11/2011 14:10
6	9	Canal Cacoos	-2.32	2.27	6.58	5.58	12.17	12/12/2011 15:45
7	11	Bela Romao	-2.29	2.26	6.75	5.83	12.58	15/1/2012 6:30
8	17	Sao Luis inlet	-2.32	2.21	6.42	5.83	12.25	24/5/2012 16:30
9	19	Centro Nautica	-2.37	2.21	6.33	5.75	12.08	8/7/2012 6:35
10	20	Bar de Gina	-2.28	2.24	6.33	5.75	12.08	31/7/2012 1:55
11	22	Quatro Aguas	-2.24	2.21	6.5	5.67	12.17	28/11/2012 14:25
12	25	Poita Nave Pegos	-2.3	2.2	6.42	5.5	11.92	12/5/2013 3:45
<b>AVERAGE</b>			<b>-2.31</b>	<b>2.26</b>	<b>6.48</b>	<b>5.71</b>	<b>12.19</b>	
<b>STANDAR DEVIATION</b>			<b>0.03</b>	<b>0.05</b>	<b>0.13</b>	<b>0.18</b>	<b>0.20</b>	
<b>RANGE OF STD</b>			<b>0.07</b>	<b>0.09</b>	<b>0.26</b>	<b>0.37</b>	<b>0.39</b>	

## 4.2. Data Treatment

All the calculations are conducted during mid tide (in between Neap and Spring tide).

### 4.2.1. Raw Time Series

Time series data of water level and longitudinal component of velocity variations for complete tidal cycle were used. For each time series, the spatial water level gradient (*barotropic pressure gradient*) is determined by calculating the difference between water level of the two/three close adjacent stations for every stations in the main channel of Ria Formosa, and so does for the longitudinal/spatial velocity gradient.

### 4.2.2. Harmonic Analysis

Harmonic Analysis methods was used to obtain the best fit between the raw data and the harmonic constituent combination/superposition curve for all stations. The harmonic constituent that are taken into account are  $M_2$  and  $M_4$ , since they are the most dominant tidal constituent in Ria Formosa (Dias and Sousa, 2009a), besides  $S_2$ . The tidal constituent of  $S_2$  was not taken into account in this study because the tidal period of data used in this study is less than 24 hours. The harmonic analysis of time series computes a least squares solution fitting the input time series with currents and water level variation of input periods according

Godin, 1972 in Foreman & Henry (1989). The harmonic analysis script was written by Brian O. Blanton (Skidaway Institute of Oceanography USA - Fall 1996) and modified by Duarte N. R. Duarte (University of Algarve - Spring 2008) to allow data gaps.

#### 4.2.2.1. Tidal distortion / Tidal asymmetry

The effect of frictional distortion of the tidal curve is also considered in terms of production of the  $M_4$ ,  $M_6$  over tides from the  $M_2$  tide. The major part of the asymmetry of the tide curve can be represented by superposition of  $M_2$  and  $M_4$ , both in terms of height and velocity.

$$A = a_{M_2} \cos(\omega t - \theta_{M_2}) + a_{M_4} \cos(2\omega t - \theta_{M_4})$$

$$u = u_{M_2} \cos(\omega t - \varphi_{M_2}) + u_{M_4} \cos(2\omega t - \varphi_{M_4})$$

Where  $a$  and  $\theta$  are the amplitude and phase of tidal height, and  $u$  and  $\varphi$  are the amplitude and phase of the tidal velocity. The elevation phase of  $M_4$  relative to  $M_2$  is  $2M_2 - M_4 = 2\theta_{M_2} - \theta_{M_4}$ . The elevation amplitude ratio is  $M_4 / M_2 = a_{M_4} / a_{M_2}$ . Speer and Aubrey (1985) in Dyer (1997) have considered the implications of these ratios and show that for an elevation phase ( $2M_2 - M_4$ ) between  $0$  and  $180^\circ$  the system will be flood dominant, and for a phase of  $180^\circ - 360^\circ$  it will be ebb dominant. In either case the larger the  $M_4 / M_2$  ratio, the more distorted and the more strongly flood or ebb dominated the system becomes. Thus the dominance can be predicted from tidal analysis (Dyer, 1997).

The flood/ebb dominance is also determined from tidal current velocities. If the ebb velocity is larger than flood velocity, then it is ebb dominance (Dias et al., 2009b). The result that obtained from the tidal current analysis then is compared with the result that obtained from the tidal height analysis.

#### 4.2.2.2. Energy Flux and Dissipation

To calculate the energy flux along an estuarine channel, the equation can be written as follow (Pugh, 1987) :

$$P = \frac{1}{2} \rho g h \overline{\eta U} \quad [\text{W m}^{-1}]$$

$h$  is the undisturbed water depth along the channel,  $(\eta)$  is the amplitude of the water level, and  $(U)$  is the amplitude of the axial tidal current,  $\rho$  is water density, and  $g$  is gravity.

Dissipation energy along the channel can be reached by dividing energy flux ( $P$ ) by the distance  $L$  separating the two stations, or can be written as follow:

$$D = [P_{n+1} - P_n] / L \quad [\text{W m}^{-2}]$$

Where n is a station counter. By dividing the equation of dissipation energy (D) above with h and  $\rho$  yields the dissipation in  $\text{W kg}^{-1}$ .

An alternate estimate of tidal energy dissipation at each station can be done using the following equation (Taylor, 1919) :

$$D = \langle \rho C_d [U^2]^{\frac{3}{2}} \rangle$$

Where the bracket pair  $\langle \rangle$  represent the average over the M2 cycle,  $C_d$  is a drag coefficient and U is the tidal velocity.

#### 4.2.2.3. Error Calculation

Error estimation can be calculated using elevation and velocity root mean square errors as follows:

$$RMS_e = \sqrt{\frac{1}{nt} \sum_{i=1}^{nt} (\eta_i - \tilde{\eta}_i)^2}$$

And

$$RMS_v = \sqrt{\frac{1}{nt} \sum_{i=1}^{nt} \{(u_i - \tilde{u}_i)^2 + (v_i - \tilde{v}_i)^2\}}$$

Where  $\eta$  is the amplitude of elevation, u and v are the amplitude of depth-averaged velocities, the tilde represents numerical results, nt is the number of time step (Fortunato et al., 1997).

#### 4.2.3. Hysteresis Diagram Analysis

To calculate the phase lags and slack water between water level ( $\eta$ ) and velocity (v), a graphic time series of vertical component (water level) and graphic time series of horizontal component (longitudinal component of velocity) for each stations are established. These two graphics are combined in order to create hysteresis diagram analysis for all tidal cycles. Hysteresis diagram is created for standing tidal wave as an open ellipse and progressive wave as a line and also for the combination of the two types (Dyer, 1997). The progressive wave contribution can be estimated by measuring the time difference between high and low water and slack water. This can then be expressed as a proportion of the tidal period in degrees or in hour (Dyer, 1997).

#### 4.2.4. GIS Application

In this study, Arc GIS platform was used to determine the cross section profile for each stations which will be used to calculate the hydraulic geometrical parameters for each stations. Besides that, Arc GIS was used also to perform the spatial distribution of water level gradient, velocity gradient, volume, and residence time, and to compare the volume that goes in and out through the inlet (inlet tidal cycle volume) with the annual critical geometry volume of the lagoon which based on the water level variation during high water and low water.

##### 4.2.4.1. Hydraulic Geometrical Parameters Calculation

Hydraulic geometrical parameters that were calculated are cross-section area ( $A_{\eta,t}$ ), wet perimeter ( $P_{\eta,t}$ ), surface width ( $LS_{\eta,t}$ ), mean depth ( $h_{\eta,t}$ ) and hydraulic radius ( $R_{h\eta,t}$ ). The calculations are conducted for each stations and for each time (hourly).

To calculate the mean depth ( $h$ ) and hydraulic radius ( $R_h$ ). the equations below can be used :

$$\bar{h}_{\eta,t} = \frac{A_{\eta,t}}{LS_{\eta,t}} \quad \text{and} \quad R_{h\eta,t} = \frac{A_{\eta,t}}{P_{\eta,t}}$$

##### 4.2.4.2. Spatial Distribution Performance

###### 4.2.4.2.1. The mean velocity ( $\bar{u}_{n,t}$ ) in the water column

To calculate the mean velocity in the water column ( $\bar{u}_{n,t}$ ) for each stations and time, the integration velocity method in the water column (per linear meter) can be used. The equation can be defined as follow :

$$\bar{u}_{n,t} = \frac{1}{h} \int_0^h u_z \cdot dz$$

Where  $u_z$  is the velocity at  $z$  meter,  $z$  is the distance from the bottom, and  $h$  is the depth of the flow that are obtained from ADP (Acoustic Doppler Current Profiler).

Since the ADP measured the  $u_z$  value several meters above the beds, the interpolation technique to calculate the  $u_z$  value from bed till those several meters were addressed. To calculate those  $u_z$  value, the bed shear velocity ( $u_*$ ) and the roughness coefficient ( $z_0$ ) were determined using graphical method (open university, 2000). The equation of this graphical method can be defined as follow:

$$u_* = \text{slope\_of\_the\_graph} / 5.756$$

$$z_o = 10^{-\frac{(\text{interception\_on\_y\_axis})}{\text{slope\_of\_the\_graph}}}$$

Then  $u_z$  value on the water column can be calculated using Von Karman-Prandtl universal equation as follow:

$$u_{(z)} = \frac{u_*}{\kappa} \ln\left(\frac{z}{z_o}\right)$$

where  $\kappa$  is von karman coefficient ( $\kappa=0.41$ ).

#### 4.2.4.2.2. The mean velocity in the channel cross section ( $\langle \bar{u}_{n,t} \rangle$ )

When only one velocity profile was obtained at the middle of channel cross-section, Manning model can be used to calculate the velocities for the entire cross section ( $\langle \bar{u}_{n,t} \rangle$ ) for each stations and time, considering constant on the cross-section the roughness Manning coefficient  $C_m$  and null the transverse energy gradient ( $\frac{\partial E}{\partial y}$ ). The manning model equation can be expressed as follows:

$$\langle \bar{u}_{n,t} \rangle = \frac{1}{C_m} \cdot R_h^{\frac{2}{3}} \cdot E^{\frac{1}{2}}$$

$$\frac{\langle \bar{u}_{n,t} \rangle}{\bar{u}_{n,t}} = \frac{R_h^{\frac{2}{3}}}{\bar{h}^{\frac{2}{3}}}$$

When  $E$  represents the energy gradient of the flow;  $\langle \bar{u}_{n,t} \rangle$  is the mean velocity on the channel cross section;  $\bar{u}_{n,t}$  is the mean velocity obtained on the middle point of the cross section;  $R_h$  is the hydraulic radius of the cross section, and  $h$  is the depth of the channel (or the mean depth  $\bar{h}$ ). So to calculate the mean velocity in the channel cross section, it is assumed that the manning coefficient ( $C_m$ ) in the cross section is constant, and also the energy gradient in the cross section.

#### 4.2.4.2.3. The mean velocity in the channel cross section during flood and ebb ( $\langle \bar{u}_n \rangle_{\text{flood}}$ and $\langle \bar{u}_n \rangle_{\text{ebb}}$ )

During flood and ebb period, the mean velocity in the channel cross section for each stations were determined by summing the mean velocity in the channel cross section during flood period for mean flood velocity and during ebb period for mean ebb velocity. The equations can be written as follows :

- Mean Flood Velocity :  $\langle \bar{u}_n \rangle_{\text{flood}} = \frac{\int_{t=0}^{t=t_{\text{flood}}} \langle \bar{u}_n \rangle_t \cdot dt}{T_{\text{flood}}}$

- Mean Ebb Velocity :  $\langle \bar{u}_n \rangle_{ebb} = \frac{\int_{t=0}^{t=t_{ebb}} \langle \bar{u}_n \rangle_t \cdot dt}{T_{ebb}}$

#### 4.2.4.2.4. Net Velocity

After calculated all calculation above, net velocity, flood and ebb mean velocity, and residual velocity can be calculated.

- Net velocity =  $\langle \bar{u}_n \rangle_{flood} - \langle \bar{u}_n \rangle_{ebb}$

#### 4.2.4.2.5. Water Discharge ( $Q_n$ ) and water volume ( $V_n$ )

The water discharge/flow of water is expressed in units of volume per time. In flow measurement, flow is often estimated by determining the velocity at which water flows through a given cross-sectional area, known as general continuity equation, which defines as follows:

$$Q_{n,t} = \langle \bar{u}_{n,t} \rangle \times A_{\eta,t}$$

Then, the flooding and ebbing time must be determined to calculate the discharge and volume during the flood and ebb phase, using equation below:

$$Q_{n,t_{flood}} = \int_{t=0}^{t=t_{flood}} \left( \langle \bar{u}_{n,t} \rangle \times A_{\eta,t} \right) \cdot dt \quad \text{and} \quad Q_{n,t_{ebb}} = \int_{t=0}^{t=t_{ebb}} \left( \langle \bar{u}_{n,t} \rangle \times A_{\eta,t} \right) \cdot dt$$

Water volume for each stations during flood and ebb can be calculated using the equation as follows:

$$V_f = Q_f \times t_{flood} \quad \text{and} \quad V_e = Q_e \times t_{ebb}$$

#### 4.2.4.2.6. Residence Time (RT) calculation

The residence time (RT) is the average duration for a water molecule to pass through a subsystem of the hydrologic cycle (Chow et al., 1988) or the time required for a particle to travel from a location to the boundary of the region (Wang et al., 2004). To calculate the residence time for each stations (station 1, station 2, station 3, etc), the equation below (Sanford et al., 1992 inside Wang et al., 2004) can be used :

$$residence\_time(RT) = \frac{(V + P/2)T}{(1-b)P + RT}$$

Where V is low tide volume of the whole or a segment of the estuary, P is tidal prism, T is tidal period, b is return flow factor, and R is river discharge.

Tidal prism is equal to volume of ocean water coming into an estuary on the flood tide + volume of river discharge mixing with that ocean water. This simple equation below can be used :

$$Tidal\_prism(P) = V_{in\_flood} + V_{in\_from\_river}$$

Return flow can be define as the ratio of the difference between the outflowing ebb velocity and the incoming flood velocity (Moore et al., 2006). To calculate the return flow factor (b), the equation below can be used :

$$b = \frac{v_{M2} - U}{v_{M2} + U}$$

Where  $v_{M2}$  is the vertically averaged amplitude of the M2 tidal harmonic over the period for which the slope was determined and U is the vertically averaged axial velocity (tides removed), which can be obtained using equation as follows (Moore et al., 2006):

$$C_d U^2 = -gh \frac{\partial \eta}{\partial x}$$

Where  $C_d$  is drag coefficient, g is the acceleration gravity, h is the mean depth of the cross section at the mouth of estuary, and  $d\eta/dx$  is the average water level slope along the axis.

To obtain drag coefficient  $C_d$ , the equation below (Soulsby, 1997) can be used :

$$\tau_o = \rho \cdot C_d \cdot \bar{u}^2$$

$$\tau_o = \rho \cdot (u_*)^2$$

Or other  $C_d$  equation below could also be used (Bricker, J.D. Et al, 2005) :

$$C_d = \left( \frac{\kappa}{\ln\left(\frac{z}{z_0}\right)} \right)^2 \rightarrow C_{100} = \left( \frac{\kappa}{\ln\left(\frac{100}{z_0}\right)} \right)^2 .$$

Where  $z_0$  is the zero velocity level on the depth profile ( $u=0$  m/s at  $z=z_0$ ) or roughness coefficient,  $\kappa$  is von karman-prandtl coefficient,  $\rho$  is water density,  $\tau_o$  is bed shear stress,  $\bar{u}$  is the depth averaged current velocity, and  $u_*$  is shear velocity.

#### 4.2.4.2.7. GIS performance

After calculating the residence time in each stations, the spatial residence time variation can be shown using interpolation method of IDW (Inverse Distance Weight) in GIS software using radius setting of 4 points and distance of 4000 m. To determine and evaluate the suitable area for shellfish pond, the average current velocity, maximum flood current, and

residence time are displayed using Geographical Information System (GIS) software application and overlaid each other, so then the best combination of the physical and hydrodynamic requirement for shellfish to grow can be obtained.

To find the suitable place for clam culture, it is needed to know the residence time and the shear stress of the water inside the lagoon. In areas where the water exchanges on almost every tide, the environmental conditions allow the development of a diverse and productive benthic population (Gamito, 1997). Variations in habitat parameters greatly affect the physiological state and the growth of bivalves. To achieve success in shellfish marine culture, environmental parameters favorable for the cultured species and the characteristics of potential sites for growing up must be determined. The survival and growth of species are influenced by substrate (muddy sand or firm mud) and is correlated with current speed. Growth rates could be increased by the breakdown of vertical gradients through turbulent mixing by waves and currents (Congleton et al., 1999).

A specification for shellfish growing sites would include bottom type, intertidal elevation, tidally integrated current velocity and a maximum current velocity. The site requirements for shellfish to grow up could include the following specifications (Congleton et al., 1999):

- A bottom type of sand, mudflat, and silty mud.
- An elevation between 1.22 and 1.83 m below mean sea level (with average low water of 2 m below mean sea level) would be submerged most of the time with access at low tide.
- An average current velocity between 9 and 10 cm/s.
- A maximum flood tide current velocity less than 20 cm/s.

For benthic invertebrates that reproduce via planktonic larvae, variation in the delivery of larvae to benthic habitats is a fundamental determinant of recruitment rates and population structure. The veliger larva is the primary dispersal stage for most estuarine bivalve and gastropod molluscs. Mollusc veligers are relatively poor swimmers, with net horizontal swimming velocities in the order of  $10^{-4} \text{ ms}^{-1}$ . They are incapable of significant directed motion in the horizontal plane since horizontal current velocities in most environments greatly exceed this value. Veligers are free to maneuver in the horizontal plane only during low flow periods or in the benthic boundary layer, where friction reduces the mean flow velocity. In contrast, mollusc larvae are more proficient at vertical swimming, and it is hypothesized that cued vertical migration may allow for retention within estuarine

systems. Vertical current velocities are generally low compared with vertical swimming velocities, and mollusc larvae are certainly capable of traversing significant vertical distances during a tidal. However, they are always transported horizontally near the velocity of the ambient flow (Roegner, 2000).

#### **4.2.4.3. Comparison study of tidal inlet volume and annual critical geometry volume of the lagoon**

The comparison study between the tidal inlet volume calculation (V) which had been calculated in the previous sub chapter 4.2.4.2.5 and the tidal annual critical geometry water volume of the lagoon is conducted to ensure a good agreement between them. The latter estimation can be performed by overlaying the two condition of Ria Formosa during low and high water in GIS software application.

To calculate the tidal annual critical geometry water volume of the lagoon, the critical level of water surface (low water and high water level variation/deformation) for each stations were over layed above the bathymetry surface using GIS software application to display the spatial distribution of the critical level water surface inside the Ria Formosa lagoon. Overlaying this critical level of water surface with the lagoon bathymetry can determine the water geometry volume. Then, the difference and comparison between the tidal inlet volume calculation (V) and the annual critical geometry water volume of the lagoon can be carried out. The bathymetry data was referred to the thesis book of Miguel (2013).

## 5. Result and Discussions

### ❖ Assumptions :

1. to calculate and interpolate the  $z_0$  (roughness coefficient) and  $u^*$  (shear stress), the 3 points of bottom velocity data are used because the regression line and equation of these 3 points are better than 4 or 5 points approaches. Besides that, there is no big difference of the average velocity among them.
2. The water density assumed to be constant (1024 kg/m<sup>3</sup>).
3. To calculate the mean velocity in the channel cross section, it is assumed that the manning coefficient ( $C_m$ ) in the cross section is constant, and also the energy gradient in the cross section.

### 5.1. Harmonic Analysis Fit and Proper test of the data

As explained in the methods above, each station has time series data of water level and longitudinal component of velocity variations. These data must be treated to get the best fit and proper test in order to do further tidal analysis such as creating hysteresis diagram analysis, creating smooth time series graph of water level and longitudinal component of velocity.

#### *Harmonic Analysis Fit and Proper test and Error Calculation*

The fit and proper test of the raw field data was conducted using M2 and M4 component of the tide, since those two components are the main components in tidal harmonic constituents in shallow water (Dias and Sousa, 2009a). The fitting result of tidal velocity and tidal height gives amplitude and phase of the tidal harmonic constituent M2 and M4 which can be seen in **Table 5.1** and **Table 5.1**, consecutively. From **Table 5.1**, it could be observed that Armona inlet has the highest M2 tidal velocity amplitude followed by Faro Olhao inlet. While the highest M4 tidal velocity amplitude was occurred in Sao Luis inlet. **Table 5.2** gives information that Armona inlet has the highest M2 tidal elevation amplitude, but not for M4, so it means that Armona inlet is not a very shallow environment and does not have strong asymmetrical behaviour of the tide, because tidal constituent of M4 has strong connection with the tidal asymmetry and shallow environment.

**Table 5.1.** The tidal velocity amplitude and phase of tidal harmonic constituents M2 and M4 for each stations

no	station	Tidal current / velocity					
		M2			M4		
		Periode (hour)	amplitude (m/s)	phase (°)	Periode (hour)	amplitude (m/s)	phase (°)
1	bela romao	12.58	0.09	136.87	6.29	0.06	107.87
2	cacoos	12.17	0.20	102.77	6.09	0.10	144.00
3	boia V3	12.17	0.47	281.26	6.09	0.22	53.51
4	quatro aguas	12.17	0.19	277.43	6.09	0.09	83.11
5	culatra	12.50	0.14	166.98	6.25	0.10	126.73
6	centro nautico	12.08	0.45	82.29	6.04	0.06	88.36
7	bar da gina	12.08	0.46	83.61	6.04	0.05	158.58
8	sao luis inlet	12.25	0.80	105.30	6.13	0.43	106.95
9	Faro-Olhao inlet	11.92	0.83	99.61	5.96	0.07	93.93
10	Armona inlet	12.25	0.86	90.66	6.13	0.28	118.63
11	nave pegos	11.92	0.10	109.41	5.96	0.02	287.25
12	marim	12.17	0.40	84.81	6.09	0.12	186.04
<b>average</b>		<b>12.19</b>	<b>0.42</b>		<b>6.09</b>	<b>0.13</b>	

**Table 5.2.** The tidal height / elevation / water level amplitude and phase of tidal harmonic constituents M2 and M4 for each stations

no	station	tidal height / elevation / water level					
		M2			M4		
		Periode (hour)	amplitude (m)	phase (°)	Periode (hour)	amplitude (m)	phase (°)
1	bela romao	12.58	1.00	7.07	6.29	0.05	123.40
2	cacoos	12.17	1.14	17.79	6.09	0.04	166.18
3	boia V3	12.17	1.22	352.02	6.09	0.07	169.32
4	quatro aguas	12.17	1.13	359.03	6.09	0.10	131.28
5	culatra	12.50	1.09	1.76	6.25	0.05	140.99
6	centro nautico	12.08	1.08	348.12	6.04	0.06	145.73
7	bar da gina	12.08	1.17	350.24	6.04	0.05	149.98
8	Sao Luis inlet	12.25	0.94	2.00	6.13	0.04	81.98
9	Faro-Olhao inlet	11.92	1.17	350.98	5.96	0.06	115.41
10	Armona inlet	12.25	1.22	352.11	6.13	0.04	156.17
11	nave pegos	11.92	1.13	0.70	5.96	0.11	130.19
12	marim	12.17	1.16	355.56	6.09	0.05	167.47
<b>average</b>		<b>12.19</b>	<b>1.12</b>		<b>6.09</b>	<b>0.06</b>	

Previously, the research related to tidal harmonic constituent in Ria Formosa had also been conducted by Baptista (1987), it could be seen in **Table 5.3**. Compared to the current

data, it could be observed that the tidal height amplitude does not change a lot from time to time, while the phases could not be compared because the phase could change a lot due to the change of hydrodynamic pattern and geometry of Ria Formosa.

**Table 5.3.** The tidal height / water level amplitude and phase of tidal harmonic constituents M2 and M4 (Baptista, 1987)

station	height					
	M2			M4		
	periode (hour)	amplitude (m)	phase (hour)	periode (hour)	amplitude (m)	phase (hour)
Armona inlet	12.421	0.985	2.026	6.21	0.01	1.276
barra de faro olhao	12.421	0.983	2.25	6.21	0.028	3.999
cais comerciale	12.421	0.985	2.504	6.21	0.065	4.386
barra do Ancao	12.421	0.856	2.079	6.21	0.024	4.466
cais da lota de olhao	12.421	0.983	2.396	6.21	0.019	5.906

Besides the amplitude and phase calculation result, the fit and proper test of harmonic analysis also give the average root mean square calculation which are 7.5 % of velocity root mean square and 6.75% of elevation root mean square, respectively (**Table 5.4**).

**Table 5.4.** Root Mean Square calculation

Stations	Root Mean Square	
	velocity root mean square	water level root mean square
Faro-Olhao inlet	0.052	0.054
Armona inlet	0.077	0.058
Culatra	0.039	0.052
Boia V3	0.178	0.103
Marim	0.113	0.039
Canal Cacoos	0.027	0.062
Bela Romao	0.070	0.082
Sao Luis inlet	0.132	0.072
Centro Nautica	0.058	0.066
Bar de Gina	0.054	0.129
Quatro Aguas	0.053	0.046
Poita Nave Pegos	0.047	0.049
<b>average</b>	0.075	0.068
<b>in percentage (%)</b>	7.495	6.756

### Tidal Distortion and Tidal Asymmetry

The tidal distortion and tidal asymmetry analysis were also carried out to define the flood/ebb dominance and the strength of the domination. From **Table 5.5**, it could be seen the tidal amplitude ratio for tidal elevation and velocity, and also the tidal current strength comparison between flood current and ebb current. From the tidal elevation amplitude ratio, Nave Pegos and Quatro Aguas stations are the most distorted stations, because the larger the  $aM_4/aM_2$  ratio, the more distorted and the stronger flood or ebb dominated the system becomes. Meanwhile from the tidal current amplitude ratio, Culatra and Bela Romao have the highest ratio which means they also have large distortion factor.

**Table 5.5.** Tidal Distortion and Tidal Asymmetry Analysis (amplitude ratio and flood/ebb strength comparison)

no	station	Amplitude ratio ( $aM_4/aM_2$ )		tidal current velocity (m/s)		
		elevation or height	Velocity/current	Flood	Ebb	description
1	bela romao	0.0479	0.69	-0.12	0.06	flood dominant
2	cacoés	0.0388	0.50	-0.13	0.15	ebb dominant
3	boia V3	0.0547	0.46	-0.50	0.30	flood dominant
4	quatro aguas	0.0924	0.49	-0.15	0.10	flood dominant
5	culatra	0.0422	0.72	-0.08	0.16	ebb dominant
6	centro nautica	0.0587	0.13	-0.28	0.33	ebb dominant
7	bar da gina	0.0388	0.10	-0.28	0.32	ebb dominant
8	Sao Luis inlet	0.0471	0.54	-0.63	0.46	flood dominant
9	Faro-Olhao inlet	0.0531	0.09	-0.57	0.47	flood dominant
10	Armona inlet	0.0348	0.32	-0.50	0.63	ebb dominant
11	nave pegos	0.0957	0.20	-0.10	0.04	flood dominant
12	marim	0.0430	0.30	-0.24	0.30	ebb dominant
<b>average</b>		0.0539	0.3782	-0.2967	0.2768	

In some study, the flood/ebb dominance were determined using the tidal elevation phase of tidal constituent M2 and M4, which is  $2M_2 - M_4 = 2\theta_{M_2} - \theta_{M_4}$ . While, for this particular study, the phase of tidal constituent M2 and M4 will not be used to determine the system dominance since the time measurements for each stations in this study are different, so it might not seem very reliable to refer the system dominance using tidal constituent phase. Therefore, to show the system dominance, tidal current velocity are used to determine whether the system are flood dominant or ebb dominant (**Table 5.5**). If the ebb velocity is larger than flood velocity, then it is ebb dominance (Dias et al., 2009b), and so otherwise.

According to tidal current velocity analysis, some of the stations belong to flood dominant system and some others belong to ebb dominant. The flood dominant stations based on tidal current velocity result are Bela Romao, Boia V3, Quatro Aguas, Sao Luis inlet, Faro-Olhao inlet, and Nave Pegos. While the ebb dominant stations are Cacoes, Culatra, Centro Nautica, Bar da Gina, Armona inlet, and Marim.

However, this result is different with the finding of Dias and Sousa (2009a) and Salles et al (2005). Their result showed that Sao Luis inlet and Faro-Olhao inlet are belong to ebb dominance system area in Ria Formosa, while Armona inlet is flood dominance in Dias and Sousa (2009a) and ebb dominance in Salles et al (2005). This difference is due to the fact that the determinant factor for flow dominance only considered the magnitude of tidal current velocity, while sometimes the duration of flood and ebb could also be a determinant factor for flow dominance. Longer duration of the flood (ebb) may be associated with flood (ebb) dominance, due to the existence of strong residual circulation between inlets. Where in fact, the larger flood (ebb) discharge in a shorter period does not necessarily lead to stronger flood (ebb) currents (Dias and Sousa, 2009a).

Due to this reason, the ebb and flood dominant were also determined using flood and ebb duration period (**Table 5.6**). Based on tidal phase period, it could be seen that Faro Olhao inlet and Armona inlet are belong to flood dominant system area, whereas Sao Luis inlet is belong to ebb dominant system area. The result gained from tidal phase (flood / ebb) duration period (**Table 5.6**) is totally different with the result from tidal current analysis (**Table 5.5**) except for Faro Olhao inlet, Culatra, and Nave Pegos. As stated by Dias and Sousa (2009a), both of them (the magnitude of tidal current velocity and flood/ebb duration period) need to be taken into consideration in deciding whether the system is ebb or flood dominant. In this case, Faro Olhao inlet and Nave Pegos can be considered as flood dominant system, while Culatra can be considered as ebb dominant system.

**Table 5.6.** Flood / Ebb Dominance based on Tidal Phase Period

No	station	T flood	Tebb	description
1	bela romao	4.5525	7.8682	ebb dominant
2	cacoos	7.8277	4.5929	flood dominant
3	boia V3	4.5364	7.8843	ebb dominant
4	quatro aguas	5.5949	6.8246	ebb dominant
5	culatra	3.1504	9.2702	ebb dominant
6	centro nautica	6.3952	6.0254	flood dominant
7	bar da gina	6.5123	5.9083	flood dominant
8	Sao Luis inlet	5.0932	7.3274	ebb dominant
9	Faro-Olhao inlet	6.3688	6.0518	flood dominant
10	Armona inlet	6.9414	5.4792	flood dominant
11	nave pegos	8.399	4.0217	flood dominant
12	marim	7.4893	4.9312	flood dominant

*Energy Flux and Energy Dissipation*

Faro Olhao inlet has the highest tidal energy flux, which is 77,364.5 W/m (Table 5.7). Compare to the flux energy in other stations, flux energy which occurred in the inlets (Faro Olhao inlet, Armona inlet, and Sao Luis inlet) are higher than the energy flux of other stations inside the main channel. It indicates the energy in the main channel decrease with the distance from the ocean (inlets).

**Table 5.7.** Tidal energy flux and dissipation for each stations due to M2 and M4 tidal constituent

No	stations	Drag Coefficient (Cd)	Energy Flux (Pflux, W/m)	Dissipation energy of M2 (W/m <sup>2</sup> )	Dissipation energy of M2 and M4 (W/m <sup>2</sup> )
1	Faro-Olhao inlet	0.0034	77364.5	2.021	2.590
2	Armona inlet	0.0172	45867.4	11.345	26.352
3	Culatra	0.0068	9608.7	0.018	0.093
4	Boia V3	0.0152	19037.1	1.645	5.100
5	Marim	2.3297	16439.0	155.335	342.188
6	Canal Cacoos	0.0155	9088.0	0.122	0.410
7	Bela Romao	0.1244	3052.8	0.083	0.403
8	Sao Luis inlet	0.0020	28166.3	1.049	3.862
9	Centro Nautica	0.0013	16142.6	0.120	0.172
10	Bar de Gina	0.0179	13948.9	1.773	2.355
11	Quatro Aguas	0.0065	10163.6	0.043	0.142
12	Poita Nave Pegos	0.0038	3373.5	0.004	0.007

Dissipation energy of DM2 and DM2M4 were also calculated for each stations (Table 5.7). The addition of the M4 overtide barely changes energy dissipation using M2 alone and

the change showed the increasing magnitude of M2 alone. From **Table 5.7**, it could be seen that the dissipation energy in the inlet is higher than the dissipation energy inside the main channel of Ria Formosa, except for Marim, Bar de Gina, and Boia V3. This condition happened due to the fact that the energy flux already decrease with the distance from the ocean and the stronger tidal current velocity of the tide occurred in the inlet and decrease with the distance from the ocean, especially in Ria Formosa, where large number of the area in the main channel were covered by salt marshes. Besides calculating dissipation energy for each stations, tidal energy dissipation along the channel were also calculated (**Table 5.8**). Since Ria Formosa has several inlets, so to observe the importance of each inlets, Ria Formosa need to be divided into three small regions which are west region (Sao Luis inlet, Centro Nautico, and Bar de Gina), middle region (Faro Olhao inlet, Quatro Aguas, Nave Pegos, Cacoos, Boia V3, and Culatra), and east region (Armona inlet, Culatra, Boia V3, Marim, and Bela Romao) (**Fig 5.1**).

**Table 5.8.** Tidal energy dissipation along the channel stations and the reference distance among the adjacent station in Ria Formosa

	station	Distance (m)	dissipation energy along the stations (W/m <sup>2</sup> )
west region	Centro Nautico - Sao luis inlet	3251	3.70
	Bar de Gina - Sao luis inlet	4331	3.28
middle region	Quatro Aguas - Faro Olhao inlet	7356	9.14
	Nave Pegos - Faro Olhao inlet	8364	8.85
	Cacoos - Faro Olhao inlet	2845	24.00
	Boia V3 - Faro Olhao inlet	3987	14.63
	Culatra - Faro Olhao inlet	3515	19.28
east region	Culatra - Armona inlet	3860	9.39
	Boia V3 - Armona inlet	5000	5.37
	Marim - Armona inlet	1900	15.49
	Bela Romao - Armona inlet	3820	19.45
Among other adjacent stations	bar de gina-centro nautico	1090	2.01
	centro nautico-quatro aguas	4020	1.49
	nave pegos-quatro aguas	1010	6.72
	boiav3-culatra	1810	5.21
	marim-boiaV3	4800	0.54
	bela romao-marim	3400	3.94
	Sao Luis inlet - Faro-Olhao inlet	8000	6.15
	cacoos-boiaV3	1890	5.26
	cacoos-quatro aguas	5800	0.19

From **Table 5.8**, it could be seen that the highest dissipation energy was occurred between Cacoés and Faro Olhao inlet, which is 24 W/m<sup>2</sup>. It indicates the biggest difference in energy flux between Cacoés and Faro Olhao inlet and the shortest distance between these two. The lower energy flux in Cacoés station indicates the shallower area in that station and apparently there are a huge mudflat area near and around this station.

## 5.2. Longitudinal and Temporal gradients of water level and velocity in the main channel

In this particular study, the explanation of the longitudinal and temporal gradients of water level and velocity are divided into three division regions which consist of west region, middle region, and east region (**Fig 5.1**).



**Fig 5.1.** Region division in Ria Formosa (West region : Sao Luis inlet, Centro Nautica, Bar de Gina ; Middle region : Faro Olhao inlet, Quatro Aguas, Nave Pegos, Canal Cacoés, Culatra, Boia V3; East region : Armona inlet, Bela Romao, Marim, Boia V3, Culatra).

### 5.2.1. Longitudinal gradients of water level and velocity in the main channel

Longitudinal gradients of water level and velocity will give the information about the water circulation pattern in the main channel of Ria Formosa. To define the longitudinal gradient of water level and velocity, it is needed to know the distance among the adjacent stations in Ria Formosa (**Table 5.8**).

In this case, the water circulation pattern inside Ria Formosa will be presented in five particular of time in which Faro Olhao inlet was acted as a reference point. Those are during high water in Faro Olhao inlet (0 h), during ebbing period in Faro Olhao inlet (3 h), during low water in Faro Olhao inlet (6 h), during flooding period in Faro Olhao inlet (9 h), and back

to high water (12 h). **Table 5.9** and **Table 5.10** give the information about the water level and velocity gradient inside the main channel of Ria Formosa in those particular time.

**Table 5.9.** Water level gradient among adjacent stations at 0 hour, 3 hours, 6 hours, 9 hours and 12 hours.

stations	water level gradient ( $d\eta/dx$ )				
	at t1 (0 h)	at t4 (3 h)	at t7 (6 h)	at t10 (9 h)	at t13 (12 h)
bar de gina-centro nautico	0.0000984	0.0000138	-0.0000690	-0.0000512	0.0000956
centro nautico-Sao Luis inlet	0.0000203	-0.0000586	-0.0000635	0.0000877	0.0000386
centro nautico-quatro aguas	-0.0000135	-0.0000567	0.0000183	0.0000456	0.0000016
nave pegos-quatro aguas	0.0000019	0.0000345	-0.0000014	-0.0000305	-0.0000068
Faro-Olhao inlet-quatro aguas	0.0000098	-0.0000282	-0.0000001	0.0000151	0.0000151
Faro-Olhao inlet-cacoos	0.0000303	-0.0001898	-0.0000421	0.0001806	0.0000622
Faro-Olhao inlet-culatra	0.0000227	-0.0000623	-0.0000257	0.0000578	0.0000318
boiav3-culatra	0.0000506	-0.0000930	-0.0000930	0.0001131	0.0000781
culatra-Armona inlet	-0.0000304	0.0000494	0.0000367	-0.0000458	-0.0000419
marim-Armona inlet	-0.0000317	0.0000444	0.0000262	-0.0000323	-0.0000379
marim-boiav3	-0.0000070	0.0000125	0.0000157	-0.0000182	-0.0000104
bela romao-marim	-0.0000425	0.0000544	0.0000602	-0.0000577	-0.0000588
Faro-Olhao inlet-boiav3	-0.0000030	-0.0000127	0.0000195	-0.0000003	-0.0000073
Sao Luis inlet - Faro-Olhao inlet	-0.0000240	0.0000213	0.0000352	-0.0000267	-0.0000288
cacoos-boiav3	-0.0000520	0.0002592	0.0001047	-0.0002729	-0.0001093
cacoos-quatro aguas	-0.0000025	0.0000575	0.0000205	-0.0000696	-0.0000114

**Table 5.10.** Velocity gradient among adjacent stations at 0 hour, 3 hours, 6 hours, 9 hours, and 12 hours.

station	velocity gradient ( $dv/dx$ )				
	at t1 (0 h)	at t4 (3 h)	at t7 (6 h)	at t10 (9 h)	at t13 (12 h)
bar de gina-centro nautico	-0.0000344	0.0000612	-0.0000079	0.0000318	-0.0000177
centro nautico-Sao Luis inlet	0.0001151	-0.0001202	-0.0000297	0.0000281	0.0001814
centro nautico-quatro aguas	0.0000106	0.0001622	0.0000111	-0.0001525	-0.0000190
nave pegos-quatro aguas	-0.0000881	0.0002437	0.0000800	-0.0003218	-0.0001005
Faro-Olhao inlet-quatro aguas	-0.0000284	0.0001334	0.0000310	-0.0001344	-0.0000555
Faro-Olhao inlet-cacoos	-0.0000179	0.0001831	0.0000709	-0.0002470	-0.0000682
Faro-Olhao inlet-culatra	-0.0000269	0.0001678	-0.0000004	-0.0002783	-0.0000749
boiav3-culatra	0.0002090	-0.0003843	-0.0000837	0.0001471	0.0002330
culatra-Armona inlet	0.0000103	-0.0002150	0.0000601	0.0002072	0.0000719
marim-Armona inlet	0.0000125	-0.0002822	-0.0000334	0.0001677	0.0001188
marim-boiav3	-0.0000758	0.0001221	0.0000062	-0.0000936	-0.0000853
bela romao-marim	0.0000091	-0.0001211	0.0000518	0.0000902	0.0000198
Faro-Olhao inlet-boiav3	-0.0001182	0.0003216	0.0000375	-0.0003115	-0.0001713
Sao Luis inlet - Faro-Olhao inlet	-0.0000202	0.0000161	-0.0000120	0.0000399	-0.0000348
cacoos-boiav3	-0.0002503	0.0006806	0.0000794	-0.0006592	-0.0003626
cacoos-quatro aguas	-0.0000272	0.0000794	0.0000045	-0.0000492	-0.0000370

**Water circulation pattern during high water in Faro Olhao inlet (0 hour)**

Water circulation pattern during high water event in Faro Olhao inlet as a reference point (0 hour) can be seen in **Fig 5.2** below. During high water, from **Fig 5.2**, it is obviously that the water flows from ocean to inner part (flood) of the main channel of Ria Formosa through inlets (Faro Olhao inlet and Armona inlet). However, the opposite condition occurred in Sao Luis inlet. The water does not go inside the main channel through Sao Luis inlet, but go outside instead. It indicates that Sao Luis inlet is not as strong as Faro Olhao and Armona inlet. Besides that, Bar de Gina and Nave Pegos stations showed the opposite direction of the flow (ebb) among the rest. This condition occurred probably due to Praia de Faro bridge between Bar de Gina and Centro Nautico station which caused the convergence / funnel effect.

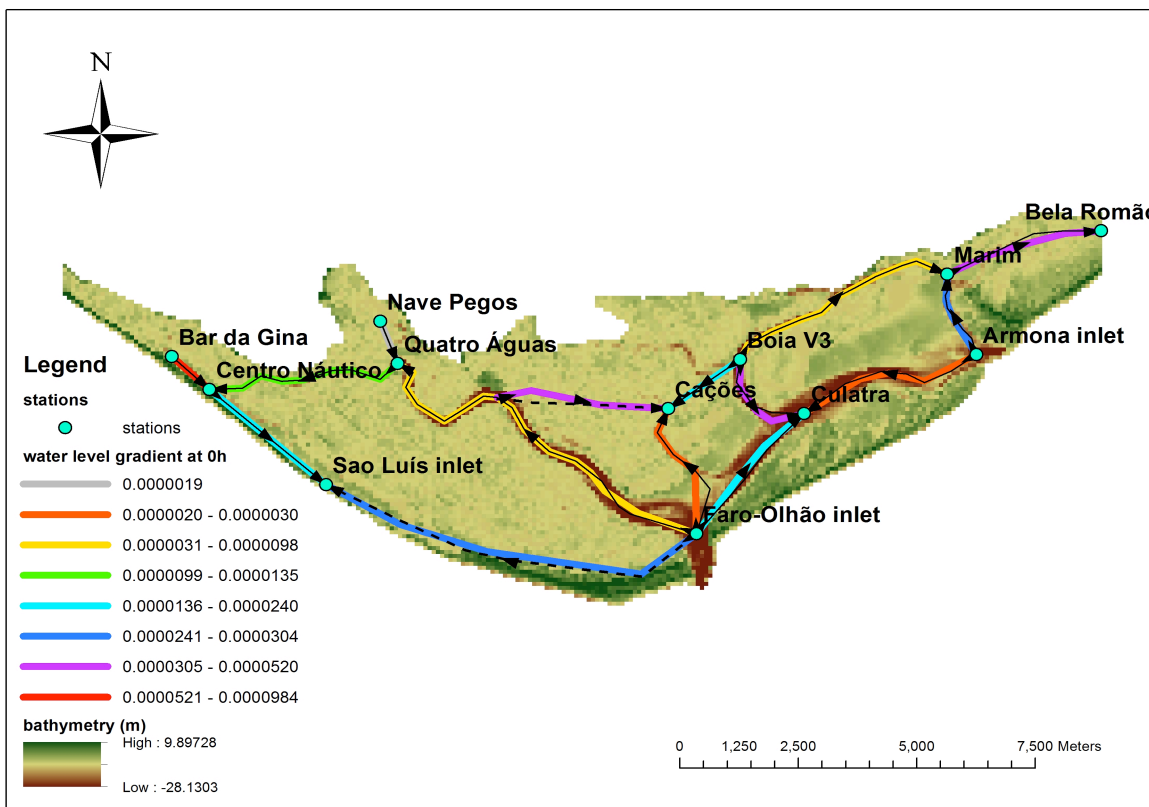


**Fig 5.2.** Water circulation patterns inside the main channel of Ria Formosa based on water level gradient at 0 hour (at high water in Faro Olhao inlet)

The interesting part in this water circulation pattern is Faro Olhao inlet plays an important role as a pathway for the most ocean water to go inside Ria Formosa. Faro Olhao inlet has very important role in transporting the water from the ocean to the middle and west region of Ria Formosa compare to Sao Luis inlet. While in the east region, Armona inlet play

an important role in transporting the water inside Ria Formosa in east region. This finding was strengthened by the finding of Salles et al (2005) which stated the tidal prisms through Faro Olhao and Armona inlet ranging from 40 - 80 % and 12 - 50 % of total tidal prism, respectively.

From velocity or tidal current gradient (**Fig 5.3**), it could be seen the flooding event occurred during high water. The interesting part which need to be pointed out is the velocity direction from Sao Luis inlet to Faro Olhao inlet. Even though the water goes from Faro Olhao inlet to Sao Luis inlet during this time, but the velocity has different path direction. It means that the velocity tend to decelerate the movement of water from Faro Olhao inlet to Sao Luis inlet. This condition occurred due to retention effect caused by salt marshes area between Sao Luis inlet and Faro Olhao inlet.

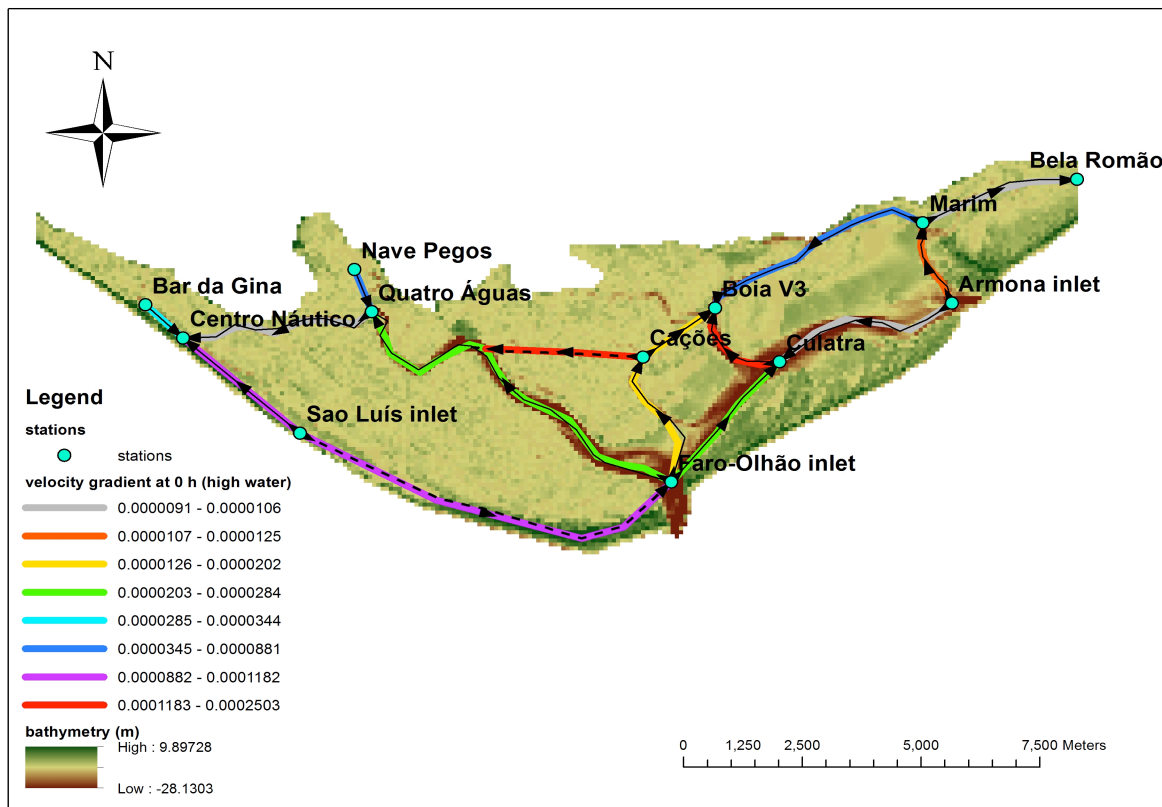


**Fig 5.3.** The tidal current circulation patterns inside the main channel of Ria Formosa at 0 hour (at high water in Faro Olhao inlet)

### ***Water circulation pattern during ebbing period in Faro Olhao inlet (3 hour)***

Water circulation pattern at 3 hour during ebbing period in Faro Olhao inlet as reference point can be seen in **Fig 5.4**. The water from the west region and middle region of Ria Formosa goes outside Ria Formosa through Faro Olhao inlet, not from Sao Luis inlet, even the water from Sao Luis inlet goes outside through Faro Olhao inlet. This occurrence

proved the strength of Faro Olhao inlet and showed the important role of Faro Olhao inlet in comparison to Sao Luis inlet. So it means during the ebbing period in Faro Olhao inlet, Sao Luis inlet showing flood occurrence. This occurrence apparently differs from the reality. In reality, during the ebbing period in Faro Olhao inlet, Sao Luis inlet also has ebb flow from centro nautico. Although Sao Luis inlet is not as strong as Faro Olhao inlet, but Sao Luis inlet still play an important role in transferring the water. While, in the east region of Ria Formosa, Armona inlet also play an important role as an escaping way for the water during ebbing event.

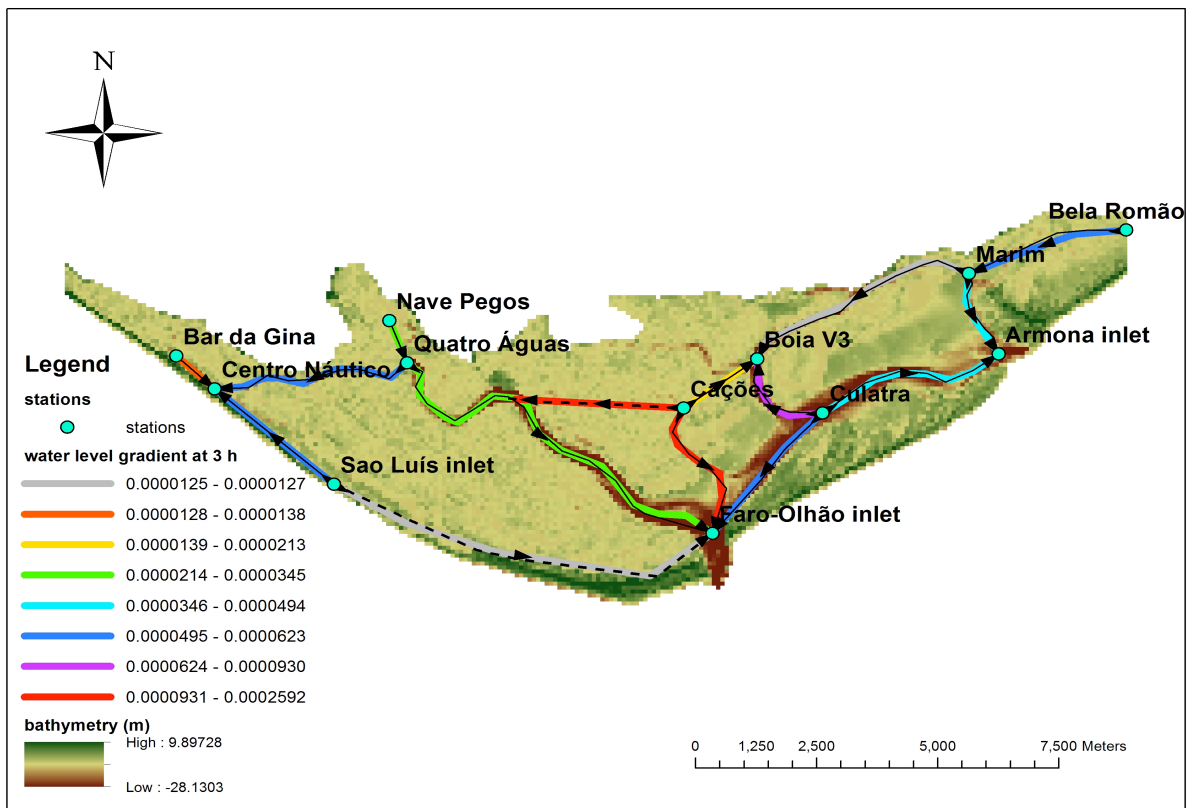


**Fig 5.4.** Water circulation pattern inside the main channel of Ria Formosa based on water level gradient at 3 hours (at ebbing period in Faro Olhao inlet)

**Fig 5.5** showed the velocity or tidal current circulation inside Ria Formosa during ebbing period. Even though, the water gradient showed the water flows from Sao Luis inlet to Faro Olhao inlet, the velocity direction tends to move to the opposite direction, which is from Faro Olhao inlet to Sao Luis inlet. It means there is a deceleration flow in this case and also it showed Sao Luis inlet plays role during ebb event, though the role is not very significant.

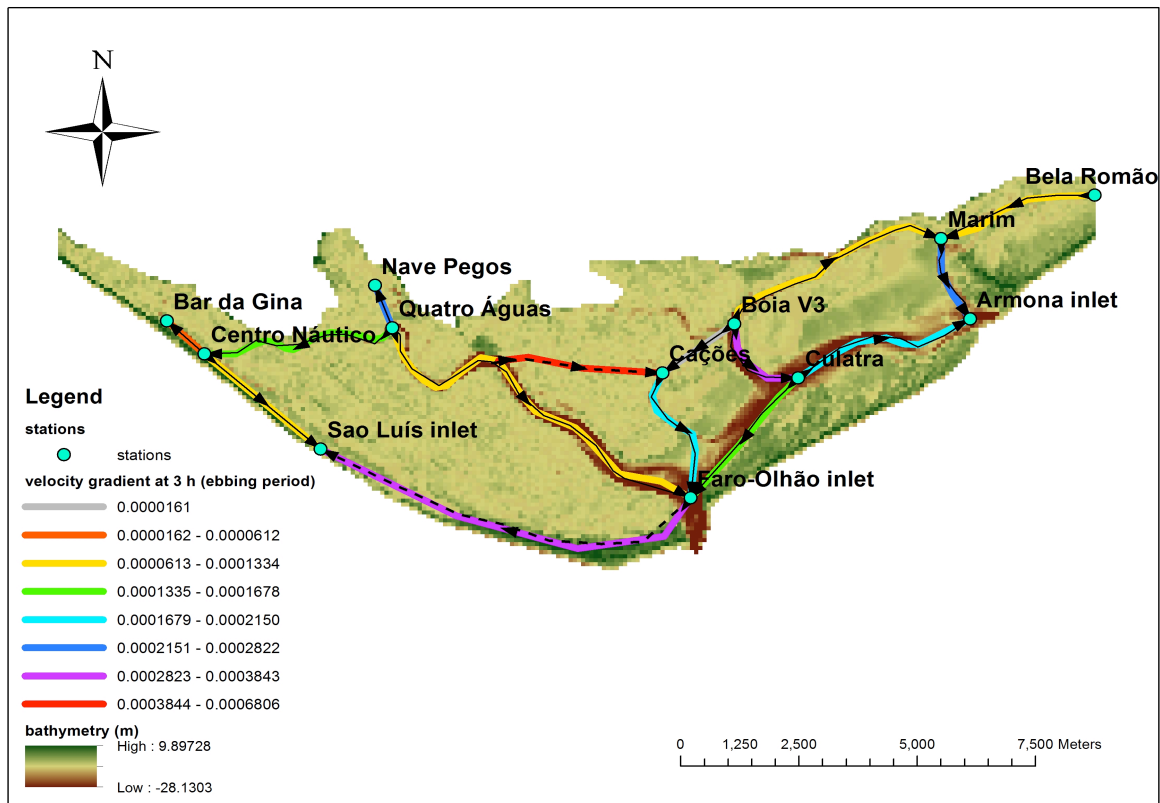


**Fig 5.5.** The tidal current circulation pattern inside the main channel of Ria Formosa at 3 hours (at ebbing period in Faro Olhao inlet)

#### *Water circulation pattern during low water in Faro Olhao inlet (6 hour)*

During the low water occurrence in Faro Olhao inlet (**Fig 5.6**), the water which is coming from the west region of Ria Formosa goes outside through Faro Olhao inlet, so does for the middle region of Ria Formosa. While for the east region, Armona inlet become a pathway for the water to go outside the Ria Formosa system. Besides the pathway of water flow direction, **Fig 5.6** also showed the magnitude of the water level gradient. The bigger water level gradient means the steeper of the slope, the more water goes through it and the faster water flows. In this case, the water which flows from Quatro Aguas station to Faro Olhao inlet showed a small water level gradient, which means the water goes slowly from Quatro aguas station to Faro Olhao inlet.

**Fig 5.7** showed the tidal current circulation inside Ria Formosa during low water in Faro Olhao inlet. During the low water occurrence, almost all the water which has been transported to Ria Formosa before, goes outside the system. This **Fig 5.7** could be the end of the ebbing period, in which some of them showing the retardation velocity which decelerate the ebb flow.

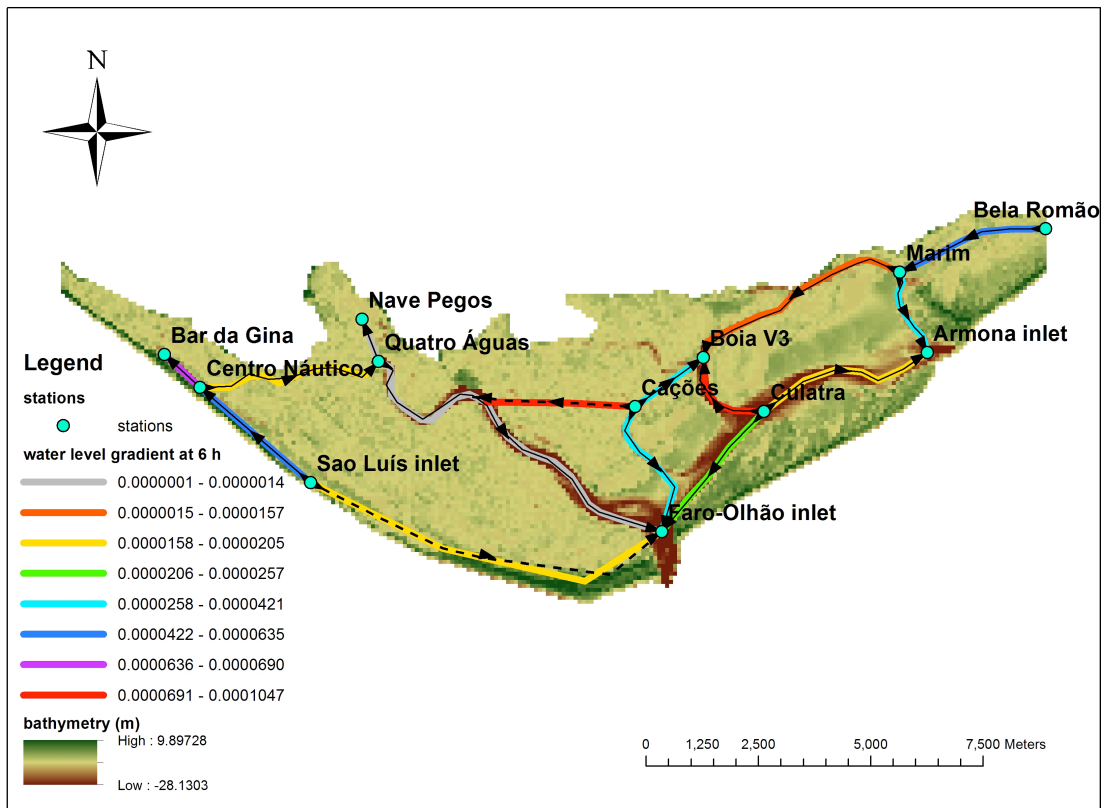


**Fig 5.6.** Water circulation pattern inside the main channel of Ria Formosa based on water level gradient at 6 hours (at low water in Faro Olhao inlet)

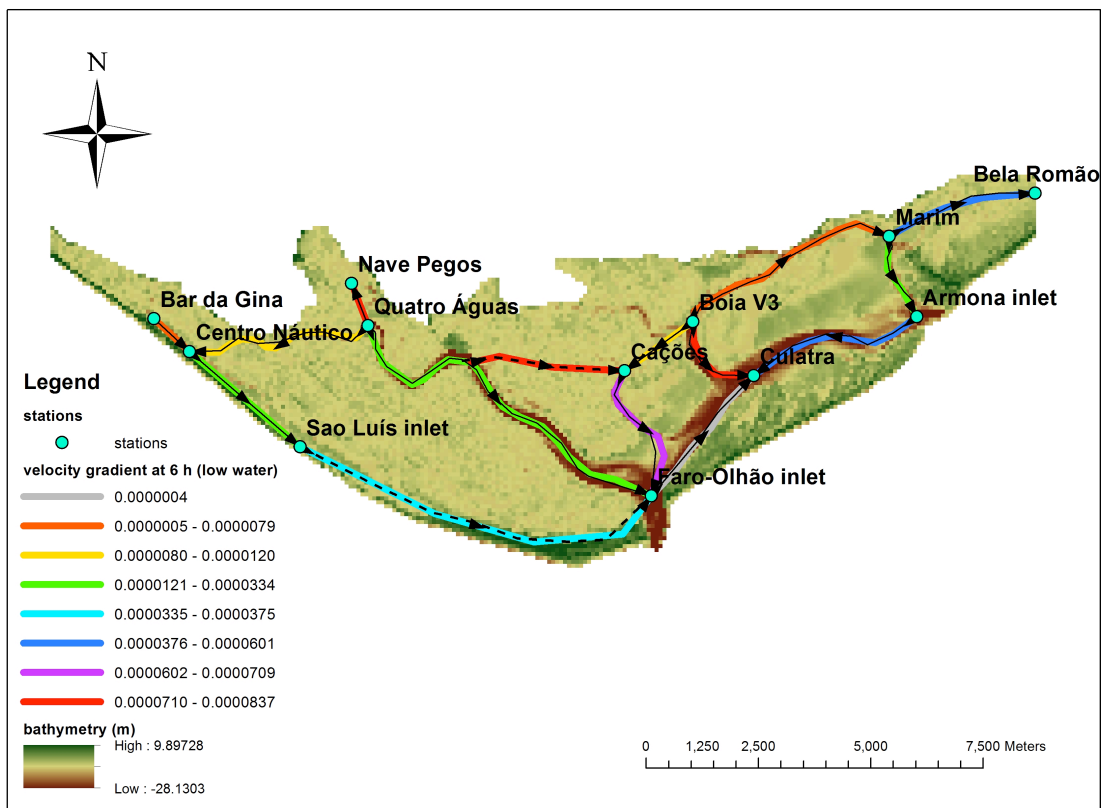


**Fig 5.7.** The tidal current circulation pattern inside the main channel of Ria Formosa at 6 hours (at low water in Faro Olhao inlet)

### *Water circulation pattern during flooding in Faro Olhao inlet (9 hour)*

The same statement could also be withdrawn by seeing the water circulation pattern based on water level gradient in Ria Formosa during flood occurrence in Faro Olhao inlet (**Fig 5.8**). The important role of Faro Olhao inlet as the pathway for the water to goes inside Ria Formosa system could be seen clearly in **Fig 5.8**. Although, Sao Luis inlet located in the west region of Ria Formosa, the role of Sao Luis inlet for the west region of Ria Formosa is not very significant. While, for the east region of Ria Formosa, Armona inlet showed the significance role of its as an inlet.

Besides the inlets, several stations also showed interesting behaviour, such as Boia V3, Culatra, and Cacoés. These three stations are the intersection points for three pathways. From **Fig 5.8** it could be seen that Boia V3 has the higher water level compared to Cacoés and Culatra, so the water goes from Boia V3 to its surrounding.

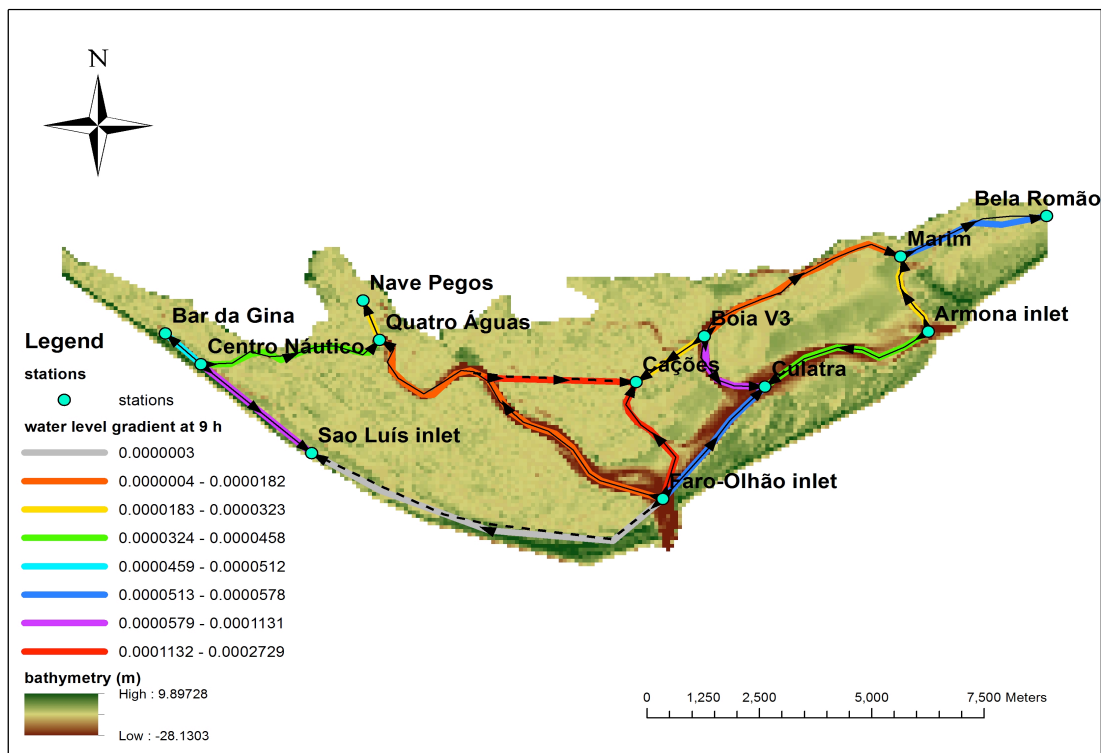


**Fig 5.8.** Water circulation pattern inside the main channel of Ria Formosa based on water level gradient at 9 hours (at flooding period in Faro Olhao inlet)

The tidal current circulation inside Ria Formosa at 9 hour (**Fig 5.9**) showed the flood current coming from the ocean. For west and middle region of Ria Formosa, the flood current goes mainly from Faro Olhao inlet to the channel inside Ria Formosa, while for the east region of Ria Formosa, Armona inlet let the flood current to explore the east region of Ria Formosa, which includes Culatra, Marim, Boia V3, and Bela Romao stations.

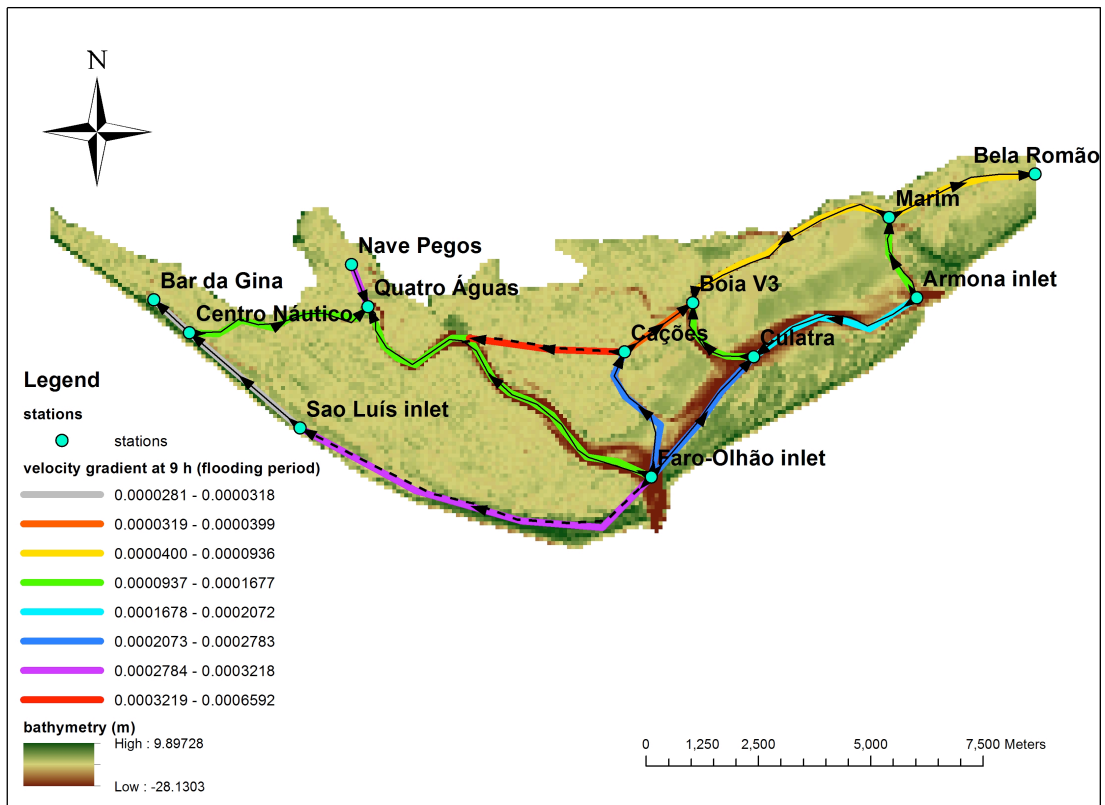


**Fig 5.9.** The tidal current circulation pattern inside the main channel of Ria Formosa at 9 hours (at flooding period in Faro Olhao inlet)

#### *Water circulation pattern during high water in Faro Olhao inlet (12 hour)*

Tidal cycle usually has period of time around 12 - 13 hours in which the high water occurrence is being repeated after that tidal period. **Fig 5.10** and **Fig 5.11** showed the water circulation pattern based on water level gradient and tidal current circulation inside Ria Formosa system at 12 hour (during high water occurrence in Faro Olhao inlet). The circulation pattern of this hour is almost similar with the circulation pattern occurred at 0 hour, except for the pathway from centro nautico to quatro aguas station and from quatro aguas to nave pegos station. This could happened probably due to the full tidal cycle has not been reached. So there is a slightest different result with the circulation pattern at 0 hour.

As Bela Romao station acts in this particular study as the representative of Fuzeta inlet in the eastern part of Ria Formosa, but it can not be defined that the action or occurrence in this station is similar with Fuzeta inlet station. Nevertheless, Bela Romao station can be used as a reference control of Fuzeta inlet in the eastern part of Ria Formosa lagoon.

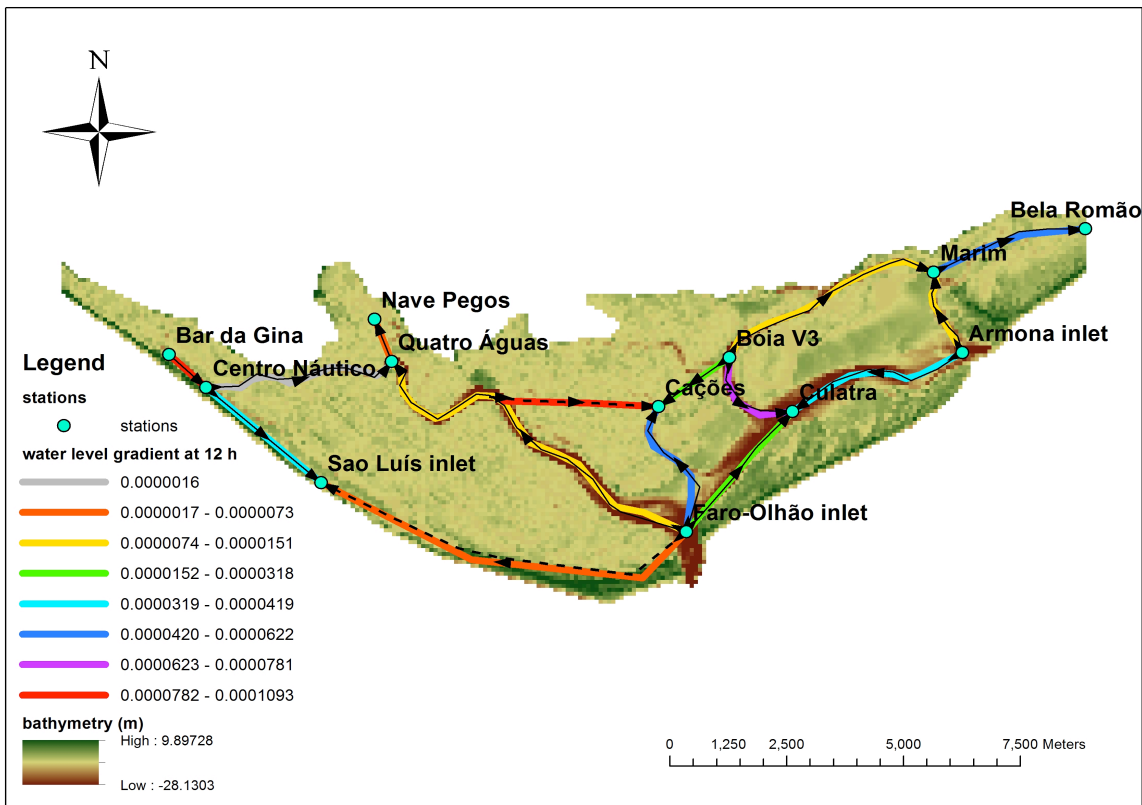


**Fig 5.10.** Water circulation pattern inside the main channel of Ria Formosa based on water level gradient at 12 hours (at high water)

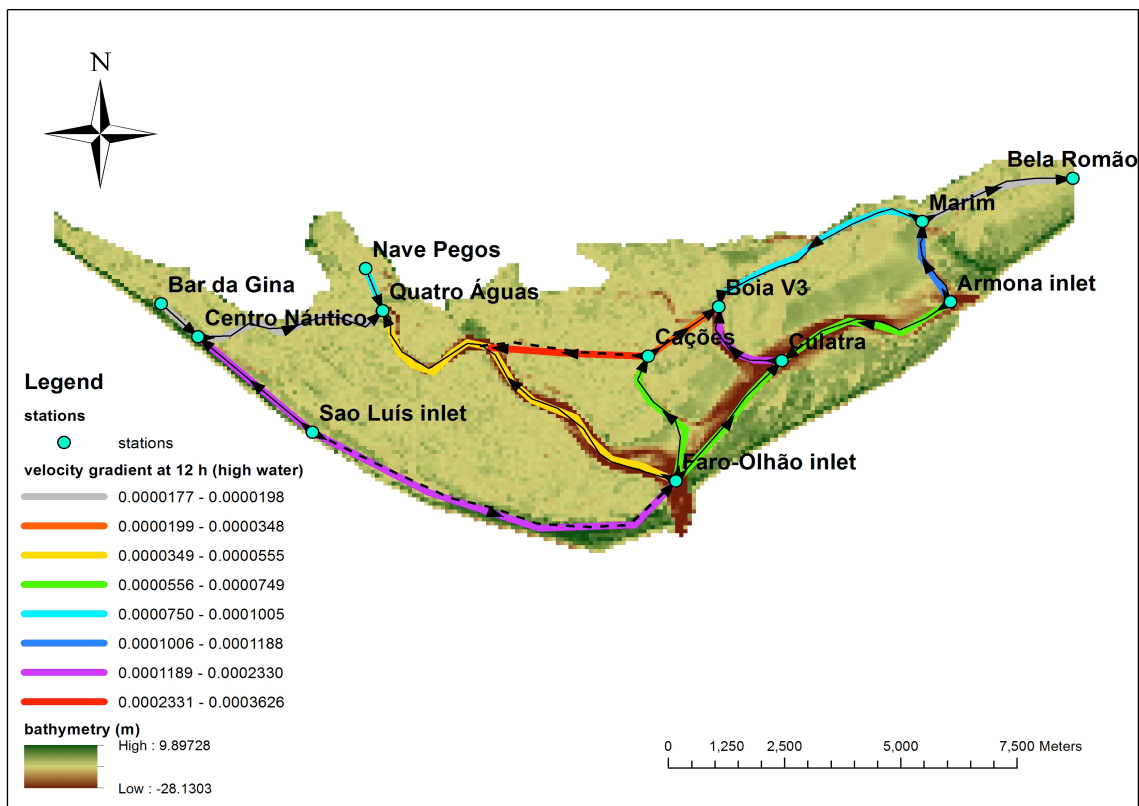


**Fig 5.11.** The tidal current circulation pattern inside the main channel of Ria Formosa based on velocity/tidal current gradient at 12 hours (at high water)

## 5.2.2. Temporal gradients of water level and velocity in the main channel

Temporal gradients of water level and velocity among stations leads to the calculation of velocity and acceleration of the tide to reach the stations. In this case, the explanation of the temporal gradients of water level and velocity are divided into five parts which consist of all stations, inlets, west region, middle region, and east region of Ria Formosa (**Fig 5.1** in the previous sub chapter).

### 5.2.2.1. For all stations

From **Fig 5.12**, it could be seen that the biggest water level temporal gradient for all stations during high water occurrence occurred between station Boia V3 and Sao Luis inlet, and so does for low water occurrence. The bigger of the difference of water level measurement and the shorter difference of time, the bigger water level temporal gradient will be. While, The biggest velocity temporal gradient occurred between station Bela Romao and Armona inlet (**Fig 5.13**). From **Fig 5.13**, it could be seen that several stations have the opposite behaviour of velocity variation, such as Quatro Aguas and Boia V3. When other stations have ebb current behaviour, Quatro Aguas and Boia V3 have the opposite behaviour, which is flood current. This condition occurred probably due to Quatro Aguas and Boia V3 are belong to the intersection point station, where the water can come from several direction of the stations.

Besides water level variation and velocity variation, hysteresis diagram analysis for all stations (**Fig 5.14**) is also need to be evaluated in order to understand the behaviour of the tide in Ria Formosa and also to see the connection or relation between water level and velocity in each stations. **Fig 5.14** showed the strength of the flood and ebb velocity are higher during high water level in inlets than other stations. So it means the magnitude of velocity decrease with the distance from the ocean, due to the friction which encounters the flow inside the main channel. While during low water, the strength of ebb and flood current seems to be equal among the stations except for Faro Olhao inlet, Armona inlet, Sao Luis inlet, and Boia V3. This finding showed the importance of these four stations in term of tidal current strength. Furthermore, **Fig 5.14** also showed the asymmetrical behaviour of every stations in term of tidal current velocity and water level. The most asymmetrical behaviour was shown in Sao Luis inlet and Boia V3 station.

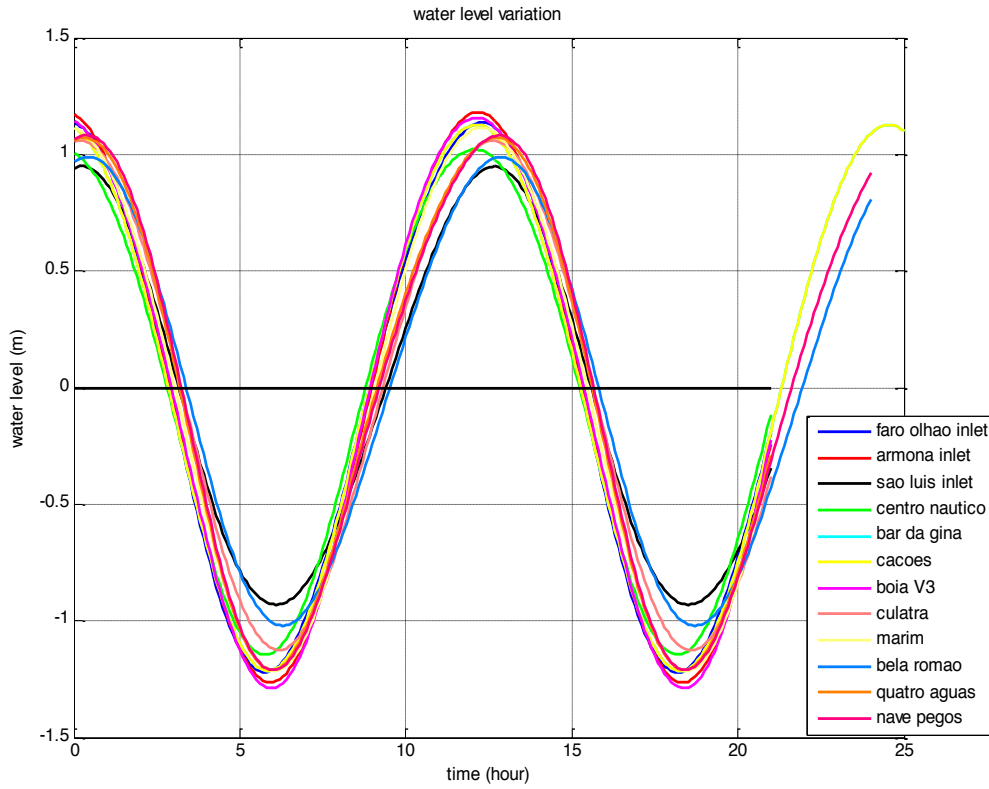


**Fig 5.12.** Water level variation for all stations

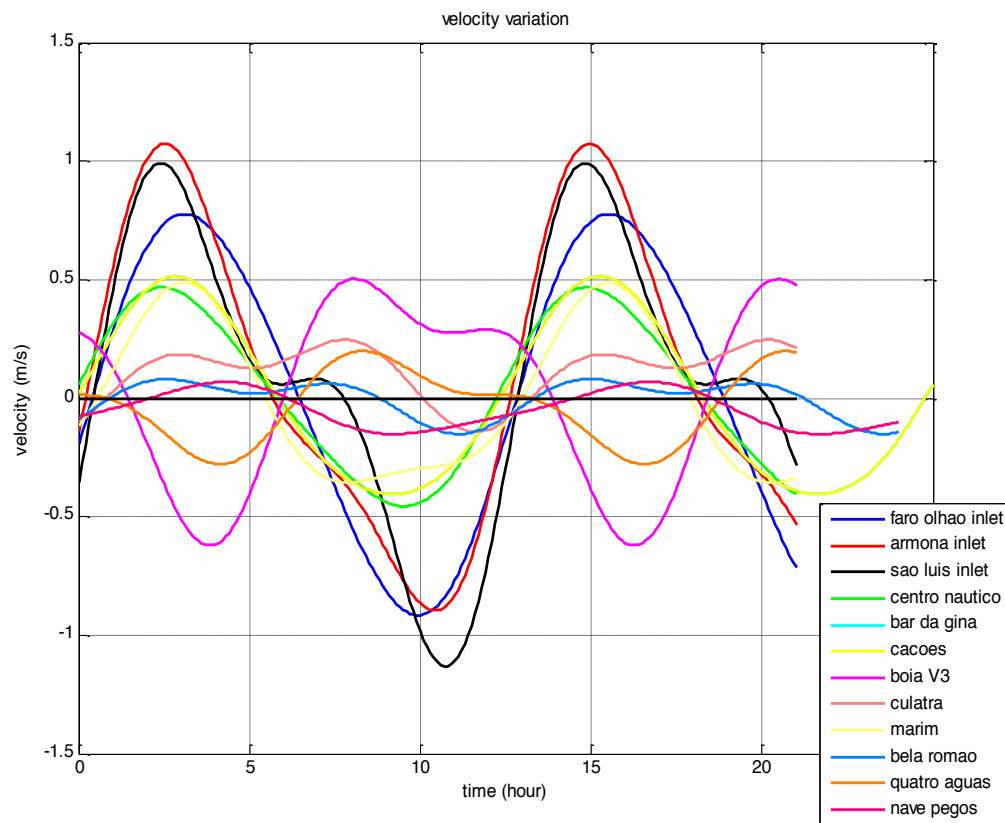


**Fig 5.13.** Velocity variation for all stations

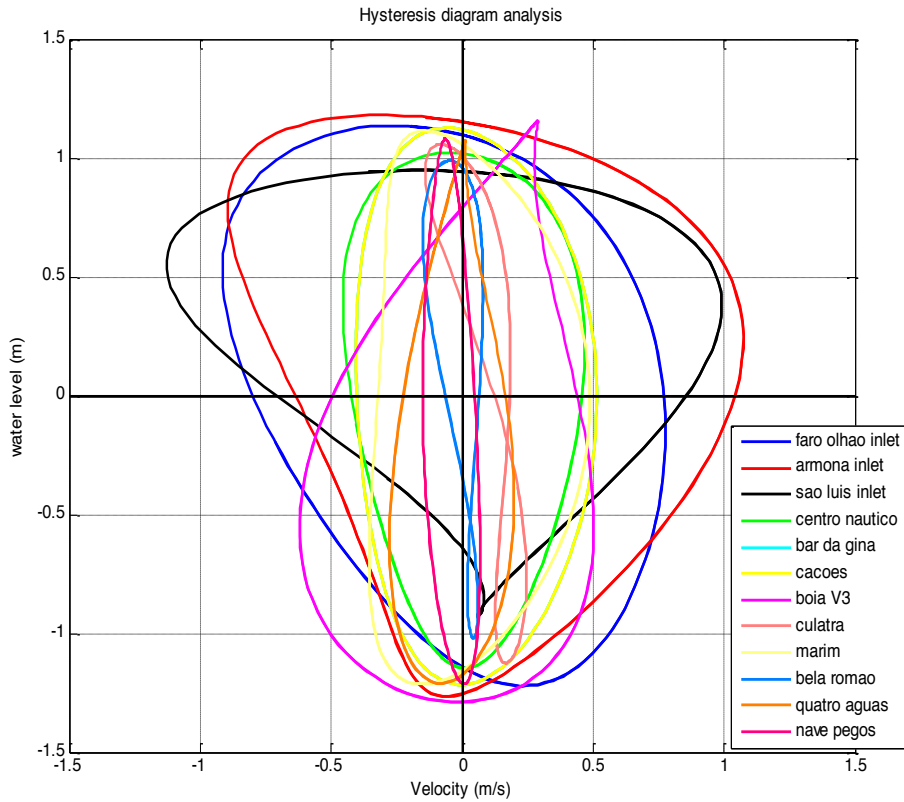


**Fig 5.14.** Hysteresis Diagram for all stations

**Table 5.11** showed the tidal amplitude during high water and low water for the raw data and harmonic analysis. Based on the harmonic analysis, the maximum amplitude during high water occurred at Armona inlet, while during low water occurred at Boia V3 station. Furthermore, based on the raw data, the maximum tidal amplitude during low water also occurred at Boia station, while during high water, the maximum amplitude occurred at Bar de Gina. Besides tidal amplitude, **Table 5.11** also showed the percentage difference (error) between the raw data and harmonic analysis, and it appeared to be 12% for the average error of high water and 9% for the average error of low water.

**Table 5.11.** tidal amplitude of harmonic analysis and raw data in all stations

station	date	start time	end time	harmonic analysis (HA) tide amplitude (m)		raw data (RAW) tide amplitude (m)		the percentage difference of RAW-HA	
				high water	low water	high water	low water	high water	low water
Faro-Olhao inlet	6/3/2011	4:15:00	22:15:00	1.136	-1.220	1.239	-1.329	8%	8%
Armona inlet	9/11/2011	2:45:00	21:45:00	1.180	-1.265	1.309	-1.405	10%	10%
Culatra	10/15/2011	4:45:00	22:45:00	1.058	-1.125	1.184	-1.218	11%	8%
Boia V3	10/24/2011	1:10:00	20:10:00	1.156	-1.289	1.288	-1.536	10%	16%
Marim	11/10/2011	14:10:00	9:10:00	1.114	-1.214	1.203	-1.294	7%	6%
Canal Cacoés	12/12/2011	15:45:00	4:45:00	1.118	-1.175	1.273	-1.197	12%	2%
Bela Romão	1/15/2012	6:30:00	4:30:00	0.990	-1.021	1.236	-1.156	20%	12%
Sao Luis inlet	5/24/2012	16:30:00	11:30:00	0.948	-0.930	1.124	-1.007	16%	8%
Centro Nautica	7/8/2012	6:35:00	1:35:00	1.021	-1.146	1.165	-1.288	12%	11%
Bar de Gina	7/31/2012	1:55:00	22:55:00	1.126	-1.216	1.384	-1.483	19%	18%
Quatro Aguas	11/28/2012	14:25:00	9:25:00	1.072	-1.210	1.155	-1.271	7%	5%
Poita Nave Pegos	5/12/2013	3:45:00	0:45:00	1.081	-1.211	1.160	-1.285	7%	6%
max amplitude				1.180	-0.930	1.384	-1.007	average	average
min amplitude				0.948	-1.289	1.124	-1.536	12%	9%

### *Phase Lag*

The phase lag calculation among all the adjacent stations can be seen in **Table 5.12**. From **Table 5.12**, it could be seen that the maximum phase lag of high water level occurred between cacoés and boia V3 station. Although, they are very close to each other in term of distance location, but the high water level phase lag seems showing the greatest difference. This could be happened due to there is huge impediment that separate them to each other, such as huge salt marshes areas. In this case, it could be stated that the higher phase lag, the higher distortion will be. Meanwhile, the shortest phase lag in high water level occurred between bar de gina and centro nautico stations, where indeed they are close in term of distance and they showed that they are in phase actually.

In the case of low water level, the greatest phase lag occurred between Faro Olhao inlet and Cacoés, while bar de gina - centro nautico and marim - boia v3 are the stations which are in phase in term of low water occurrence, so there is no phase lag between them. This condition occurred probably because they are so close to each others in term of distance. Besides water level phase lag, **Table 5.12** also gives information about velocity or tidal current phase lag. so it can be known the time length between the adjacent station to achieve high ebb or flood velocity for both of them.

**Table 5.12. Phase Lag**

stations	Phase lag (hour)							
	high water	low water	Zero water level (from HW to LW)	Zero water level (from LW to HW)	high velocity	low velocity	Zero velocity level (from Hvel to Lvel)	zero velocity level (from Lvel to Hvel)
bar de gina-centro nautico	0.000	0.000	0.036	0.113	0.400	0.300	0.006	0.123
centro nautico-sao luis inlet	0.600	0.300	0.350	0.616	0.000	1.100	1.928	0.630
centro nautico-quatro aguas	0.600	0.200	0.375	0.349	5.800	5.400	5.022	5.822
nave pegos-quatro aguas	0.100	0.000	0.051	0.063	4.000	5.100	5.297	4.320
faro-olhao inlet-quatro aguas	0.400	0.200	0.320	0.212	5.200	5.800	5.642	6.004
faro olhao inlet-cacoes	0.900	0.900	0.905	0.950	0.200	1.100	1.063	0.396
faro-olhao inlet-culatra	0.300	0.400	0.363	0.385	4.700	1.600	3.634	0.415
boiav3-culatra	0.500	0.200	0.286	0.377	0.300	4.600	3.750	5.177
culatra-armona inlet	0.400	0.300	0.324	0.336	5.300	1.100	4.401	0.610
marim-armona inlet	0.100	0.100	0.136	0.103	0.600	2.500	0.212	0.336
marim-boiaV3	0.200	0.000	0.098	0.143	5.000	4.000	4.017	5.451
bela romao-marim	0.600	0.300	0.342	0.448	0.500	3.200	3.316	0.379
faro-olhao inlet-boiav3	0.200	0.200	0.077	0.008	5.000	6.100	4.996	5.592
sao luis inlet - faro olhao inlet	0.400	0.300	0.296	0.479	0.700	0.700	0.700	0.033
cacoes-boiaV3	1.100	0.700	0.828	0.942	5.200	5.100	3.933	5.196
cacoes-quatro aguas	0.500	0.700	0.585	0.738	5.400	5.400	4.580	5.608
faro olhao inlet - armona inlet	0.100	0.100	0.039	0.048	0.600	0.400	0.768	0.195
sao luis inlet - armona inlet	0.500	0.200	0.256	0.431	0.100	0.200	2.076	0.228

### 5.2.2.2. For inlets

Inlets are the most important and crucial part of every lagoon, because it creates a connection between the ocean and the water inside the lagoon. In this particular study, there are three inlets involved and one station as the reference control of the Fuzeta inlet in the eastern part of Ria Formosa.

**Fig 5.15** and **Fig 5.16** give the water level variation profile and velocity variation profile in the inlets, respectively. From **Fig 5.15**, it could be seen that Armona inlet has the maximum tidal amplitude among all others. Besides that, Armona inlet is the first inlet where the higher water occurred. The sequence of the high water occurrence among all inlets can be written as Armona inlet - Faro Olhao inlet - Sao Luis inlet - Bela romao station. While the sequence of the low water occurrence among all inlets are Faro Olhao inlet - Armona inlet - Sao Luis inlet - Bela romao (**Fig 5.15**). The phase lag of high water level occurrence and low water level occurrence among all inlets can be seen in **Table 5.13**.

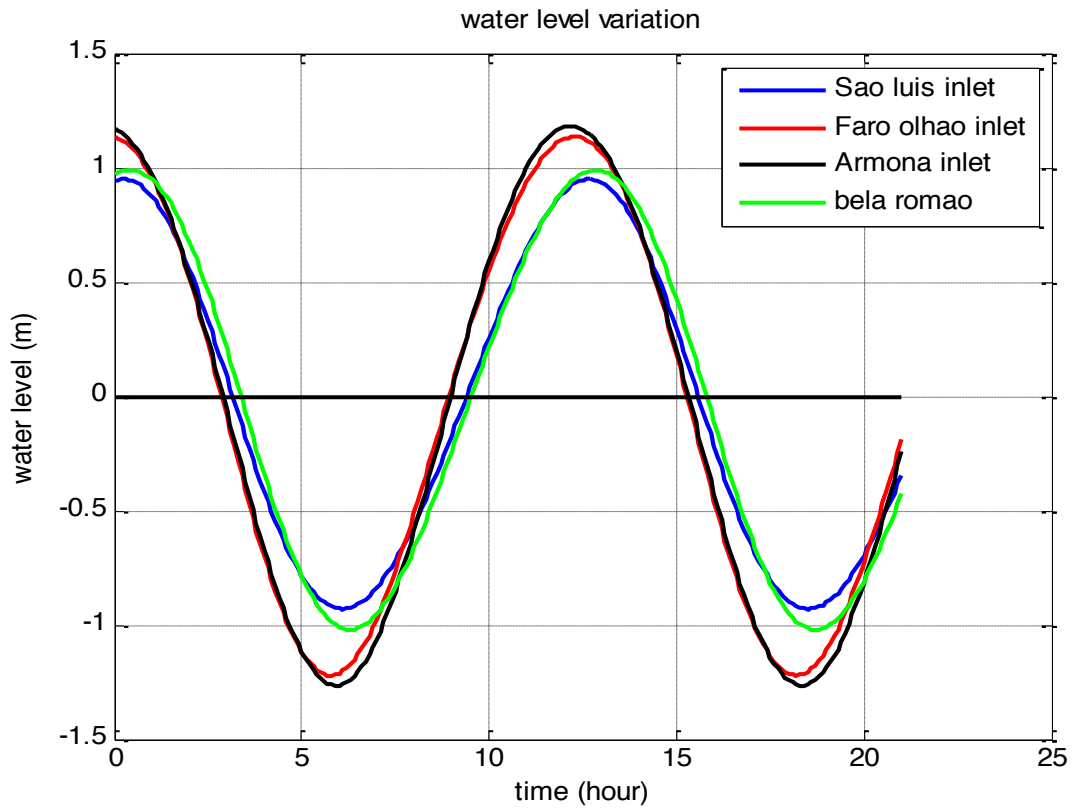


**Fig 5.15.** Water level variation for inlets

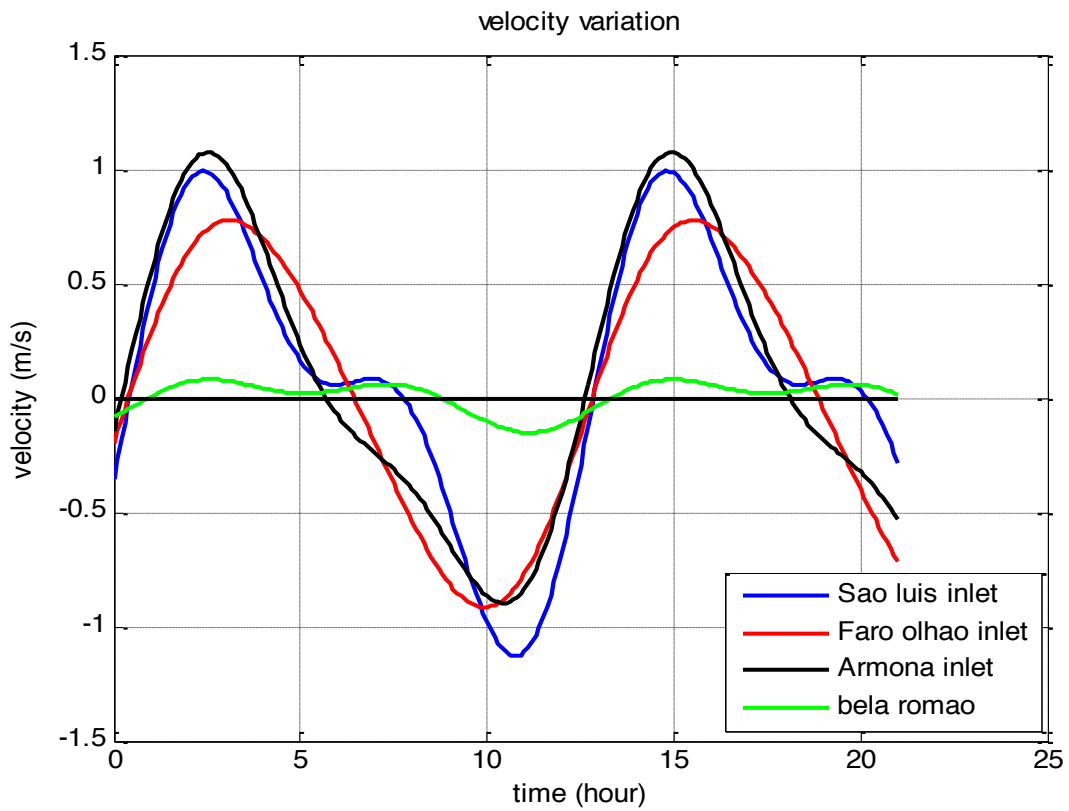


**Fig 5.16.** Velocity variation for inlets

From **Fig 5.16**, it could be seen that Armona inlet has the maximum ebb velocity, while Sao Luis inlet has the maximum flood velocity. As mentioned before, the tidal current velocity can be an indication whether the inlet tends to be ebb dominant or flood dominant. In this case, Armona inlet can be stated as ebb dominant inlet according to tidal current strength, while Sao Luis inlet is flood dominant inlet. Among all inlet station, Bela romao seems to have the lowest ebb and flood velocity. This can be ignored since actually Bela romao is not the real inlet, it is just the reference control station for Fuzeta inlet in the eastern part of Ria Formosa. From **Fig 5.16**, it could be seen also that the maximum velocity in Faro Olhao inlet is lower than maximum velocity in Armona inlet. This is probably due to the breakwaters that had been artificially built in the Faro Olhao inlet. The time difference between maximum velocity and between minimum velocity among the inlets can be seen in **Table 5.13**.

Besides water level time variation and velocity time variation, the hysteresis diagram analysis has also been carried out to see the behaviour relationship between water level and velocity variation among all the inlets (**Fig 5.17**). From this figure, it could be seen that Sao Luis inlet has the strong flood velocity and Armona inlet has the strong ebb velocity. The strong ebb and flood current velocities were occurred in high water level phase for all the inlets.

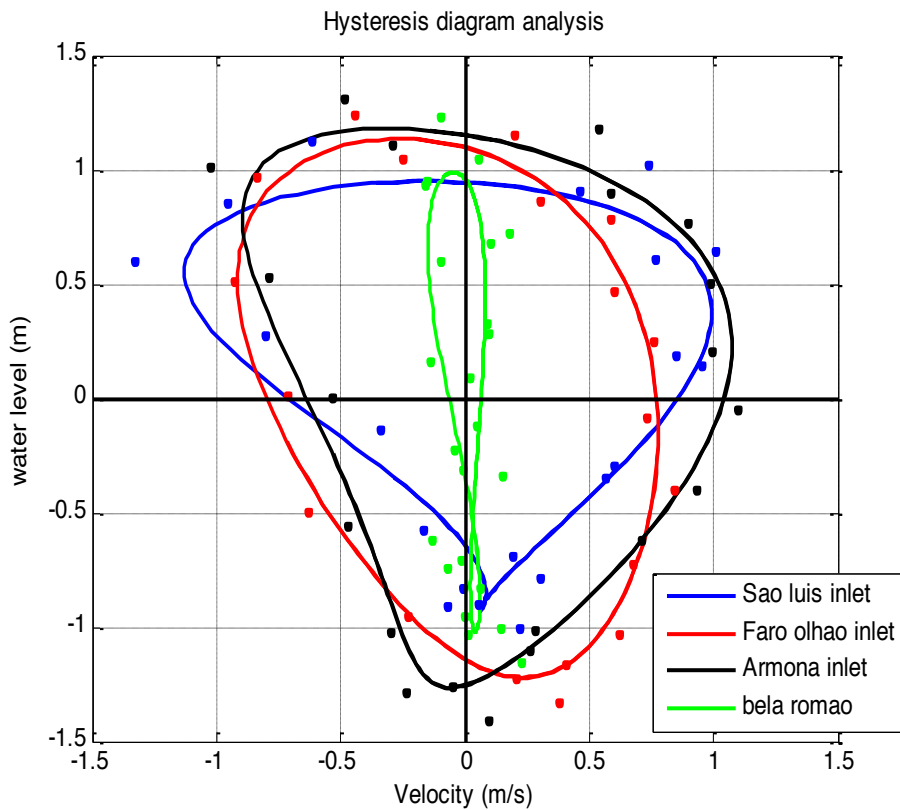


**Fig 5.17.** Hysteresis Diagram Analysis for inlets

The interesting part that need to be pointed out from **Fig 5.17** is the asymmetrical behaviour of Sao Luis inlet. During high water occurrence, Sao Luis inlet showed the strong current in term of flood and ebb current velocity, otherwise during low water occurrence, Sao Luis inlet showed the opposite condition with the weak current in term of flood and ebb current. Furthermore, From **Fig 5.17**, it could be seen that the maximum high slack water was occurred in Armona inlet, while the maximum low slack water was occurred in Faro Olhao inlet. The slack water analysis will be carried out later in this sub chapter.

As mentioned before, **Table 5.13** showed the phase lag calculation among the inlets in Ria Formosa. From **Table 5.13**, it could be seen that the high water in sao luis inlet occurred 24 minutes after the occurrence in Faro Olhao inlet and 30 minutes after occurrence in Armona inlet. So it means the delay of the high water occurrence between Armona inlet and Faro Olhao inlet are 6 minutes, in which the high water occurred first in Armona inlet then Faro Olhao inlet. Whereas the low water level occurred first in Faro Olhao inlet, then 6 minutes later the low water occurred in Armona inlet.

**Table 5.13.** Phase lag among the inlets in Ria Formosa

inlet stations	phase lag (hour)		phase lag (minute)		time difference (hour)		time difference (minute)	
	high water	low water	high water	low water	Max velocity	Min velocity	Max velocity	Min velocity
sao luis inlet - faro olhao inlet	0.4	0.3	24	18	0.7	0.7	42	42
sao luis inlet - armona inlet	0.5	0.2	30	12	0.1	0.2	6	12
sao luis inlet - bela romao	-0.2	-0.2	-12	-12	0.1	0.3	6	18
faro olhao inlet - armona inlet	0.1	-0.1	6	-6	0.6	0.4	36	24
faro olhao inlet - bela romao	-0.6	-0.5	-36	-30	0.5	1.1	30	66
armona inlet - bela romao	-0.7	-0.4	-42	-24	0	0.6	0	36

The time difference of maximum and minimum velocity between inlets could also be seen in **Table 5.13**. The biggest time difference of maximum velocity occurred between Sao luis inlet and Faro Olhao inlet which is 42 minutes. Whereas the biggest time difference of minimum velocity happened between Faro Olhao inlet and Bela romao station which the delay almost one hour.

### 5.2.2.3. For West Region of Ria Formosa

In this particular study, the west region of Ria Formosa consists of several stations which are Bar da Gina, Centro Nautico, and Sao luis inlet. As mentioned before in the

previous sub chapter about longitudinal gradient, Sao Luis inlet does not play a big significant role compared to Faro Olhao inlet, but indeed it has role to balance and transfer the water inside and outside Ria Formosa lagoon.

The water level time variation and velocity time variation can be seen in **Fig 5.18** and **Fig 5.19**, respectively. From **Fig 5.18**, it could be seen that both the highest and lowest water level occurred in Bar de Gina. The greatest water level gradient occurred between Bar de Gina and Sao Luis inlet. Since Sao Luis inlet has the smallest tide height and tide amplitude among other stations in the west region of Ria Formosa, so during the high water period the direction of the water flows always goes toward Sao Luis inlet, while during low water period, the direction of the water flows goes to the opposite direction (**Fig 5.18**).

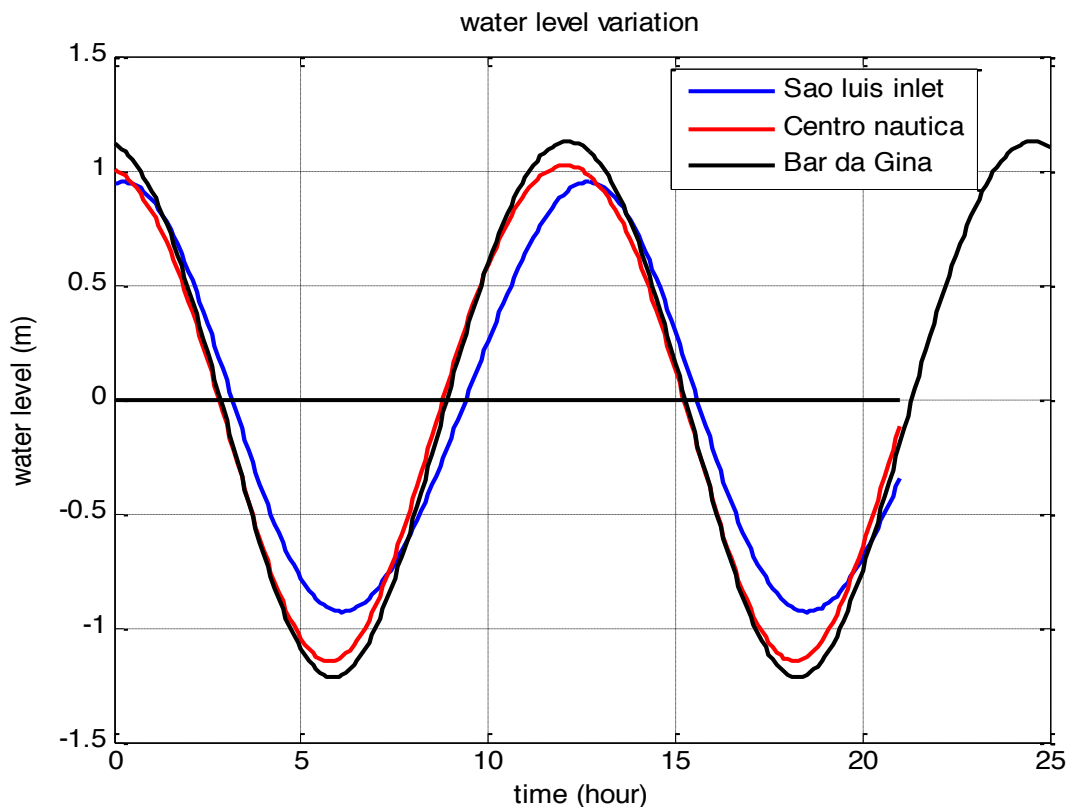


**Fig 5.18.** Water level variation for west region of Ria Formosa

The velocity variation in the west region of Ria Formosa seems to have big oscillation pattern (**Fig 5.19**). **Fig 5.19** showed that Sao Luis inlet has the maximum flood and ebb velocity field in the west region of Ria Formosa. So even though the water level variation of Sao Luis inlet is not that high, but it has strong tidal current amplitude.

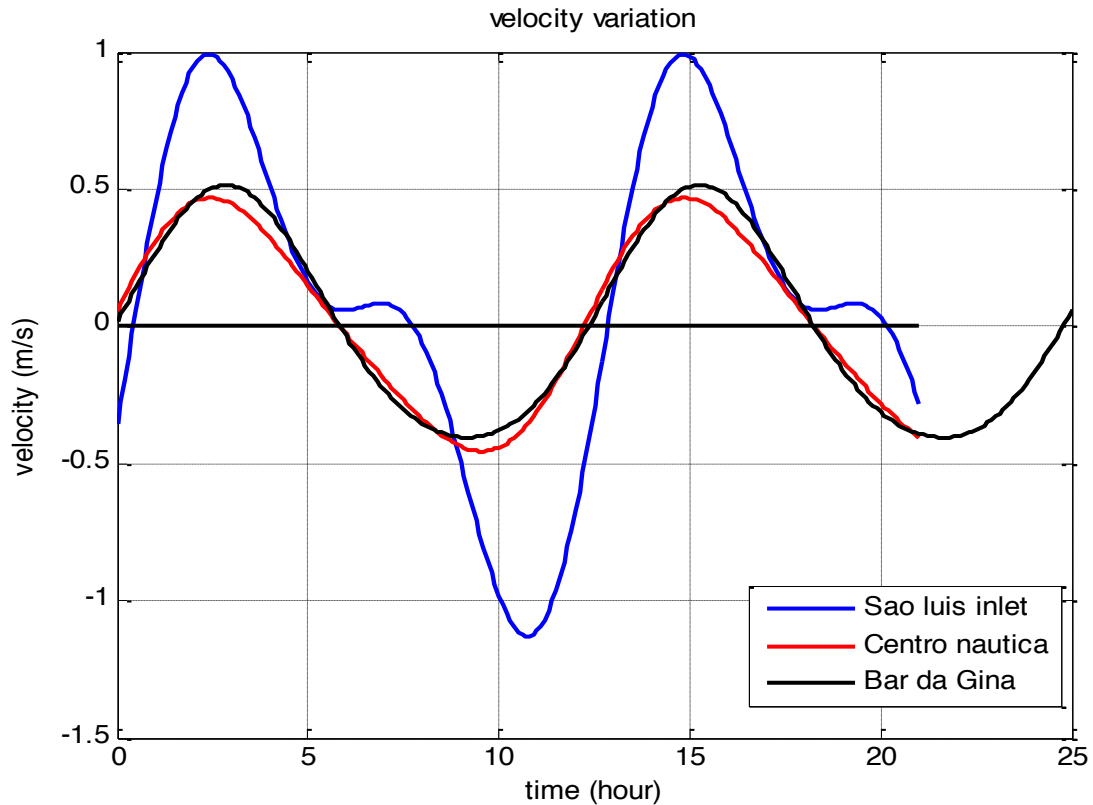


**Fig 5.19.** Velocity variation for west region of Ria Formosa

Besides water level variation and velocity variation, hysteresis diagram analysis for west region of Ria Formosa has also been carried out to see the performance behavior of the stations which located in the west region of Ria Formosa (**Fig 5.20**). From this figure, it could be seen that Sao Luis has the strong ebb and flood current and it has strong tidal asymmetry behaviour, while in term of water level, Sao Luis inlet has minimum high water occurrence and maximum low water occurrence compared to other stations in the west region of Ria Formosa. It means that during high water occurrence the water flows from Bar da Gina and Centro Nautica station to Sao Luis inlet. Besides that, Sao Luis inlet also has ebb current only during the lowest water level phase.

Furthermore, from **Fig 5.20**, it could be seen that Centro Nautico and Bar de Gina stations has more or less similar behaviour relationship between water level and velocity variation. This could be due to the closer distance and the similar location characteristic between them.

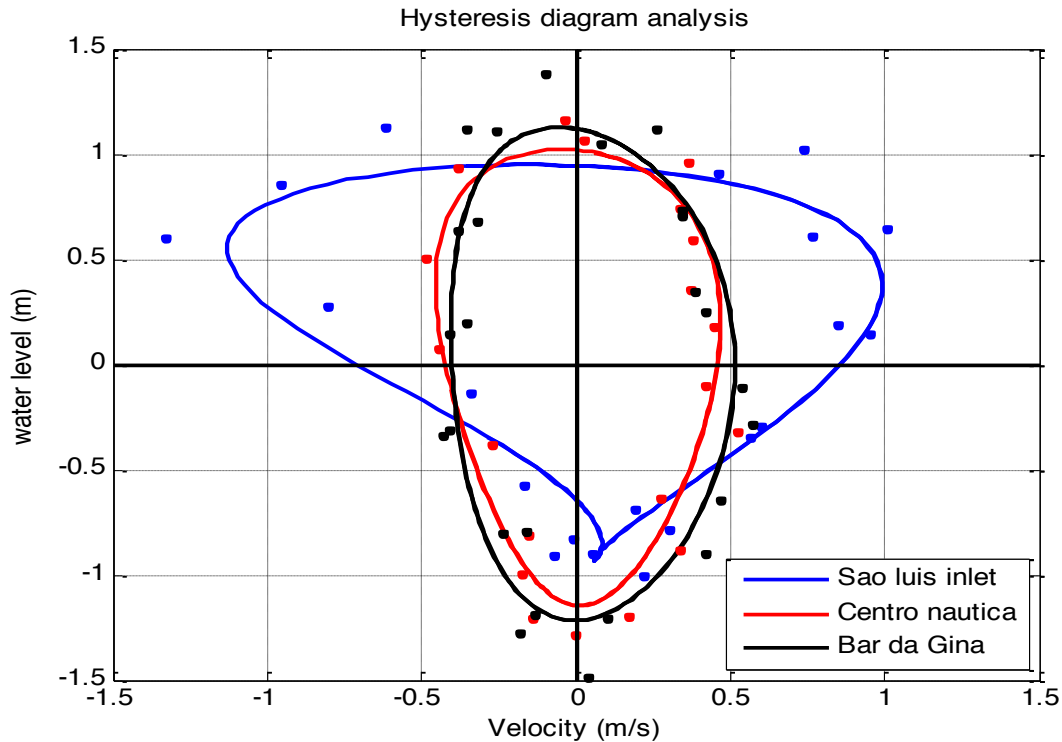


**Fig 5.20.** Hysteresis Diagram Analysis for west region of Ria Formosa

#### 5.2.2.4. For middle region of Ria Formosa

The middle region of Ria Formosa consists of several stations, which are Faro Olhao inlet, Cacoés, Boia V3, Culatra, Quatro Aguas, and Nave Pegos stations. The water level variation and velocity variation for those station can be observed in **Fig 5.21** and **Fig 5.22**. As mentioned before in the previous sub chapter, Faro Olhao inlet plays an important and significant role in controlling the water circulation in Ria Formosa. It could be seen from **Fig 5.21** and **Fig 5.22** in which Faro Olhao inlet has higher tidal amplitude and the strongest tidal current in term of flood and ebb current. Furthermore, from **Fig 5.21**, it could be seen that Boia V3 and Faro Olhao inlet almost have the same water level variation, but still there is a slightest different between them in which the water could flow between them. In term of velocity variation (**Fig 5.22**), Faro Olhao inlet and boia V3 have the opposite tidal current occurrence. In a certain period of time, if Faro Olhao inlet has ebb current, Boia V3 station will have flood current. However, there is similarity between them which is they have strong ebb and flood current. Furthermore, from **Fig 5.22**, it could be seen that there are strong oscillation fluctuation of tidal current velocity in almost of the stations in the west region of Ria Formosa, especially in Culatra and Quatro Aguas.

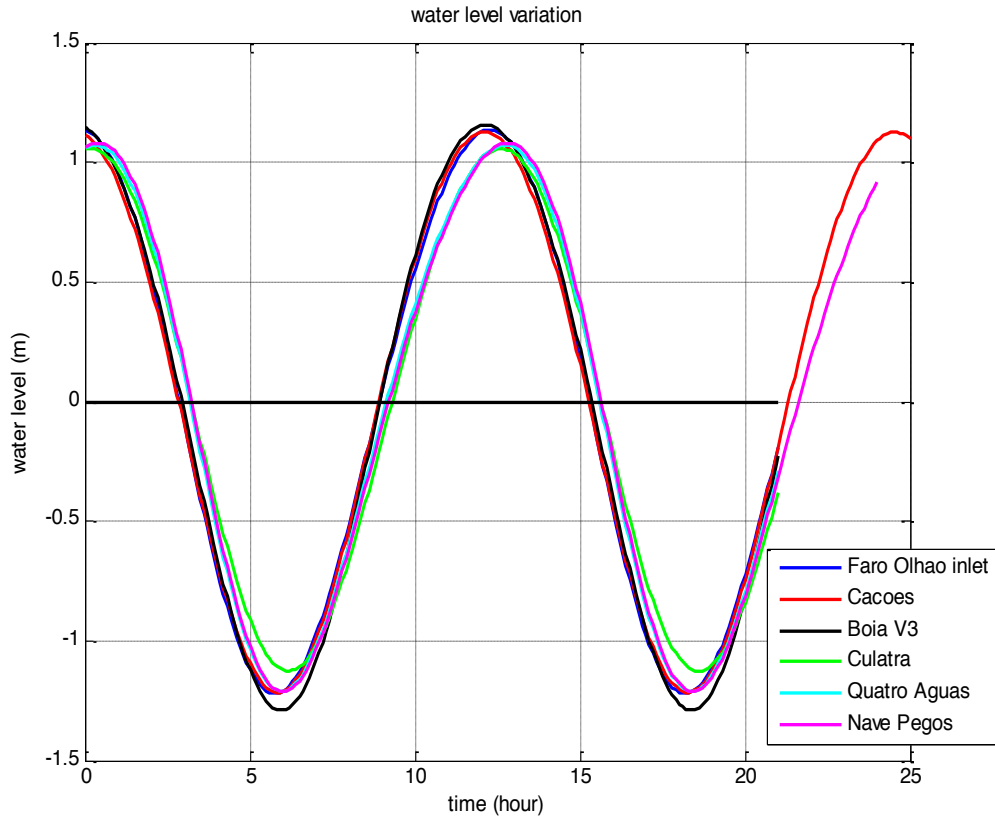


**Fig 5.21.** Water level variation for middle region of Ria Formosa

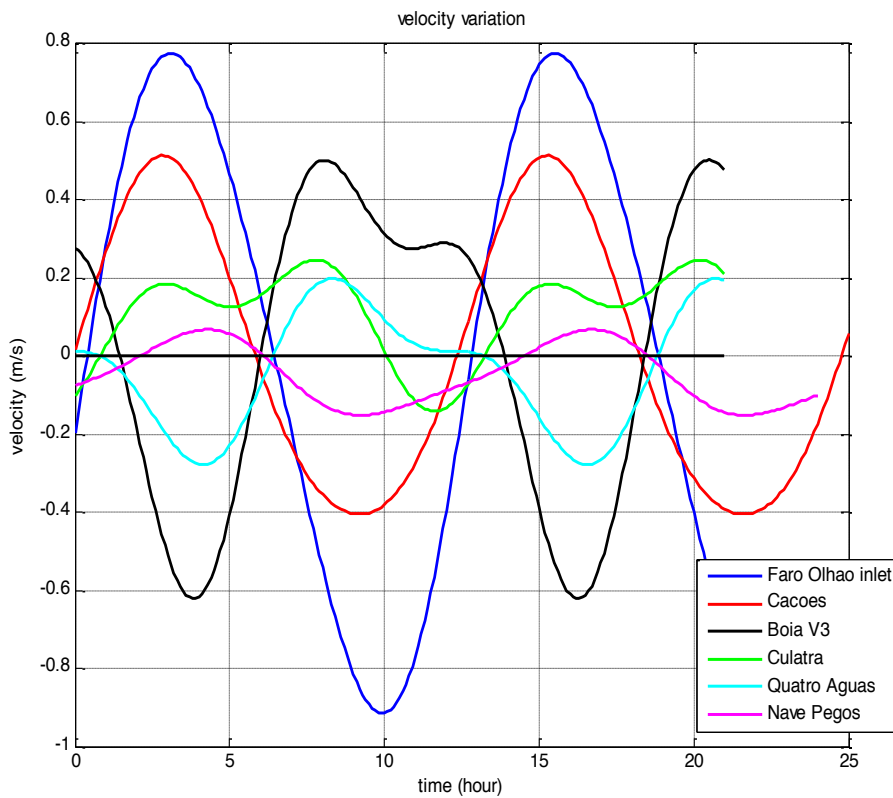


**Fig 5.22.** Velocity variation for middle region of Ria Formosa

Besides water level variation and velocity variation, hysteresis diagram analysis was also carried out in the middle region of Ria Formosa (**Fig 5.23**). From this figure, it could be seen that Faro Olhao inlet has strong ebb and current velocity during high water and low water level. The interesting thing that need to be pointed out from this figure is the Boia V3 station behaviour. During high water level occurrence, Boia V3 seems to have strong ebb current velocity, while during low water level, the strength of the flood and ebb current are almost similar. The most asymmetrical behaviour is also belong to Boia V3 station.

Furthermore, other stations in the middle region of Ria Formosa also showed the unique behaviour, such as Culatra and Quatro Aguas. This could be due to the strongest oscillation fluctuation of the tidal current velocity in which it can be caused by the shallow environment in the station because of the salt marshes area or muddy sediment area.

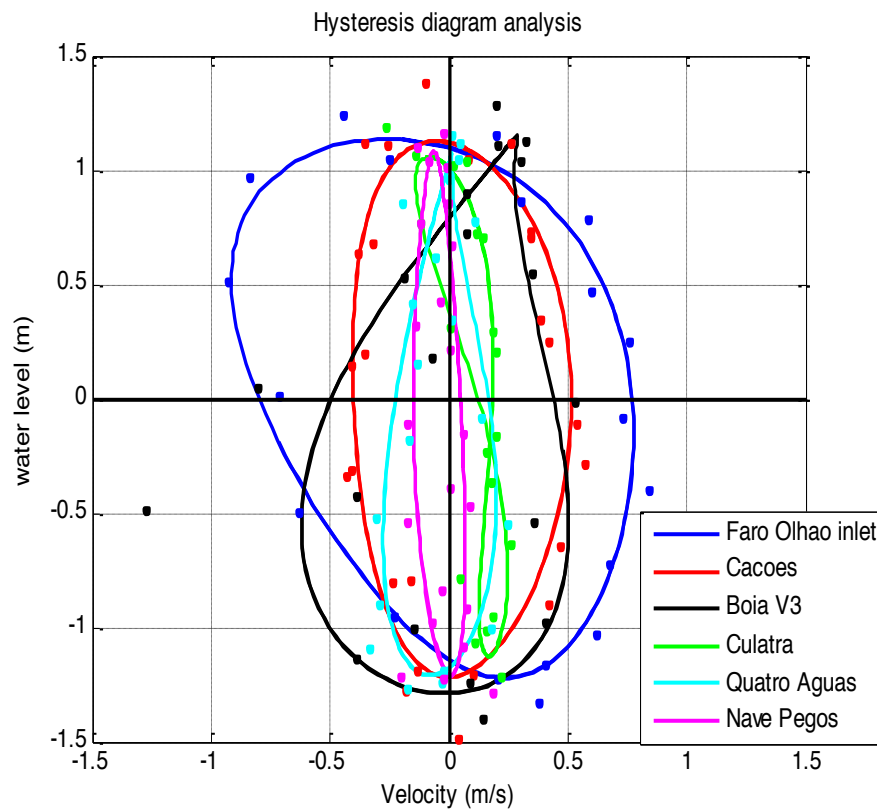


**Fig 5.23.** Hysteresis Diagram Analysis for middle region of Ria Formosa

#### 5.2.2.5. For East region of Ria Formosa

East region of Ria Formosa consists of Bela romao station, Marim station, Boia V3 station, Culatra station, and Armona inlet station. The water level variation and velocity variation for east region of Ria Formosa can be seen in **Fig 5.24** and **Fig 5.25**. During the high water occurrence, Armona inlet has the maximum tidal amplitude. While during low

water, Boia V3 seems to have the maximum tidal amplitude (**Fig 5.24**). The biggest water level temporal gradient occurred between Armona inlet and Bela romao station. because apparently they have big difference in term of water level tidal amplitude. In this region section of Ria Formosa, Armona inlet play an important and significant role as an inlet, especially in exchanging water in and out of east region of Ria Formosa.

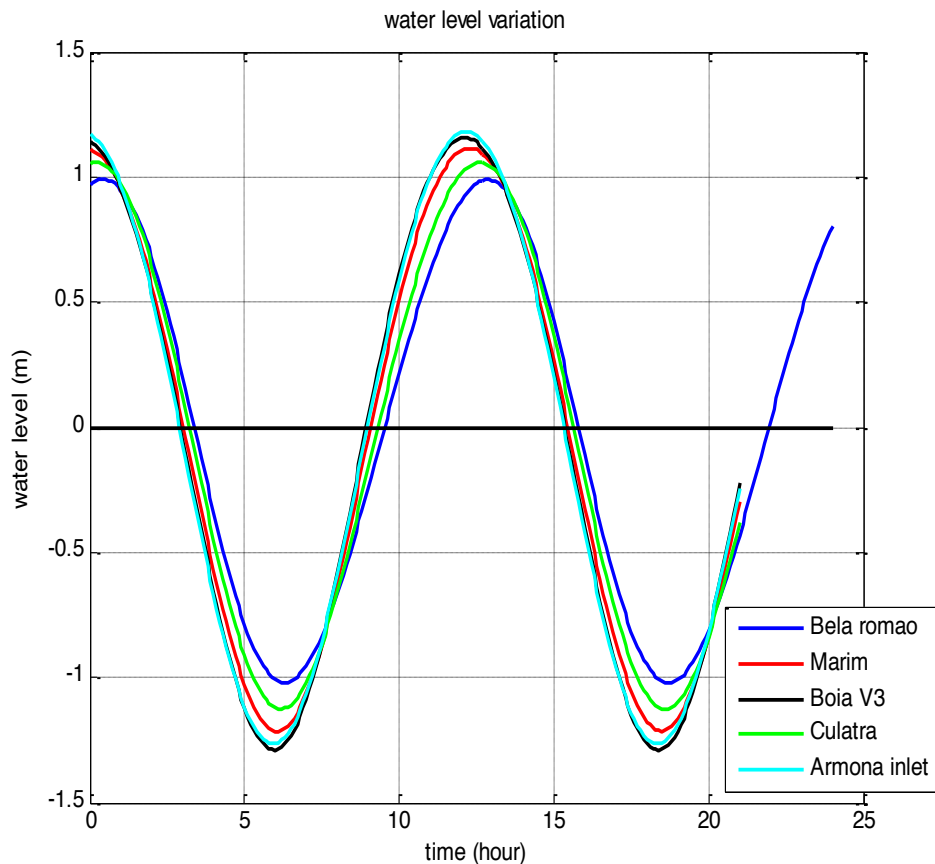


**Fig 5.24.** Water level variation for east region of Ria Formosa

The velocity variation among the stations showed a great variation of time, especially between Armona inlet and Boia V3. The different phase of current occurred between these two. If the ebb current occurred in Armona inlet, otherwise flood current occurred in Boia V3 (**Fig 5.25**). Besides that, the velocity variation in other stations are also interested to be observed, such as in Culatra and Bela Romao. These two stations showed a great fluctuation of tidal current which can be caused by shallow environment. Apparently, it has been known that Culatra is a muddy flat intersection point station in which the water flows to this station comes not only from one direction, but can be simultaneously coming from several different directions. So it could possibly caused the sediment settling in this station where the flows which bring sediment encountered.

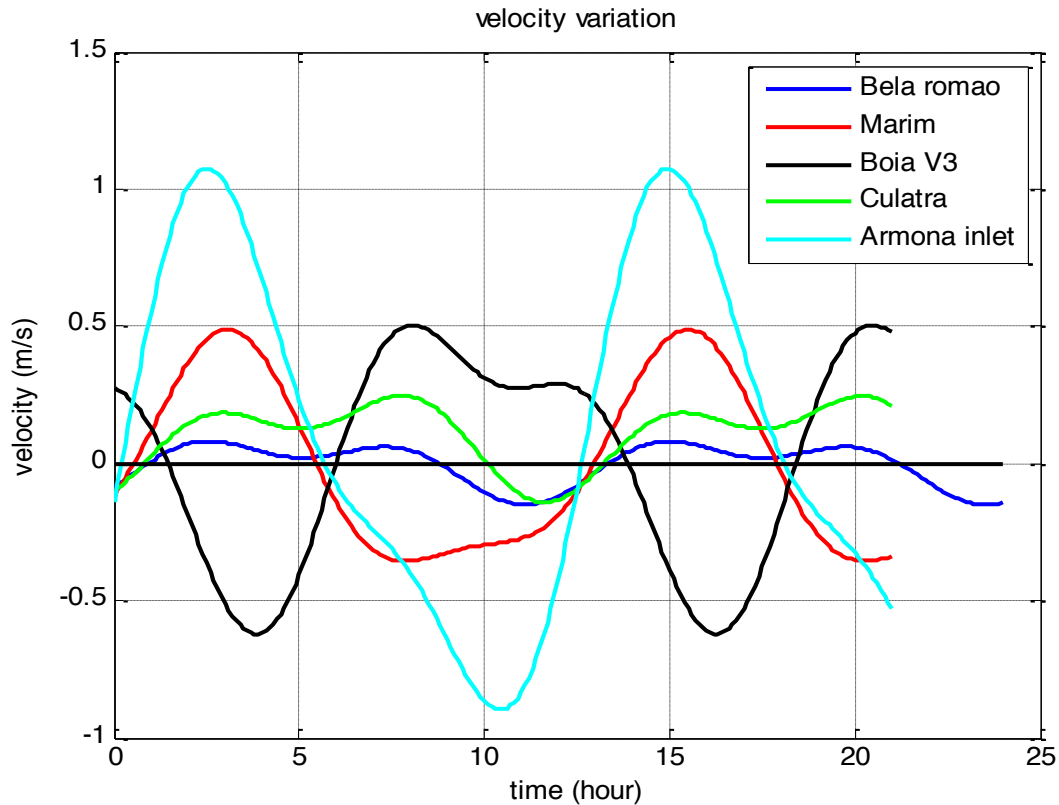


**Fig 5.25.** Velocity variation for east region of Ria Formosa

Besides water level and velocity variation, hysteresis diagram analysis for east region of Ria Formosa was also conducted to see the relationship behavior between water level variation and velocity variation (**Fig 5.26**). From this figure, it could be seen that Armona inlet has the strongest flood and ebb current during high water, while during low water, Boia V3 station seems to have the strongest flood current.

Furthermore, from **Fig 5.26**, it could be seen that Culatra and Bela Romao have almost the same diagram behavior due to the strong velocity fluctuation behaviour. Meanwhile Marim station also showed an unique behaviour, in which it has almost the same magnitude of flood current during high and low water occurrence.

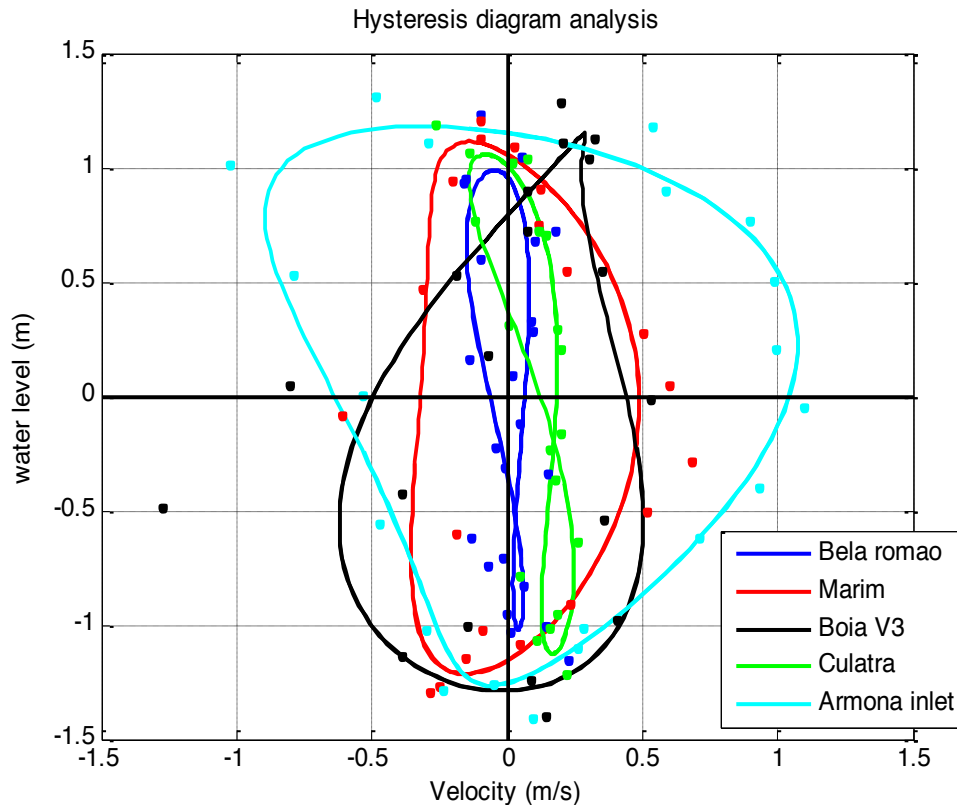


**Fig 5.26.** Hysteresis Diagram Analysis for east region of Ria Formosa

### *Slack Water*

Following the hysteresis diagram analysis, the slack water calculation also can be derived from the hysteresis diagram analysis. The slack water is a period of cessation in the strong flow of a current of water, especially at high or low tide. **Table 5.14** gives the information about the slack water for each stations during high and low water level.

From **Table 5.14**, it could be seen that Boia V3 has the maximum high slack water time and the minimum low slack water time. While Cacoés station has the minimum high slack water and Culatra station has the maximum low slack water. These three station has the maximum and minimum slack water time due to its shallow environment. Boia V3 and Culatra have been known as an intersection point station where the water flow can come from three different directions and sometimes it caused sediment settling in those station area due to the sediment carried by the water flows. Besides Boia V3 and Culatra, Cacoés station has also been known as a mud flat and salt marshes area which located in between Cais Comerciale and Boia V3. Cacoés has also a connection to the Faro Olhao inlet.

**Table 5.14.** The slack water for all stations

no	station	slack water (hour)	
		high water level	low water level
1	bela romao	0.4381	2.4856
2	cacoes	0.0145	1.3135
3	boia V3	1.7738	0.0104
4	quatro aguas	0.5265	0.4018
5	culatra	0.6332	3.8829
6	centro nautico	0.1242	0.0290
7	bar da gina	0.2469	0.0346
8	Sao Luis inlet	0.1508	1.6575
9	Faro-Olhao inlet	0.5181	0.6493
10	Armona inlet	0.4231	0.2183
11	nave pegos	1.7027	0.1037
12	marim	0.6590	0.5304
<b>average</b>		0.6009	0.9431

### 5.3. Volume and Discharge of flood and ebb phase

In this particular study, it is also studied the volume and discharge of the water pass through the stations (**Table 5.15**). It is obviously that Faro Olhao inlet and Armona inlet have the maximum volume of water and maximum water discharge both for ebb and flood occurrence. From this finding, it could be stated that Faro Olhao inlet and Armona inlet play an important role as an inlet in Ria Formosa lagoon. While Sao Luis inlet also plays role as an inlet in Ria Formosa lagoon, especially in the west region of Ria Formosa, but not in a significant role. It could be seen from the magnitude of the volume and water discharge in **Table 5.15**. This finding is similar with the finding of Salles et al (2005) which stated that the tidal prisms through Faro Olhao and Armona inlet ranging from 40 - 80 % and 12 - 50 % of total tidal prism, respectively. Besides that, this finding is also similar with the finding of Pacheco et al (2010) which stated that during spring tide, Faro Olhao, Armona, and Sao Luis inlet account for 61%, 23%, and 8% of tidal prism, respectively and during neap tide, Faro Olhao and Armona inlet share the tidal prism (45% and 40% respectively), with Sao Luis inlet having reduced importance. The inlet tidal prism during spring and neap tide according to Pacheco et al. (2010) can be seen in **Table 5.16**.

**Table 5.15.** Volume and Discharge of flood and ebb during tidal cycle

no	station	Discharge (m <sup>3</sup> /second)		Discharge residual (m <sup>3</sup> /s)	Volume (m <sup>3</sup> )		Volume residual (m <sup>3</sup> )
		flood	ebb		flood	ebb	
1	bela romao	-8.5E+02	5.9E+02	-2.5E+02	-3.0E+06	2.1E+06	-9.0E+05
2	cacoos	-3.2E+03	2.4E+03	-8.6E+02	-1.2E+07	8.5E+06	-3.1E+06
3	boia V3	-7.2E+02	9.0E+02	1.7E+02	-2.6E+06	3.2E+06	6.3E+05
4	quatro aguas	-1.0E+03	9.6E+02	-7.4E+01	-3.7E+06	3.5E+06	-2.7E+05
5	culatra	-1.3E+03	5.6E+03	4.3E+03	-4.6E+06	2.0E+07	1.6E+07
6	centro nautico	-1.4E+03	1.5E+03	6.3E+01	-5.1E+06	5.4E+06	2.3E+05
7	bar da gina	-9.4E+02	9.1E+02	-3.3E+01	-3.4E+06	3.3E+06	-1.2E+05
8	sao luis / Ancao inlet	-2.7E+03	2.7E+03	-9.5E+01	-9.9E+06	9.5E+06	-3.4E+05
9	faro - olhao inlet	-1.6E+04	1.1E+04	-4.5E+03	-5.6E+07	4.0E+07	-1.6E+07
10	Armona inlet	-8.1E+03	7.1E+03	-9.5E+02	-2.9E+07	2.6E+07	-3.4E+06
11	nave pegos	-3.6E+03	5.3E+02	-3.1E+03	-1.3E+07	1.9E+06	-1.1E+07
12	marim	-1.2E+03	1.0E+03	-2.2E+02	-4.5E+06	3.7E+06	-7.9E+05

**Table 5.16.** Inlet tidal prism during spring and neap tide (Pacheco et al., 2010)

	Ancão		Faro-Olhão		Armona
	Inlet Channel	Faro Channel	Inlet Channel	Olhão Channel	Inlet Channel
<i>Spring-tides</i>					
Flood <i>P</i> (m <sup>3</sup> )	8.28E + 06	3.41E + 07	6.64E + 07	2.49E + 07	2.11E + 07
Ebb <i>P</i> (m <sup>3</sup> )	-8.93E + 06	-3.37E + 07	-6.19E + 07	-2.20E + 07	-2.59E + 07
Residual <i>P</i>	-6.53E + 05	3.69E + 05	4.48E + 06	2.98E + 06	-4.74E + 06
Flood <i>U</i> (m/s)	0.58	0.23	0.50	0.34	0.31
Ebb <i>U</i> (m/s)	-0.80	-0.24	-0.52	-0.28	-0.43
Residual <i>U</i> (m/s)	-0.23	-0.01	-0.02	0.06	-0.12
Flood <i>T</i> (h)	6.6	6.4	6.4	6.2	6.4
Ebb <i>T</i> (h)<	5.9	6.1	6.1	6.3	6.1
<i>Neap-tides</i>					
Flood <i>P</i> (m <sup>3</sup> )	1.85E + 06	1.03E + 07	1.98E + 07	1.06E + 07	1.56E + 07
Ebb <i>P</i> (m <sup>3</sup> )	-1.56E + 06	-1.56E + 07	-1.77E + 07	-3.34E + 06	-1.76E + 07
Residual <i>P</i>	2.85E + 05	-5.32E + 06	2.02E + 06	7.29E + 06	-2.00E + 06
Flood <i>U</i> (m/s)	0.20	0.07	0.17	0.16	0.23
Ebb <i>U</i> (m/s)	-0.27	-0.11	-0.15	-0.09	-0.21
Residual <i>U</i> (m/s)	-0.07	-0.03	0.02	0.07	0.02
Flood <i>T</i> (h)	7.4	5.8	6.3	8.4	5.6
Ebb <i>T</i> (h)	5.1	6.7	6.2	4.1	6.9

#### 5.4. Spatial variability of residence time

In this study, residence time is an important and significant parameter that need to be carefully taken care of. Because this residence time play a significant role in determining the best place for the seashells to grow, besides average current velocity and maximum flood current. The spatial variability of residence time in all the stations can be seen in **Table 5.17**

and Fig 5.27.

From Table 5.17 and Fig 5.27, it could be seen that the higher residence time occurred in Marim stations, which is 6.7 days. It is probably due to the salt marshes area which covers the surrounding area in Marim station. Whereas the smaller residence time used to occurred in the inlet station because the water keeps exchanging in and out to and from the Ria Formosa lagoon (Duarte et al., 2005 and 2008), and it is obviously that inlets must have low residence time compare to other stations.

Besides that in the west region and middle region of Ria Formosa, it could be seen from Fig 5.27, the residence time is lower than 0.95 days, which means there is a good exchanging of water between the ocean and the west and middle region of Ria Formosa lagoon. While in the east region of the Ria Formosa lagoon, the water exchange seems a bit delay, probably due to a lot of friction existed in the east region of Ria Formosa, such as dunes, salt marshes area, and mud flat.

**Table 5.17** Spatial variability of residence time in all stations

ID	Stations	X	Y	ref	Residence time (days)
1	Barra Faro-Olhão	23380.87	-299044	ADP-BFO	0.5
2	Barra Armona	29290.71	-295059	TP2-BArmona	1.1
3	Barra S Luís	15564.26	-297957	240512	0.5
4	Cais Centro Náutico	13102.33	-295835	120611	0.8
5	Bar da Gina	12309.32	-295100	190712	1.7
6	Esteiro Cações	22787.09	-296264	30911	0.2
7	Boia V3	24307.06	-295167	271111	2.4
8	Culatra	25659.83	-296369	260412	0.2
9	Marim	28678.3	-293269	90911	6.7
10	Bela Romão	31924.71	-292305	181211	0.4
11	Quatro Águas	17077.1	-295254	231112	0.3
12	Estaleiro Nave Pegos 46ENP	16709.33	-294315	231112	0.2

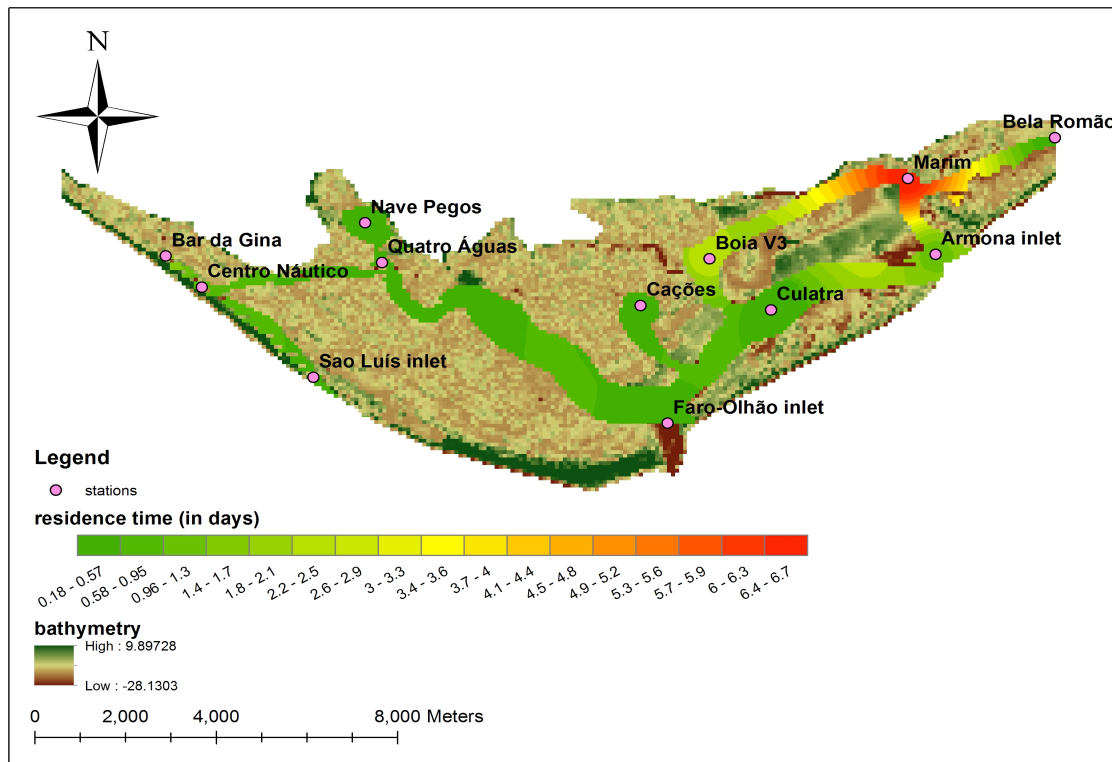


**Fig 5.27.** Spatial variability of Residence time

## 5.5. Preliminary study in determining the suitable area for seashell ponds using Arc GIS

To determine and evaluate the suitable area for shellfish pond, all of the calculation results of maximum flood current, average current velocity, and residence time are displayed using Geographical Information System (GIS) software application, so then the best combination of the physical and hydrodynamic requirement for shellfish to grow can be obtained.

As mentioned before in previous chapter, the site requirements for shellfish to grow up could include the following specifications (Congleton et al., 1999):

- A bottom type of sand, mudflat, and silty mud.
- An elevation between 1.22 and 1.83 m below msl (with average low water of 2 m below msl) would be submerged most of the time with access at low tide.
- An average current velocity between 0.09 and 0.1 m/s.
- A maximum flood tide current velocity less than 0.2 m/s.

Besides those specifications, to find the suitable place for clam culture, it is needed to know the residence time. In areas where the water exchanges on almost every tide, the environmental conditions allow the development of a diverse and productive benthic

population (Gamito, 1997).

**Table 5.18** showing the residence time, average current velocity, and maximum flood current for each stations in Ria Formosa lagoon. From this table, it could be seen that in term of average current velocity, Bela Romao, Quatro Aguas, Nave Pegos, Culatra, and Cacoés seems to have a good condition for seashell to grow (the average current velocity range is in between 0.08-0.14 m/s). While in term of maximum flood current, Culatra, Bela Romao, and Nave Pegos seems to have good condition for seashell to grow (the maximum flood current range is less than 0.2 m/s). In term of residence time, Cacoés, Culatra, Bela Romao, Quatro Aguas, and Nave Pegos seems to have good condition for seashells to grow since it has lower residence time where the good water exchange can occur.

**Table 5.18.** Residence Time, Average current velocity, and Maximum Flood Current for each stations in Ria Formosa lagoon

No	Stations	Residence time (days)	average current vel (m/s)	max flood current (m/s)
1	Faro Olhao inlet	0.49	0.55	0.94
2	Armona inlet	1.15	0.57	1.02
3	Sao Luis inlet	0.49	0.54	1.30
4	Centro Nautico	0.78	0.29	0.49
5	Bar da Gina	1.65	0.30	0.42
6	Cacoés	0.24	0.13	0.28
7	Boia V3	2.35	0.32	1.24
8	Culatra	0.22	0.14	0.14
9	Marim	6.74	0.28	0.64
10	Bela Romao	0.37	0.09	0.16
11	Quatro Águas	0.28	0.13	0.33
12	Nave Pegos	0.18	0.08	0.18

The spatial variability of Maximum Flood Current (m/s) and Average Current velocity (m/s) in Ria Formosa can be seen in **Fig 5.28** and **Fig 5.29**, respectively. From these two figures, it can be concluded that the suitable area for the seashell to have better grow are in Nave Pegos, Culatra, Cacoés, and Bela Romao. Giving an outlook to residence time, these four stations seems to have lower residence time, so it means the good water exchange can occur in these four stations, because in areas where the water exchanges on almost every tide, the environmental conditions allow the development of a diverse and productive benthic population (Gamito, 1997).

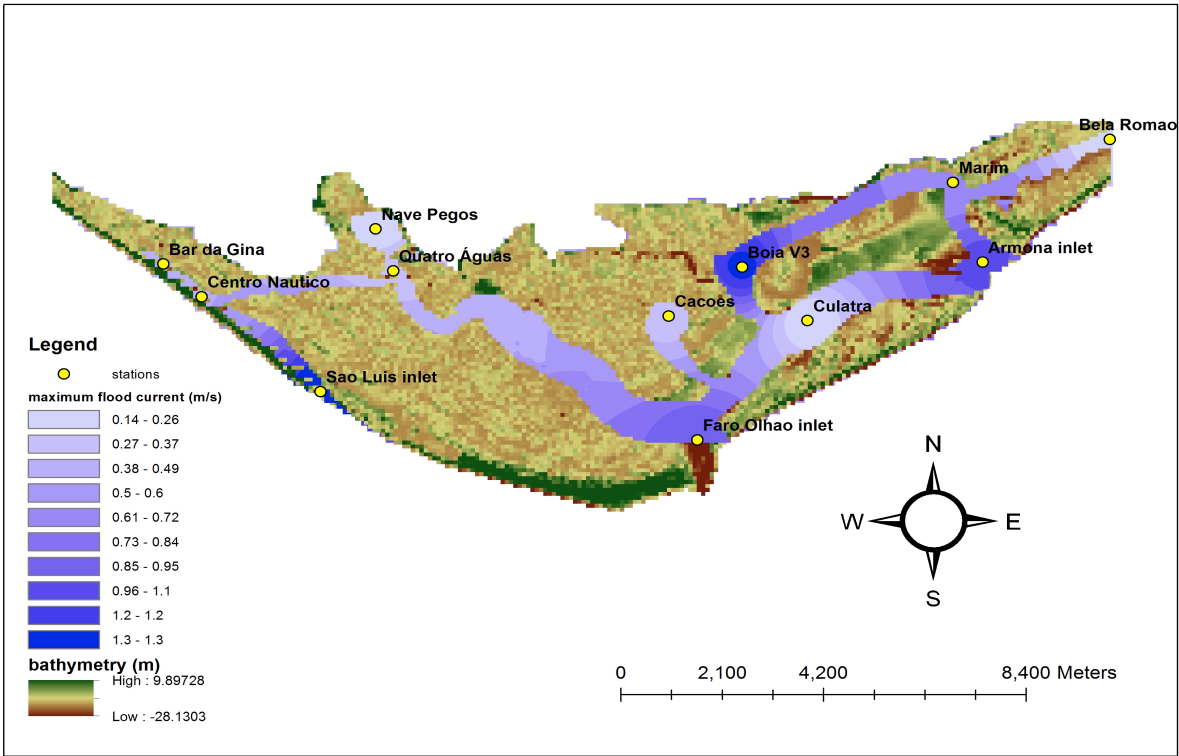


Fig 5.28 Spatial variability of Maximum Flood Current (m/s) in Ria Formosa lagoon

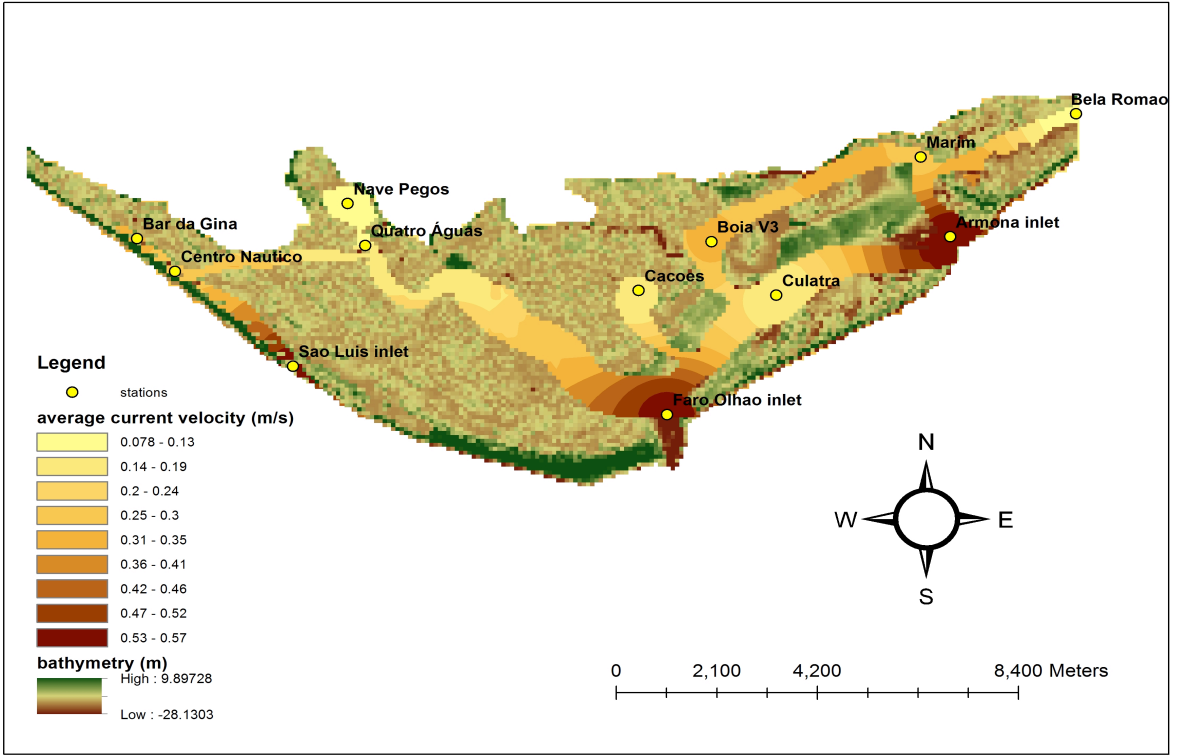


Fig 5.29 Spatial variability of Average Current Velocity (m/s) in Ria Formosa lagoon

5.6. Comparison study between inlet tidal cycles volume and geometric volume

In this study, the comparison study between the inlet tidal cycles volume and

geometric volume which based on the water level variation during high water and low water was carried out to ensure a good agreement between them. The former calculation result can be seen in **Table 5.19**. Whereas, the latter estimation was performed by overlaying the two condition of Ria Formosa during low water and high water variation for every stations in GIS (**Fig 5.30 and Fig 5.31**).

*Inlet tidal cycle volumes*

**Table 5.19 . Inlet tidal cycle volume calculation**

no	inlets	Volume (m3)		
		flood	ebb	residual
1	Sao Luis inlet	-9,889,991.66	9,546,655.50	-343,336.16
2	Faro-Olhao inlet	-55,877,916.33	39,728,095.80	-16,149,820.54
3	Armona inlet	-29,068,878.33	25,642,417.39	-3,426,460.94
4	Bela Romao	-3,042,007.38	2,139,710.77	-902,296.61
<b>total</b>		<b>-97,878,793.70</b>	<b>77,056,879.46</b>	<b>-20,821,914.24</b>

*Geometrical volumes*

Volume during High water

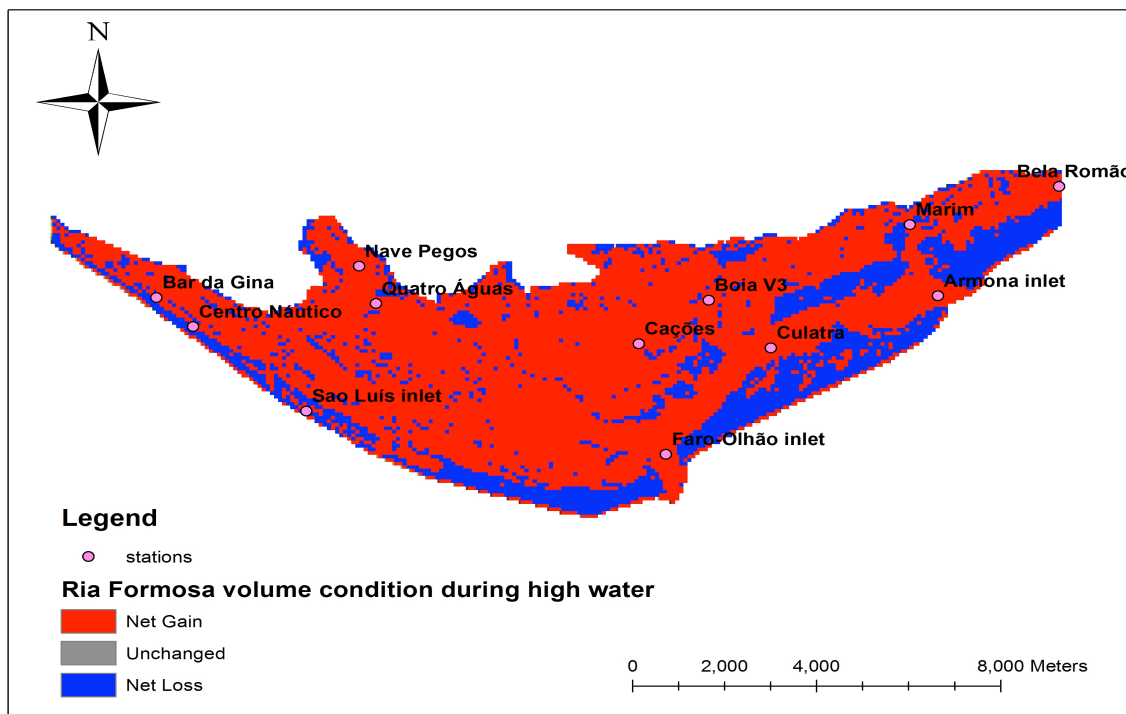


**Fig. 5.30** Ria formosa condition during high water level

Volume of the area submerged (net gain) = 89,904,710 m<sup>3</sup>

Volume of the area emerged (net loss) = 13,757,944 m<sup>3</sup>

## Volume during Low water

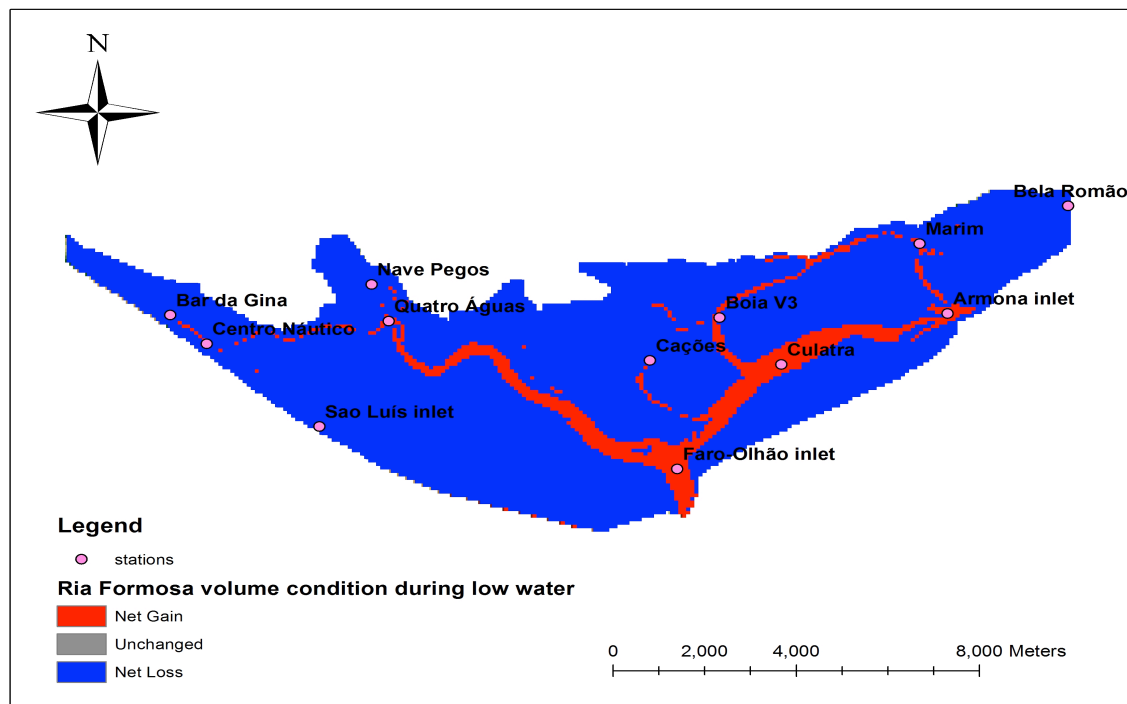


**Fig 5.31.** Ria formosa condition during low water level

Volume of the area submerged (net gain) = 26,299,267 m<sup>3</sup>

Volume of the area emerged (net loss) = 138,977,801 m<sup>3</sup>

Volume of the water that enter Ria Formosa during low and high water

= Volume of the area submerged during high water - Volume of the area submerged during low water

= 89,904,710 - 26,299,267 m<sup>3</sup>

= 63,605,444 m<sup>3</sup>

From this volume comparison, the difference volume calculation can be estimated (Table 5.20). From Table 5.20, it could be seen that the magnitude of the volume which calculated using inlet tidal cycle volume is much higher than the geometrical volume, because during the calculation time, the error could be involved and it could increase the error of calculation in the end. Besides that, the inlet tidal cycle volume calculation considered not only the water level variation but also the variation of the tidal current velocity in which often tidal current variation is very fluctuating, so this could be the reasons why there is such big difference between inlet tidal cycle volume calculation and geometrical calculation.

**Table 5.20.** The difference estimation between inlet tidal cycle volume and geometrical volume

	inlet tidal cycle volume (m3)	geometrical volume (m3)	inlet tidal cycle volume - geometrical volume (m3)	difference estimation percentage	Area of Ria Formosa (m2)	tidal height difference estimation (m)
flood	97,878,793	63,605,444	34273350	35.02%	88506398	0.387
ebb	77,056,879	63,605,444	13451435	17.46%	88506398	0.152

From **Table 5.19**, it could be seen that the difference estimation percentage during the flood and ebb are 35.02 % and 17.46 %, respectively. Besides that, from **Table 5.19**, it could be seen also the tidal height difference calculation for flood and ebb which are 38 cm for flood and 15 cm for ebb.

## 6. Conclusions

This study was enabled to obtain the hydrodynamic water circulation pattern in the main channel of Ria Formosa based on tidal dynamic analysis. The harmonic analysis of fit and proper test showed a good agreement between the raw data and the harmonic constituent combination/superposition curve of M2 and M4, in which the average root mean square calculation are 7.5 % of velocity root mean square and 6.75% of elevation root mean square, consecutively.

The spatial and temporal gradient of water level and longitudinal component of velocity in the main channel enabled to describe a good water circulation pattern, even though there are some errors in the direction of water circulation pattern and in the magnitude of water level gradient or velocity gradient. These happened due to some limitations committed in this study. The limitation of this study is the difference time scale of data collection due to the limitation of equipment (ADP / Acoustic Doppler Current Profiler ). The result of this water circulation pattern in the main channel of Ria Formosa showed the significance role of Faro Olhao inlet and Armona inlet and less significance role of Sao Luis inlet in the main channel of Ria Formosa system.

Tidal asymmetry and tidal distortion using harmonic analysis showed the flood and ebb dominance system in Ria Formosa, in which Faro Olhao inlet and Nave Pegos stations are belong to flood dominant system, while Culatra is belong to ebb dominant system. Other stations can not be defined specifically due to the different result of tidal current analysis and tidal phase (ebb/flood) duration period analysis. Besides that, this study also found that higher distortion can be indicated by the higher phase lag and also shallow areas will induce the strength of tidal asymmetry behaviour.

The energy flux calculation showed the highest energy is lied in the inlets of Ria Formosa lagoon and decrease with the distance from the inlets and the highest volume and highest discharge magnitude obviously can also be found in the inlets of Ria Formosa, since they have directly connection to the ocean. While the highest dissipation energy was occurred in between Cacoés station and Faro Olhao inlet which indicates the biggest difference in energy flux and the shortest distance between these two. The lower energy flux occurrence in Cacoés station indicates the shallow environment in this station. From this tidal energy dissipation calculation, it is also found that tidal dissipation has higher values in areas where the tidal currents are stronger.

The spatial variability of residence time in each stations and the preliminary study of the suitable area for seashell ponds were obtained in this study. It is shown that in the west

and middle region of Ria Formosa, there seems to have a good water exchange indication, while in east region of Ria Formosa, a high residence time magnitude is found. It means there is a bit delay in exchanging the water in and out of east region of Ria Formosa. The finding result of this spatial residence time variability was combined with the average current velocity and maximum flood current and found that Nave Pegos, Culatra, Cacoés, and Bela Romão stations are the suitable area for seashell to grow.

To ensure a good agreement of this tidal analysis study, the comparison study between inlet tidal cycle volume and geometric volume calculation were carried out. The results showed a big difference between inlet tidal cycle volume and geometric volume calculation in which about 35.02 % of volume difference during flood and 17.46 % of volume difference during ebb. This difference occurred because the inlet tidal cycle volume calculation considered not only the water level variation but also the variation of the tidal current velocity in which often tidal current variation is very fluctuating.

The future development of this work will allow to gain a quality level of understanding of the system in Ria Formosa. As mentioned in the beginning before, this thesis could possibly give contribution as a preliminary study for the fisherman to find the suitable place for doing clam aquaculture or clam harvesting. Hence, from the Eco-hydrological perspective, the result of this study could be used as a management tool for the decision maker to handle the anthropogenic activities such as dredging activity, inlet opening, etc that can give impact to the biota life in Ria Formosa.

## 7. References

- Baptista, Antonio M. (1987). " Propagacao de Mare e circulacao hidrodinamica na Ria de Faro e Zona costeira Adjacente Estudo preliminar em modelo matematico". Lisboa, departamentos de hidraulica nucleo de estuarios. Proc. 64/1/6352
- Bebiano, M. J. (1995). "Effects of pollutants in the Ria Formosa Lagoon, Portugal." Science of the Total Environment **171**(1-3): 107-115.
- Bjorn, Kjerfve (1994). "Coastal Lagoons". *Coastal lagoon processes*. Elsevier. pp. 1–3. ISBN 978-0-444-88258-5. Retrieved 31 March 2012.
- Bricker, J. D., Inagaki S., Monismith, S.G. (2005). "Bed Drag Coefficient Variability under Wind Waves in a Tidal Estuary". *Journal Hydraulic Engineering* 131 : 497-508.
- Brito, A. C., A. Newton, T.F. Fernandes, P. Tet (2011). "The role of microphytobenthos on shallow coastal lagoons: A modelling approach." Biogeochemistry **106**(2): 207-228.
- Chow, V. T., D. R. Maidment, L. W. Mays (1988). "Applied Hydrology". McGraw-Hill series in water resources and environmental engineering. McGraw-Hill Book Company : ISBN 0-07-010810-2.
- Coelho, M. R., M. J. Bebianno, and W.J. Langston (2002). "Organotin levels in the Ria Formosa lagoon, Portugal." Applied Organometallic Chemistry **16**(7): 384-390.
- Congleton Jr, W. R., B. R. Pearce, M.R. Parker, B.F. Beal (1999). "Mariculture siting: a GIS description of intertidal areas." Ecological Modelling **116**(1): 63-75.
- Csanady, G. T. (1976). "Mean Circulation in Shallow Seas." J Geophys Res **81**(30): 5389-5399.
- Davis, R., D.M. Fitzgerald. 2004. *Beaches and Coasts*. Blackwell Science Ltd. Malden, MA.
- Dias, J. M., and Sousa, M. C. (2009a). "Numerical modeling of Ria Formosa tidal dynamics." *Journal Coastal Research*, SI 56 (Proceeding of the 10<sup>th</sup> International Coastal Symposium), 1345-1349. Lisbon, Portugal, ISBN 0749-0258.
- Dias, J. M., M. C. Sousa, X. Bertin, A.B. Fortunato, A. Oliveira (2009b). "Numerical modeling of the impact of the Ancão Inlet relocation (Ria Formosa, Portugal)." Environmental Modelling and Software **24**(6): 711-725.
- Duarte, P., B. Azevedo, A. Pereira (2005). "Hydrodynamic modeling of Ria Formosa (South Coast of Portugal) with Ecodynamo." DITTY report : EESD Project EVK3-CT-2002-00084
- Duarte, P., B. Azevedo, M. Guerreiro, C. Ribeiro, R. Bandeira, A. Pereira, M. Falca, D. Serpa, J. Reia (2008). "Biogeochemical modelling of Ria Formosa (South Portugal)." Hydrobiologia **611**(1): 115-132.

- Dyer, Keith R. (1997). "Estuaries : A Physical Introduction". 2<sup>nd</sup> edition. Institute of Marine Studies, University of Plymouth, UK. John Wiley and Sons : ISBN 0-471-97470-6 (alk. Paper).
- Falcao, M. & C. Vale (2003). "Nutrient dynamics in a coastal lagoon (Ria Formosa, Portugal): the importance of lagoon-sea water exchanges on the biologic productivity". Ciencias Marinas 29(3): 425–433.
- Foreman, M. G. G. & Henry, R. F. (1989) The harmonic analysis of tidal time series. Adv. Water Resources, 12:109-120.
- Fortunato, A. B., A. Oliveira, and A. M. Baptista (1997). "On the effect of tidal flats on the hydrodynamics of the Tagus estuary. Oceanologica Acta (1999) vol. 22 - No. 1. 31-44.
- Gamito, S. (1997). "Sustainable management of a coastal lagoonal system (Ria Formosa, Portugal): an ecological model for extensive aquaculture." International Journal of Salt Lake Research 6(2): 145-173.
- Ghil, M., Y. Feliks, and L. Sushama (2002). "Baroclinic and barotropic aspects of the wind-driven ocean circulation." Physica D: Nonlinear Phenomena 167(1-2): 1-35.
- Guimaraes, M. H. M. E., A. H. Cunha, R. L. Nzinga, J. F. Marques (2012). "The distribution of seagrass (*Zostera noltii*) in the Ria Formosa lagoon system and the implications of clam farming on its conservation." Journal for Nature Conservation 20(1): 30-40.
- Kennish, M. J. (1986). "Ecology of Estuaries. Volume I: Physical and Chemical Aspects." Boca Raton, FL: CRC Press, Inc. ISBN 0-8493-5892-2.
- Kusky, Timothy, ed. (2005). "Encyclopedia of Earth Sciences. New York: Facts on File. P. 245. ISBN 0-8160-4973-4
- Luketina, D. (1998). "Simple tidal prism models revisited. Estuarine, Coastal and Shelf Science; Vol. 46. pp. 77-84.
- Martins, F., P. Pina, S. Calado, S. Delgado, and R. Neves. (2003). "A coupled hydrodynamic and ecological model to manage water quality in Ria Formosa coastal lagoon." Advance in Ecological Science 18 : 93-100.
- Mendonca, Ana (2001). "Simulacao da hidrodinamica de mare na Ria Formosa com um modelo de elementos finitos." Thesis book. Portugal : Universidade do Algarve.
- Miguel, Tiago (2013). "Evolução espaço-temporal da batimetria dos principais canais da Ria Formosa recorrendo à aplicação de SIGs." Thesis book. Portugal : Universidade do Algarve.
- Moore, W. S., J. O. Blanton, and S. B. Joye. (2006). "Estimates of Flushing times, Submarine

- groundwater discharge, and Nutrient fluxes to Okatee estuary, South Carolina." Journal of Geophysical Research, Vol. 111, CO9006, doi 10.1029/2005 JC003041, 2006.
- Mudge, S. M., J. D. Icelly, and A. Newton (2007). "Oxygen depletion in relation to water residence time." Journal of Environmental Monitoring, DOI :10.1039/b708178b.
- Mudge, S. M., J. D. Icelly, and A. Newton (2008). "Residence times in a hypersaline lagoon: Using salinity as a tracer." Estuarine, Coastal and Shelf Science **77**(2): 278-284.
- Newton, A., Mudge, S.M. (2003). "Temperature and salinity in a shallow, mesotidal lagoon, the Ria Formosa, Portugal". Estuarine, Coastal and Shelf Science **57**, 73–85.
- Nobre, A.M., Ferreira, J.G., Newton, A., Simas, T., Icelly, J.D., Neves, R., (2005). "Management of coastal eutrophication: integration of field data, ecosystem-scale simulations and screening models". Journal of Marine Systems **56**, 375e390.
- O'Brien, M.P. 1931. Estuary tidal prisms related to entrance areas. Civil Engineer; Vol. 1. pp. 738-739.
- Open University. 2000. Waves, Tides and Shallow-Water Processes, Second Edition. United Kingdom : Butterworth-Heinemann publication. ISBN - 10 : 0750642815.
- Pacanowski, R. C., and S. M. Griffies (2000), MOM 3.0 manual, technical report, 680 pp., Geophys. Fluid Dyn. Lab., Princeton, N. J.
- Pacheco, A., Vila-Concejo, A., Ferreira, O., and Dias, J.A. (2006). "Recent bathymetric evolution of the Faro Channel (Algarve, Portugal)". 4<sup>th</sup> symposium on the Iberian Atlantic Margin.
- Pacheco, A., Ferreira, O., Williams, J.J. , Garel. O., Vila Concejo, A., Dias, J.A (2010). "Hydrodynamics and equilibrium of a multiple- inlet system". Marine Geology **274** : 32-42.
- Pugh, D. (1987). "Tides, Surges and Mean Sea-Level: A handbook for engineers and scientists." John Wiley, Chichester, UK.
- Reed, R. E., H. B. Glasgow, J.M. Burkholder, C. Brownie (2004). "Seasonal physical-chemical structure and acoustic Doppler current profiler flow patterns over multiple years in a shallow, stratified estuary, with implications for lateral variability." Estuarine, Coastal and Shelf Science **60**(4): 549-566.
- Roegner, G. C. (2000). "Transport of molluscan larvae through a shallow estuary." Journal of Plankton Research **22**(9): 1779-1800.
- Salles, P., (2001). "Hydrodynamic Controls on Multiple Tidal Inlet Persistence". Ph.D. thesis, University of Mexico, pp. 272.

- Salles, P., Voulgaris, G., Aubrey, D.G., (2005). "Contribution of nonlinear mechanisms in the persistence of multiple tidal inlet systems". *Estuarine, Coastal and Shelf Science* 65, 475–491.
- Schwartz, Maurice L. (2005). "Encyclopedia of coastal science". Springer. p. 263. ISBN 978-1-4020-1903-6. Retrieved 31 March 2012.
- Seim, H., J. Blanton, S. Elston (2006). "Tidal circulation and energy dissipation in a shallow, sinuous estuary." *Ocean Dynamics* 56(3-4): 360-375.
- Serpa, D., M. Falcão, P. Duarte, L.C.D Fonseca, C. Vale (2007). "Evaluation of ammonium and phosphate release from intertidal and subtidal sediments of a shallow coastal lagoon (Ria Formosa - Portugal): A modelling approach." *Biogeochemistry* 82(3): 291-304.
- Soulsby, R. (1997). *Dynamic of Marine Sands - A manual for practical applications*. Oxford, Great Britain : Thomas Telford Publications, Thomas Telford Services Ltd. ISBN : 0 7277 2584 X.
- Taylor, G. (1919). Tidal friction in the Irish Sea. *Phil. Trans. R. Soc.*, 220: 1-93.
- Van Rijn, L. C. (1990). "Principles of Fluid Flow and Surface Waves in Rivers, Estuaries, Seas, and Oceans." Book.
- Vila-Concejo, A., Ferreira, O', Matias, A., Dias, J.M.A., (2003). "The first two year of an inlet: sedimentary dynamics". *Continental Shelf Research* 23, 1425–1445.
- Wang, Z.B., Jeuken, C. , De Vriend, H.J., (1999). *Tidal Asymmetry and Residual Sediment Transport in Estuaries - A literature study and application to the western scheldt*. Z2749.
- Wang C. F., M. H. Hsu, A. Y. Kuo. (2004). "Residence time of the Danshuei River estuary, Taiwan." *Estuarine, Coastal, and Shelf Science* 60 (2004) 381-393.
- Wolanski, E. (2007) "Estuarine Ecohydrology." Amsterdam, The Netherlands: Elsevier. ISBN 978-0-444-53066-0.